

DATAComp:

In search of the next generation of multimodal datasets

Samir Yitzhak Gadre^{*2} Gabriel Ilharco^{*1} Alex Fang^{*1} Jonathan Hayase¹ Georgios Smyrnis⁵
 Thao Nguyen¹ Ryan Marten^{7,9} Mitchell Wortsman¹ Dhruva Ghosh¹ Jieyu Zhang¹
 Eyal Orgad³ Rahim Entezari¹⁰ Giannis Daras⁵ Sarah Pratt¹ Vivek Ramanujan¹
 Yonatan Bitton¹¹ Kalyani Marathe¹ Stephen Mussmann¹ Richard Vencu⁶
 Mehdi Cherti^{6,8} Ranjay Krishna¹ Pang Wei Koh¹ Olga Saukh¹⁰ Alexander Ratner¹
 Shuran Song² Hannaneh Hajishirzi^{1,7} Ali Farhadi¹ Romain Beaumont⁶
 Sewoong Oh¹ Alexandros G. Dimakis⁵ Jenia Jitsev^{6,8}
 Yair Carmon³ Vaishaal Shankar⁴ Ludwig Schmidt^{1,6,7}

Abstract

Large multimodal datasets have been instrumental in recent breakthroughs such as CLIP, Stable Diffusion, and GPT-4. At the same time, datasets rarely receive the same research attention as model architectures or training algorithms. To address this shortcoming in the machine learning ecosystem, we introduce DATAComp, a participatory benchmark where the training code is fixed and researchers innovate by proposing new training sets. Concretely, we provide a testbed for dataset experiments centered around a new candidate pool of 12.8B image-text pairs from Common Crawl. Participants in our benchmark design new filtering techniques or curate new data sources and then evaluate their new dataset by running our standardized CLIP training code and testing the resulting model on 38 downstream test sets. Our benchmark consists of multiple scales, with four candidate pool sizes and associated compute budgets ranging from 12.8M to 12.8B samples seen during training. This multi-scale design facilitates the study of scaling trends and makes the benchmark accessible to researchers with varying resources.

Our baseline experiments show that the DATAComp workflow is a promising direction for improving multimodal datasets. We introduce DATAComp-1B, a dataset created using a simple filtering algorithm applied to the 12.8B candidate pool. The resulting 1.4B subset enables training a CLIP ViT-L/14 from scratch to 79.2% zero-shot accuracy on ImageNet. Our new ViT-L/14 model outperforms a larger ViT-g/14 trained on LAION-2B by 0.7 percentage points while requiring 9× less compute during training. We also outperform OpenAI’s CLIP ViT-L/14 by 3.7 percentage points, which is trained with the same compute budget as our model. These gains highlight the potential for improving model performance by carefully curating training sets. We view DATAComp-1B as only the first step and hope that DATAComp paves the way toward the next generation of multimodal datasets.

We publicly release our datasets, associated tooling, filtering baselines, and our code for training and evaluating models at www.datacomp.ai.

^{*}Equal contribution, randomly ordered. Correspondence to contact@datacomp.ai. ¹University of Washington ²Columbia University ³Tel Aviv University ⁴Apple ⁵UT Austin ⁶LAION ⁷AI2 ⁸Juelich Supercomputing Center, Research Center Juelich ⁹University of Illinois Urbana-Champaign ¹⁰Graz University of Technology ¹¹Hebrew University.

Table 1: Zero-shot performance of CLIP models trained on various datasets. Our dataset DATACOMP-1B, assembled with a simple filtering procedure on image-text pairs from Common Crawl, leads to a model with higher accuracy than previous results while using the same or less compute. Training compute is measured in the total number of multiply-accumulate operations during training (MACs). See Section 3.5 for details on the evaluation datasets.

Dataset	Dataset size	# samples seen	Architecture	Train compute (MACs)	ImageNet accuracy	Avg. performance (38 datasets)
OpenAI’s WIT [102]	0.4B	13B	ViT-L/14	1.1×10^{21}	75.5	0.61
LAION-400M [119, 23]	0.4B	13B	ViT-L/14	1.1×10^{21}	73.1	0.58
LAION-2B [120, 23]	2.3B	13B	ViT-L/14	1.1×10^{21}	73.1	0.59
LAION-2B [120, 23]	2.3B	34B	ViT-L/14	2.6×10^{21}	75.2	0.61
LAION-2B [120, 23]	2.3B	34B	ViT-H/14	6.5×10^{21}	78.0	0.64
LAION-2B [120, 23]	2.3B	34B	ViT-g/14	9.9×10^{21}	78.5	0.64
DATACOMP-1B (ours)	1.4B	13B	ViT-L/14	1.1×10^{21}	79.2	0.66

1 Introduction

The past two years have seen multiple breakthroughs in multimodal learning. A new family of models including CLIP [102], DALL-E [106, 107], Stable Diffusion [114], Flamingo [4], and GPT-4 [95] offer unprecedented generalization capabilities in zero-shot classification, text-guided image generation, and in-context learning. While these advances use different algorithmic techniques such as contrastive learning, diffusion, or auto-regressive modeling, they all rest on a common foundation: large datasets containing paired image-text examples. For instance, CLIP’s training set contains 400 million image-text pairs, and Stable Diffusion was trained on subsets of LAION-2B [120], a dataset of more than two billion image-text pairs. This new generation of image-text datasets is more than 1,000 times larger than previous training datasets such as the widely used ImageNet, which contains 1.2M images [32, 117].

Despite the central role large image-text datasets play in multimodal learning, little is known about them. Many state-of-the-art datasets are proprietary and only available in corporate research labs, as in the case of CLIP [102], DALL-E [106, 107], Flamingo [4], and GPT-4 [95]. But even for public datasets such as LAION-2B [120], it is unclear how design choices during dataset construction, such as the data source or filtering techniques, affect the resulting models. While there are thousands of ablation studies for algorithmic design choices (loss function, optimizer, model architecture, etc.), datasets are usually treated as monolithic artifacts without detailed investigation or further improvements. Moreover, datasets currently lack the benchmark-driven development process that has enabled the community to produce a steady stream of advances on the model side. These issues impede further progress in multimodal learning, as evidenced by recent work showing that public datasets currently do not match the scaling behavior of proprietary alternatives [23]. A key difficulty for improving datasets is the scarcity of data-centric benchmarks that isolate dataset enhancements from changes to the model.

In this paper, we take a step towards a more rigorous dataset development process via five contributions. Our first and central contribution is **DATACOMP, a new benchmark for multimodal dataset design**. DATACOMP flips the traditional benchmarking paradigm in machine learning where the dataset is fixed and the research community proposes new training algorithms. Instead of a fixed dataset, we hold the training code, model, and computational budget constant so that

participants innovate by proposing new training sets. To evaluate the quality of a training set, we score the resulting model with a broad testbed of 38 classification and retrieval tasks such as ImageNet [32], ImageNetV2 [112], DTD [25], EuroSAT [56], PatchCamelyon [131], SUN-397 [135], MSCOCO [21], and WinoGAViL [12].

DATAComp focuses on two key challenges that arise when assembling large training datasets: what data sources to train on, and how to filter a given data source. Each challenge corresponds to one track in our benchmark. To facilitate the *filtering track*, our second contribution is **COMMONPOOL, a dataset of 12.8B image-text pairs collected from Common Crawl**. In the filtering track, the goal of participants is to find the best subset of COMMONPOOL to train on. COMMONPOOL is currently the largest publicly released image-text dataset, exceeding the size of LAION-5B by a factor of $2.5\times$. Additionally, we apply explicit content checks and face blurring when constructing COMMONPOOL to improve the safety of image-text datasets. In the second track, *Bring Your Own Data* (BYOD), participants can leverage any data source of their choice, as long as the training data does not overlap with our evaluation testbed. Taken together, our two tracks provide a controlled environment to better understand dataset curation for multimodal learning.

Our third contribution is an investigation of **scaling trends for dataset design**. In particular, DATAComp contains *four* distinct compute and data scales. On the data side, the candidate pool for filtering ranges from 12.8M samples to 12.8B samples. On the compute side, the training budget scales accordingly from 12.8M to 12.8B samples seen during training. This choice of pool size and compute budget leads to the natural baseline of training on the entire candidate pool with a single training pass and no filtering. Expressed in GPU hours, the cost of a single training run ranges from 4 to 40,000 GPU hours on the A100 cluster we used for development. This $10,000\times$ range stems from a factor $1,000\times$ in pool size and another factor $10\times$ from scaling the model size. The different scales enable researchers with different resources to participate in our benchmark. Moreover, the multi-scale format facilitates studying scaling trends. Our results show that the order of several filtering approaches is largely consistent across multiple compute and data scales.

Our fourth contribution are **over three hundred baseline experiments** and resulting insights into how dataset curation methods compare. Our baselines span basic techniques such as removing small images or non-English captions, querying captions for relevant keywords, filtering based on image embeddings, and applying a threshold on CLIP scores. A key result from our baseline experiments is that smaller, more stringently filtered datasets can lead to models that generalize *better* than larger datasets coming from the same pool. At the 12.8B scale, our best filtering baseline increases ImageNet zero-shot accuracy by 6.9 percentage points (pp) relative to the unfiltered pool (see Table 3). For the BYOD track, our initial experiments with multiple data sources find that 109M additional data points (less than 1% of the pool size) improve the CLIP-filtered subsets of COMMONPOOL by up to 1.2 pp ImageNet accuracy at the 12.8B scale (see Table 4).

Finally, our fifth contribution is **DATAComp-1B, a new state-of-the-art multimodal dataset** that can be used as a drop-in replacement for previous image-text datasets such as LAION-2B. DATAComp-1B is a filtered subset of COMMONPOOL containing 1.4B image-text pairs and demonstrates that improving data curation can yield large performance gains. We obtained DATAComp-1B by combining our two most promising baselines from smaller scale experiments: CLIP score filtering and image-based filtering. DATAComp-1B enables training a CLIP ViT-L/14 model with a compute budget of 12.8B samples to an ImageNet zero-shot accuracy of 79.2% (see

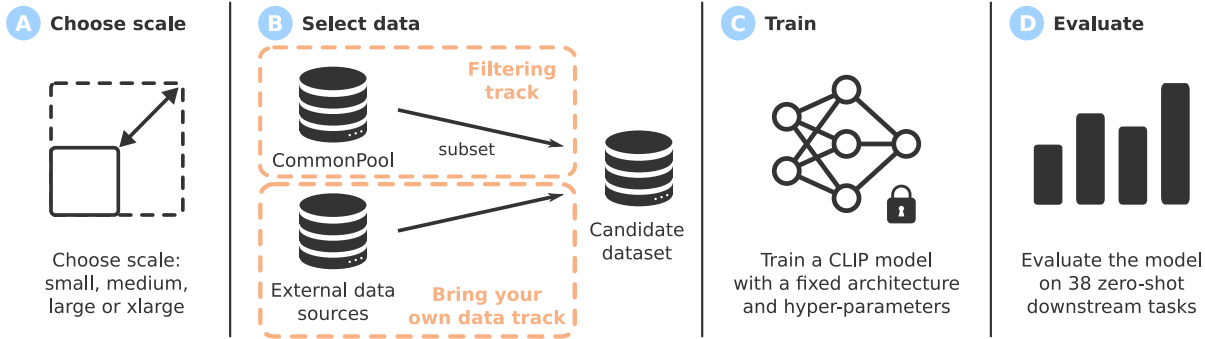


Figure 1: Participant workflow. A) Participants first choose a scale, `small`, `medium`, `large` or `xlarge`, based on their resource constraints (submission to multiple scales is allowed). B) Participants create a candidate dataset, choosing one of two tracks: *filtering*, where only image-text pairs from COMMONPOOL are allowed; or BYOD, where any data source (including COMMONPOOL) is permitted. C) Participants train a CLIP model on their candidate pool using a fixed architecture and hyperparameters (Section 3.4). D) Participants evaluate the trained model on a suite of diverse downstream tasks (Section 3.5) and submit to our leaderboard.

Table 1). This model, trained on DATACOMP-1B, outperforms a larger CLIP ViT-g/14 model trained on LAION-2B for about $3\times$ longer (34B samples seen), corresponding to an $9\times$ overall reduction in compute cost. Moreover, our model outperforms OpenAI’s original CLIP ViT-L/14 by 3.7 percentage points, which is trained with the same compute budget of 12.8B samples as our model. We view DATACOMP-1B as only the first new dataset coming out of DATACOMP and expect that future work will leverage our benchmark to discover further dataset improvements.

We hope that DATACOMP serves as a starting point for new creative research on dataset curation by making it easier to conduct controlled experiments in a shared experimental setting. To enable future work, we publicly release our candidate pools, our tooling for assembling these pools, our filtering baselines, and our code for training and evaluating models at www.datacomp.ai. We present an overview of the participant workflow in Figure 1. We believe that our infrastructure will help put research on dataset curation on rigorous empirical foundations, draw attention to this understudied research area, and lead to the next generation of multimodal datasets.

2 Related Work

Due to space constraints, we discuss work that is closest to DATACOMP here and refer the reader to Appendix C for additional related work.

The effects of data curation. Classical work considers dataset cleaning and outlier removal [65, 140, 115, 116] to discard samples that may lead to undesirable model bias. A related line of work develops coreset selection algorithms [54, 3, 41, 7, 86, 134, 27], which aim to select data subsets that lead to the same performance as training on the entire dataset. These techniques are known to scale poorly to larger data regimes [46, 2], which are critical for modern deep learning algorithms. More recent efforts in subset selection often operate on already curated datasets [90, 130, 121, 11, 28, 98]

like CIFAR-10, ImageNet or on smaller data regimes (e.g., YFCC-15M [102, 129]). These settings often do not reflect newer training paradigms that involve (1) *noisy* image-text pairs instead of category labeled images and (2) large scale datasets (e.g., billions of samples). While data-centric investigations have led to community competitions like DCBENCH [38] and DATAPERF [89], existing benchmarks have likewise operated at small data scales [92], especially when compared to datasets like LAION-2B [120], which contains over two billion images. DATACOMP bridges this gap to better align dataset curation algorithms with modern large scale image-text training.

There has also been renewed interest in dataset pruning and deduplication. Sorscher et al. [124] show that data pruning can be used to outperform traditional power-law scaling trends on ImageNet, but do not consider image-text training or larger datasets. Raffel et al. [104] attempt to remove sentence redundancies when creating the C4 corpus. Future work further demonstrated the benefits of deduplication for better language modeling [82]. Radenovic et al. [101] introduce CAT filtering for image-text datasets—a rule based system to retain high quality samples. Abbas et al. [2] introduce SemDeDup, which starts with the CAT-filtered LAION-440M subset, further employing a clustering method to remove semantic duplicates. SemDeDup improves training speed; however, the resulting models show similar zero-shot ImageNet performance when compared to models trained on the original dataset. At our largest scale, we introduce a pool of 12.8B image-text pairs, which is an order of magnitude larger than the data pools considered in either CAT or SemDeDup. Hence, we hope the DATACOMP benchmark will bootstrap future data-centric exploration at a scale that is unprecedented in non-proprietary research.

Large-scale multimodal datasets. Datasets have been instrumental to build multimodal models like CLIP [102], Flamingo [4], Stable Diffusion [114], DALL-E [106, 107] and GPT-4 [95]. These methods succeeded by training on large, heterogeneous datasets rather than solely through advanced modelling techniques. For example, OpenAI’s CLIP trains on 400M image-text pairs from the web, roughly $300\times$ the size of ImageNet [32]. Prior work on scaling image-text datasets also provides promising trends with respect to zero-shot model performance [64, 99]. Additional large scale datasets like FILIP-300M [137], FLD-900M [141], and PaLI-10B [20] were constructed to train multimodal models. However, many datasets used to train such models (including the dataset for OpenAI’s CLIP) are proprietary, making it hard to conduct data-centric investigations. Even for public image-text datasets like SBU [96], Flickr30k [139], MS-COCO [21], Conceptual Captions [122], CC12M [19], RedCaps [33], WIT [125], Shutterstock [93], YFCC-100M [129], COYO-700M [15], LAION-400M [119], or LAION-2B [120] little is known about what constitutes a good image-text dataset. Preliminary analysis suggests that different image-text data sources lead to CLIP models with different properties [93]. However, previous work is limited to smaller scale data (10-15M examples). Our work provides a testbed for conducting controlled experiments on how different data curation techniques affect models. Our benchmark spans several orders of magnitude in compute and data scale. It includes the largest publicly available collection of image-text pairs, with 12.8B samples.

3 DATACOMP

The goal of DATACOMP is to place dataset curation on rigorous empirical foundations, making it easier to conduct controlled experiments in a shared experimental setting. In contrast to traditional benchmarks where participants iterate on model design and hyperparameter tuning, DATACOMP

asks participants to design datasets that lead to high accuracy under fixed experimental conditions on the modeling side. Our benchmark focuses on large image-text datasets and evaluates a new dataset by training a CLIP model on the dataset from scratch [102]. To facilitate such investigations, we provide a candidate pool of uncurated image-text pairs crawled from the public internet.

Our benchmark offers two tracks: one where participants must use only samples from the pools we provide, and another where participants can use external data in addition to samples from our pool. Moreover, DATACOMP is structured to accommodate participants with diverse levels of computational resources: each track is broken down into four scales with varying compute requirements.

In this section, we discuss several design considerations including the benchmark tracks, experimental details for training, datasets used for evaluation, and the rules of the competition.

3.1 Competition design

The first question when designing a datasets benchmark is how to enable meaningful comparisons between different datasets. In numerous areas of machine learning, larger datasets lead to better performance [79, 70, 64, 99, 59, 23, 14, 102, 103]. Hence a natural starting point for a dataset benchmark would be to compare datasets of the same size only. While intuitive, this approach is flawed when it comes to contemporary large training sets for multimodal models. In particular, controlling the dataset size ignores the creation process behind the dataset and thereby fails to control for the actually relevant quantities: pool size and training compute. To illustrate this point, we now briefly summarize how state-of-the-art multimodal datasets are assembled.

At a high level, assembling a dataset such as LAION-2B consists of two steps. The first step is to identify one or multiple *data sources*, e.g., a web crawl such as Common Crawl or a widely used website such as Reddit. The data source should provide many training examples covering a broad distribution and come with supervision signals such as nearby text. After identifying a suitable set of data sources, the next step is to *filter* the data source to remove data points with low-quality annotations or other deficiencies (blurry images, etc.). The final dataset then contains all examples from the data sources that pass the data curation filters.

An important aspect of this dataset creation process is that *the final dataset size is a design choice* and not fixed ahead of time by the data sources. In particular, the dataset designer faces a trade-off between the dataset size (more data points are better) and data quality (higher quality data points are better). Hence the true data constraint in web-scale training set curation is not the size of the final dataset, but the size of the *candidate pool*. To make DATACOMP a realistic benchmark for dataset curation that can inform future dataset projects, we therefore fix the candidate pool participants work with in the filtering track, but otherwise give participants full control over the training set size.

Besides the size of the candidate pool, the other practically relevant constraint when training a model is the compute cost. In order to put training sets of different size on equal footing, we specify the training compute in terms of the total *number of samples seen* during training, not in terms of how many passes (epochs) the training run makes over the training set. As a concrete example, consider the 12.8B candidate pool, for which we fix a compute budget of 12.8B examples seen. A participant may choose to build a training set A with 3.2B data points by removing 75% of the candidate pool. The DATACOMP training code would then make four passes over this training set A .

Table 2: Experimental configuration for each scale. The number of samples seen during training at the largest scale is chosen to match the experimental setup from Radford et al. [102]. Training compute is measured in the total number of multiply-accumulate operations (MACs).

Scale	Model	Train compute (MACs)	Pool size and # samples seen
small	ViT-B/32	9.5×10^{16}	12.8M
medium	ViT-B/32	9.5×10^{17}	128M
large	ViT-B/16	2.6×10^{19}	1.28B
xlarge	ViT-L/14	1.1×10^{21}	12.8B

Alternatively, a participant may filter more aggressively and end up with a dataset B containing only 1.6B examples (i.e., removing 87.5% of the candidate pool). In this case, the training code would make eight passes over training set B so that the total amount of training compute remains constant (12.8B samples seen). A key result from our baselines experiments in DATACOMP is that smaller, more stringently filtered datasets can lead to models that generalize *better* than larger datasets coming from the same pool of images when the total amount of training compute is constant.

This realistic, pool-centric perspective on dataset curation is one of the key design decisions in DATACOMP. We now briefly review the other design decisions such as the division into two competition tracks, our multi-scale structure and the construction of the candidate pool. Other design decisions including our training and evaluation protocols are discussed in Sections 3.4 and 3.5.

Competition tracks. As mentioned above, the two key steps in assembling a training dataset are filtering an existing pool of data [119, 120, 15] and aggregating different data sources [31, 32]. To compare methods for these two approaches separately, DATACOMP has two tracks: *filtering*, where participants must select a subset of the samples from COMMONPOOL, and *Bring Your Own Data* (BYOD), where participants are allowed to use any source of external data. The tracks are described in Sections 3.2 and 3.3, respectively.

Competition scales. To facilitate the study of scaling trends and accommodate participants with various levels of computational resources, we structure DATACOMP using four scales of compute: **small**, **medium**, **large** and **xlarge**. Each new scale increases the number of samples seen during training by $10\times$ (from 12.8M to 12.8B samples seen), and the pool we provide by the same factor (from 12.8M samples to 12.8B samples). Table 2 describes the experimental configuration used for training at each scale.

Preprocessing and safety. Creating a dataset from a noisy web source such as Common Crawl involves many design decisions, e.g., whether one should de-duplicate images, keep only English captions, or restrict the image sizes. We decided to grant participants a high degree of autonomy and kept our initial preprocessing of COMMONPOOL to a minimum, leaving these design decisions open for exploration. Our only initial preprocessing steps are to eliminate images that appear in downstream evaluation datasets or are flagged due to safety considerations. For the latter, we take steps to eliminate illegal and explicit content and to protect the privacy of individuals. Specifically, we remove unsafe images and captions with automated filters and obfuscate faces in the candidate images we provide. Section 3.2 describes these steps in more detail.

Competition rules. We include comprehensive rules in Appendix A. Briefly, for the filtering track, we do not allow usage of test images from our evaluation suite, but do allow users to use the training

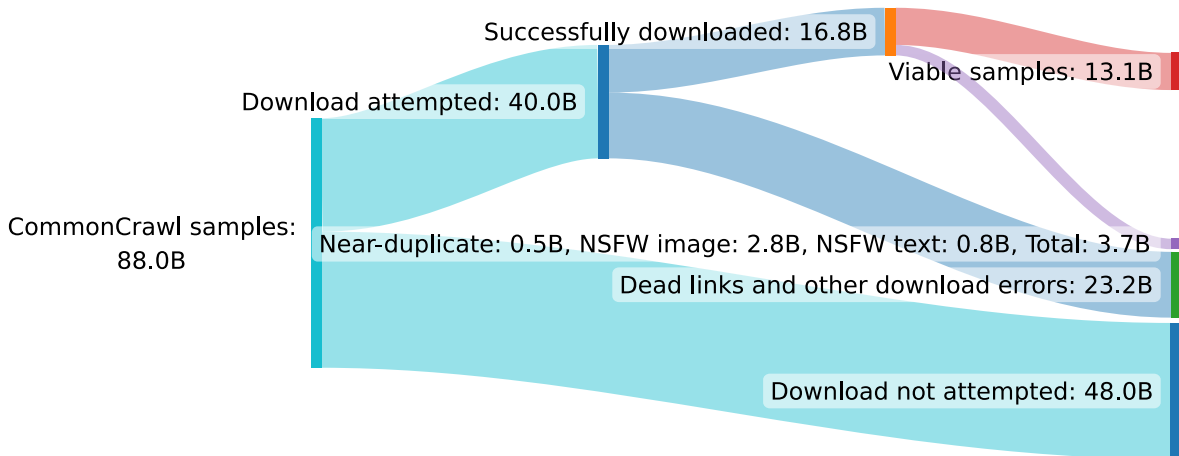


Figure 2: Data funnel going from potential samples found in Common Crawl to the 13.1B image-text pairs that were suitable for COMMONPOOL. We sampled uniformly 12.8B datapoints for the `xlarge` COMMONPOOL.

images for their filtering algorithms. For BYOD, we like-wise allow the use of training sets, but lift the restriction that COMMONPOOL must be used.

3.2 COMMONPOOL generation

We construct COMMONPOOL, a large-scale dataset of image-text pairs sourced from Common Crawl.¹ Our pool construction pipeline has four major steps: URL extraction and data download, NSFW detection, evaluation test set deduplication, and face blurring. We additionally provide metadata (e.g., CLIP features) for each sample in the pool. Starting from the `xlarge` COMMONPOOL, we take successive random subsets to create `large`, `medium`, and `small` COMMONPOOL (e.g., `medium` is a subset of `large`). An overview of the effect of each step in our pool generation pipeline is shown in Figure 2.

Extracting urls and downloading data. We first use Apache Spark [143] to extract image urls with nonempty alt-text from all Common Crawl dumps from 2014 to 2022. We deduplicate the resulting set of image url, alt-text pairs and conduct a global shuffle, which results in ~ 88 B possible samples. Not all samples are downloadable due to dead links; other samples are not suitable for inclusion in COMMONPOOL due to NSFW content or overlap with our evaluation sets. Hence, we attempt to download ~ 40 B samples using `img2dataset`² resulting in ~ 16.8 B successfully downloaded image-text pairs. For details, see Appendix D.

NSFW preprocessing. Since Common Crawl is a snapshot of the internet, we require strict preprocessing to remove unsafe content. We first use Detoxify [53] to prune samples that contain unsafe text (e.g., obscene, sexually explicit, or threatening language). We also employ an image classifier to discard explicit visual content. To do so, we train a classifier on CLIP ViT-L/14 [102] features, using the NSFW dataset used in LAION-5B [120]. We validate our classifier against the

¹<https://commoncrawl.org/>

²<https://github.com/rom1504/img2dataset/>

Google commercial image safety API. See Appendix E for details. Overall, $\sim 19\%$ of image-text pairs are considered NSFW, taking our pool of $\sim 16.8\text{B}$ downloads to $\sim 13.6\text{B}$ samples.

Evaluation set deduplication. To prevent accidental overfitting to certain test sets in our evaluation suite, we perform a thorough near-duplicate removal between the candidate pool and our evaluation sets, using a state-of-the-art image deduplication model [138]. Appendix F contains additional details. The model flags $\sim 3\%$ of the 16.8B images as near-duplicates, reducing the $\sim 13.6\text{B}$ pool to $\sim 13.1\text{B}$ samples. From here we select a random subset to get the `xlarge` pool of 12.8B samples.

Face detection & blurring. To protect the privacy of individuals, we detect and blur faces from images in our pool using a face detector [48]. As observed by Yang et al. [136], obfuscating faces has little impact on model performance, as we also observe in our experiments (Appendix G).

Pool metadata. Motivated by the LAION-400M data curation procedure, which employs similarity scores between CLIP image and text features, we compute additional metadata for each sample in COMMONPOOL. To bootstrap participants in their exploration of filtering algorithms, we provide image url, alt-text, original image width and height, CLIP image and text features, and CLIP image-text similarity scores. We also release a SHA256 hash of each image to guard against data poisoning in subsequent COMMONPOOL downloads [17]. For additional details see Appendix H. Metadata is meant to ease the computational burden on participants; however, we encourage exploring curation techniques that go beyond the provided metadata.

3.3 Bring your own data (BYOD)

While COMMONPOOL can be used to study different filtering techniques, state-of-the-art models are often trained on heterogeneous data pools from different sources. For instance, the Flamingo model [4] uses both curated data from multimodal massive web (M3W) and the ALIGN dataset [64]. To facilitate non-proprietary research on curating data from many sources, we instantiate a separate track in DATACOMP to allow participants to combine multiple data streams. For example, participants could construct a training set from CC12M [19], YFCC100M [129], and data sources they label themselves. In Section 4.2 and Appendix O.2 we describe our exploration of using other public datasets.

3.4 Training

We create a common experimental setting that enables controlled and comparable experiments by fixing the training procedure (i.e., model architecture, optimizer, loss, hyperparameters, etc.) and compute at each scale. We closely follow the training recipe used to train state-of-the-art CLIP models from Radford et al. [102], training models from scratch with a contrastive objective over images and captions. Given a set of image-caption pairs, we train an image encoder and a text encoder such that the similarity between the representations of images and their corresponding text is maximized relative to unaligned pairs.³

³More precisely, given a batch of data $\{(x_1, y_1), \dots, (x_B, y_B)\}$ with images x and captions y , we train the image encoder g and text encoder v with the loss $\ell = \frac{1}{2} \sum_{i=1}^B \frac{\sigma_{ii}}{\sum_{j=1}^B \sigma_{ij}} + \frac{1}{2} \sum_{i=1}^B \frac{\sigma_{ii}}{\sum_{j=1}^B \sigma_{ji}}$, where $\sigma_{ij} = \exp \langle g(x_i), h(y_j) \rangle$. We also use a learnable temperature parameter as in Radford et al. [102].

For each scale, we use a fixed model architecture and set of hyperparameters. We pick Vision Transformers (ViTs) [34] as the image encoder, considering the better scaling trends observed by Radford et al. [102] compared to ResNets [55]. The size of the model varies with the scale, using a ViT-B/32 for the `small` and `medium` scales, a ViT-B/16 for the `large` scale and ViT-L/14 for the `xlarge` scale. Models are trained for a fixed number of steps determined by the scale (Table 2), using the OpenCLIP repository [61]. We closely follow the training procedure from Radford et al. [102], using the Adam optimizer [72] with decoupled weight decay [85] on all weights except gains or biases with $\beta_1 = 0.9$, $\beta_2 = 0.98$ and weight decay of 0.2. For the `xlarge` scale, we use $\beta_2 = 0.95$ to prevent instability. The models are trained with automatic mixed precision and a cosine annealing learning rate schedule [84]. For the `small` scale, our internal training runs took four hours on one A100 GPU, and for the `xlarge` scale, 81 hours on 512 GPUs. Additional details including other scale-specific hyperparameters are shown in Appendix M.

3.5 Evaluation

We evaluate on an extensive suite of 38 image classification and retrieval tasks. We also provide an in-depth analysis on two fairness-related datasets, detailed in Section 5 and Appendix P. Image classification datasets range from satellite imagery recognition to classifying metastatic tissues from histopathologic scans, including (with some overlap): 22 of the datasets evaluated in Radford et al. [102], 6 ImageNet distribution shifts, 11 datasets from the Visual Task Adaptation Benchmark (VTAB) [144], and 3 datasets from the WILDS benchmark [75, 118]. Retrieval datasets include the Flickr30k [139] and MSCOCO image and text retrieval datasets [21], as well as the WinoGAViL commonsense image-text associations task [12]. To aggregate results over all evaluation tasks, we average the preferred metric for each task. As discussed in Section 3.2, we remove all test set images from the pool we provide to avoid contamination.

DATAComp adopts a zero-shot evaluation protocol, which means models are tested without training on the evaluation tasks. This approach is computationally efficient and measures a model’s ability to perform well without any additional training, in contrast to methods such as linear probing or end-to-end fine-tuning. As an additional validation step, we find a strong correlation (>0.99) between performance using a linear probe and that in a zero-shot setting, as seen in Appendix Figure 17. Additional details are in Appendix N.

4 Baselines

4.1 Filtering baselines

We study six simple filtering methods for the filtering track; see Appendix O.1 for further details.

No filtering. We simply use the entire pool as the subset, without any filtering. Since each pool size is equal to the sample budget, training consists of one pass over the data.

Random subsets. To isolate the effects of increasing the compute budget from increasing the dataset size, we form subsets consisting of 1%, 10%, 25%, 50% and 75% of the pool chosen at random.

Basic filtering. We consider a number of simple filtering operations inspired by Schuhmann et al. [119] and Byeon et al. [15]: filtering by *language* (only English captions, using either fasttext [68] or

cld3 [1]); filtering by *caption length* (over two words and 5 characters); and filtering by *image size* (smaller dimension above 200 pixels and aspect ratio below 3). We also experiment with combining the first two methods (language + caption length) and all three (language + caption length + image size). Unless otherwise specified, “basic” refers to filtering by fasttext language, caption length, and image size.

CLIP score and LAION filtering. We experiment with the main filtering strategy employed by LAION, where we take only examples where the cosine similarity score between CLIP image and text embeddings exceeds a pre-defined threshold. We investigate a range of thresholds and two OpenAI CLIP models for computing the scores: the ViT-B/32 model (as in LAION) and the ViT-L/14. Furthermore, we combine CLIP score thresholds and English filtering using cld3 in order to reproduce the LAION-2B filtering scheme. Table 14 in Appendix O.1 summarizes the different CLIP score threshold configurations.

Text-based filtering. We select examples that contain text overlapping with ImageNet class names, which serves as a proxy for relevance to downstream tasks. Specifically, we select English captions (according to fasttext) that contain words from synsets corresponding to classes in ImageNet-21K or ImageNet-1K [32].

Image-based filtering. We select a subset of examples whose visual content overlaps with ImageNet classes. After applying language (fasttext) and caption length filtering on the data, we cluster the image embeddings extracted from the OpenAI ViT-L/14 model of the candidate pool into 100K groups using Faiss [66]. We then find the nearest neighbor cluster center for every ImageNet training example, and keep examples whose corresponding cluster center is a nearest neighbor to at least one ImageNet image. We apply this procedure using either ImageNet-21K (14M images) or ImageNet-1K (1.2M images), forming two subsets.

4.2 BYOD baselines

We experiment with multiple external data sources, including four moderately sized datasets (10 to 58M samples) studied by Nguyen et al. [93]—CC12M [19], YFCC15M [129, 102], RedCaps [33] and Shutterstock [93]—and the larger LAION-2B [120]. Additional experiments, along with more details about the data sources are provided in Appendix O.2. We consider these data sources as they are and do not perform additional preprocessing. We also present experiments combining some of the data sources (using only the external datasets, or in addition to data from our pool).

5 Results and discussion

5.1 Building better datasets

Main results. Our key results are in Table 3. Most notably, the intersection between image-based filtering and CLIP score filtering taking the top 30% examples with highest scores using a ViT-L/14 model excels on most tasks. The exception is for the `small` scale and the retrieval datasets, where other filtering approaches perform better.⁴ Furthermore, other filtering strategies like basic, CLIP score, image-based, text-based filtering show better downstream performance when compared to

⁴Cherti et al. [23] also observe that models rank differently on classification and retrieval tasks.

Table 3: Zero-shot performance for select baselines in the *filtering* track. On all scales, various filtering strategies lead to better performance than using the entire pool without filtering. The intersection between imaged-based and CLIP score strategies performs well on most tasks and scales. For all metrics, higher is better (see Appendix N for details). \cap denotes the intersection between filtering strategies.

Scale	Filtering strategy	Dataset size	Samples seen	ImageNet	ImageNet dist. shifts	VTAB	Retrieval	Average over 38 datasets
small	No filtering	12.8M	12.8M	0.025	0.033	0.145	0.105	0.132
	Basic filtering	3M	12.8M	0.030	0.040	0.149	0.111	0.137
	Text-based	3.2M	12.8M	0.046	0.052	0.169	<u>0.112</u>	0.156
	Image-based	3M	12.8M	0.043	0.047	0.178	<u>0.112</u>	0.158
	LAION-2B filtering	1.3M	12.8M	0.031	0.040	0.136	0.085	0.133
	CLIP score (L/14 30%)	3.8M	12.8M	<u>0.051</u>	<u>0.055</u>	<u>0.190</u>	0.108	<u>0.172</u>
	Image-based \cap CLIP score (L/14 30%)	1.4M	12.8M	0.039	0.045	0.162	0.089	0.144
medium	No filtering	128M	128M	0.176	0.152	0.259	0.174	0.254
	Basic filtering	30M	128M	0.226	0.193	0.284	0.192	0.280
	Text-based	31M	128M	0.255	0.215	0.328	0.183	0.301
	Image-based	29M	128M	0.268	0.213	0.319	<u>0.193</u>	0.307
	LAION-2B filtering	13M	128M	0.230	0.198	0.307	0.170	0.287
	CLIP score (L/14 30%)	38M	128M	0.273	0.230	0.338	0.183	<u>0.323</u>
	Image-based \cap CLIP score (L/14 30%)	14M	128M	<u>0.297</u>	<u>0.239</u>	<u>0.346</u>	0.170	<u>0.323</u>
large	No filtering	1.28B	1.28B	0.459	0.378	0.426	0.305	0.428
	Basic filtering	298M	1.28B	0.516	0.423	0.446	0.353	0.448
	Text-based	317M	1.28B	0.561	0.465	0.465	0.352	0.466
	Image-based	293M	1.28B	0.572	0.454	0.483	0.353	0.471
	LAION-2B filtering	130M	1.28B	0.553	0.453	0.510	0.365	0.491
	CLIP score (L/14 30%)	384M	1.28B	0.578	0.474	0.538	0.342	0.520
	Image-based \cap CLIP score (L/14 30%)	140M	1.28B	<u>0.631</u>	<u>0.508</u>	<u>0.546</u>	<u>0.369</u>	<u>0.527</u>
xlarge	No filtering	12.8B	12.8B	0.723	0.612	0.611	0.441	0.611
	LAION-2B filtering	1.3B	12.8B	0.755	0.637	0.624	<u>0.503</u>	0.627
	CLIP score (L/14 30%)	3.8B	12.8B	0.764	0.655	0.643	0.468	0.641
	Image-based \cap CLIP score (L/14 30%)	1.4B	12.8B	<u>0.792</u>	<u>0.679</u>	<u>0.652</u>	0.489	<u>0.653</u>

no filtering. While Table 3 shows a summary of our key results, we present a much larger suite of experiments in Appendix Q.

DATAComp leads to better image-text datasets. We hope DATAComp catalyzes the search for the next generation of multimodal datasets. Towards this end, we contribute DATAComp-1B, which is a direct result of the DATAComp benchmark workflow. DATAComp-1B is the output from the Image-based \cap CLIP score (L/14 30%) baseline filter at the xlarge scale of the filtering track. Our dataset is comprised of 1.4B samples, which is *smaller* than the LAION-2B dataset with 2.3B samples. Additionally, DATAComp-1B is built from a smaller pool than the one used to create LAION-2B, which means direct comparisons are likely skewed in favor of LAION-2B. Nevertheless, a CLIP L/14 trained on DATAComp-1B outperforms the LAION-2B competitor by 6.1 percentage points on ImageNet as seen in Table 1. Moreover, training on DATAComp-1B improves ImageNet accuracy by 3.7 percentage points over OpenAI’s ViT-L/14 trained with the same compute budget. These results underscore the impact that DATAComp can make and provide a promising foundation upon which participants can build.

External data sources can improve performance. Table 4 shows results for several baselines in the BYOD track. Compared to the best baselines in the filtering track, training on each external

Table 4: Zero-shot performance for select baselines in the BYOD track. External data sources can be effective in isolation or in combination with CommonPool. Moreover, upsampling external curated sources can improve performance.

Scale	Data source	Dataset size	Samples seen	ImageNet	ImageNet dist. shifts	VTAB	Retrieval	Average over 38 datasets
medium	CC12M	10M	128M	0.245	0.189	0.283	0.206	0.266
	YFCC15M	15M	128M	0.232	0.137	0.263	0.174	0.251
	RedCaps	11M	128M	0.237	0.166	0.271	0.150	0.261
	Shutterstock	58M	128M	0.342	0.209	0.364	<u>0.248</u>	0.323
	4 external sources	109M	128M	<u>0.378</u>	0.262	0.392	0.210	0.348
	COMMONPOOL, CLIP score filter	38M	128M	0.273	0.230	0.338	0.183	0.323
	+ 4 external sources	147M	128M	0.372	<u>0.269</u>	<u>0.401</u>	0.203	<u>0.357</u>
large	LAION-2B	2.3B	1.28B	0.585	0.472	0.504	<u>0.399</u>	0.505
	COMMONPOOL, CLIP score filter	0.4B	1.28B	0.578	0.474	0.538	0.342	0.520
	+ 4 external sources	0.5B	1.28B	0.609	0.508	0.546	0.303	0.525
	+ 4 external sources (upsampled 2x)	0.5B	1.28B	<u>0.621</u>	<u>0.509</u>	<u>0.547</u>	0.315	<u>0.530</u>
xlarge	LAION-2B	2.3B	12.8B	0.757	0.631	0.611	<u>0.502</u>	0.612
	COMMONPOOL, CLIP score filter	3.8B	12.8B	0.764	0.655	<u>0.643</u>	0.468	<u>0.641</u>
	+ 4 external sources (upsampled 6x)	3.9B	12.8B	<u>0.776</u>	<u>0.671</u>	0.633	0.410	0.638

data source separately for the `medium` scale performs worse, but using all four sources together significantly improves accuracy, especially on ImageNet. At the `large` scale, combining CLIP-filtered data from the filtering track with external data from the four sources further boosts ImageNet accuracy by up to 4.3 percentage points. This approach also surpasses using LAION-2B. In Appendix O.2 we further examine the external data sources and show additional experiments.

English filtering is helpful but not necessary. Given that the prompts used in downstream tasks are in English, a natural question is how critical is English filtering for achieving good performance. We try filtering our pool by removing non-English captions, with both `clد3` and `fasttext` as language detectors. Although the two vastly differ in percentage of English captions detected (20% and 50% respectively), filtering with both of them results in similar performances at all scales. For basic filtering, English filtering is a key component in our best performing baselines (see Appendix Q). On the other hand, English filtering is not necessary to achieve good performance. When using English filtering in combination with CLIP score filtering, performance stays the same or decreases at all scales. Figure 24 in the appendix suggests that CLIP score filtering implicitly does some English filtering, which may be a result of the CLIP models being trained on English filtered data [102].

Trade-off between data diversity and repetition. When we have large pools of data, is it useful to see samples more than once during training? In Figure 3, we show that randomly selecting subsets of the pool typically has little effect or degrades performance; when only small fractions are used, performance drops substantially. In contrast, when filtering with CLIP scores, the optimal training set comes from selecting $\sim 30\%$ of the pool with the highest scores. The difference in performance between filtering with CLIP scores and using random subsets while using the same number of training samples again highlights the importance of different strategies for selecting samples.

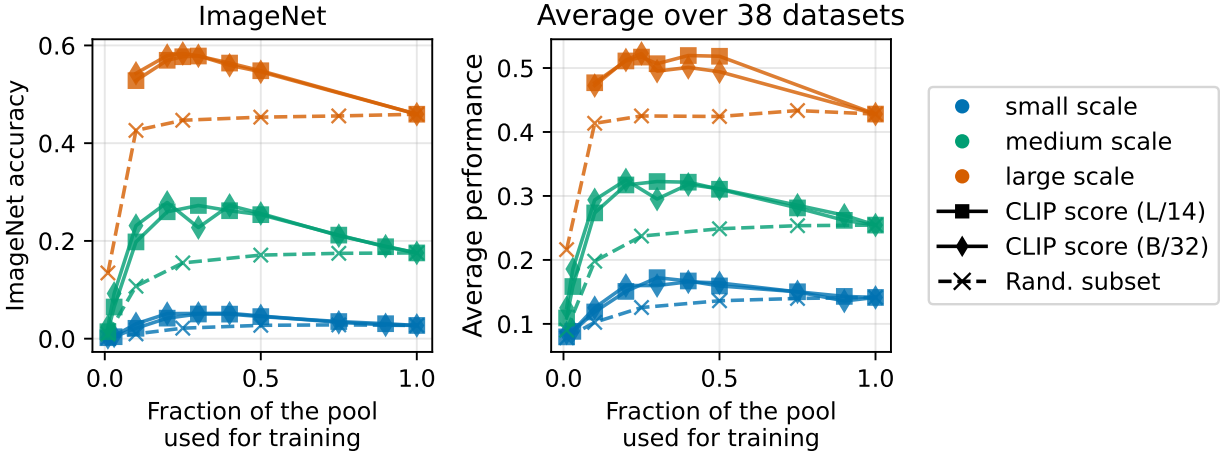


Figure 3: Performance of random subsets (dotted line) and CLIP score filtering (solid line) when varying the subset size. When taking random subsets larger subsets are always better, but other filtering functions such as CLIP score perform best with subsets of intermediate size.

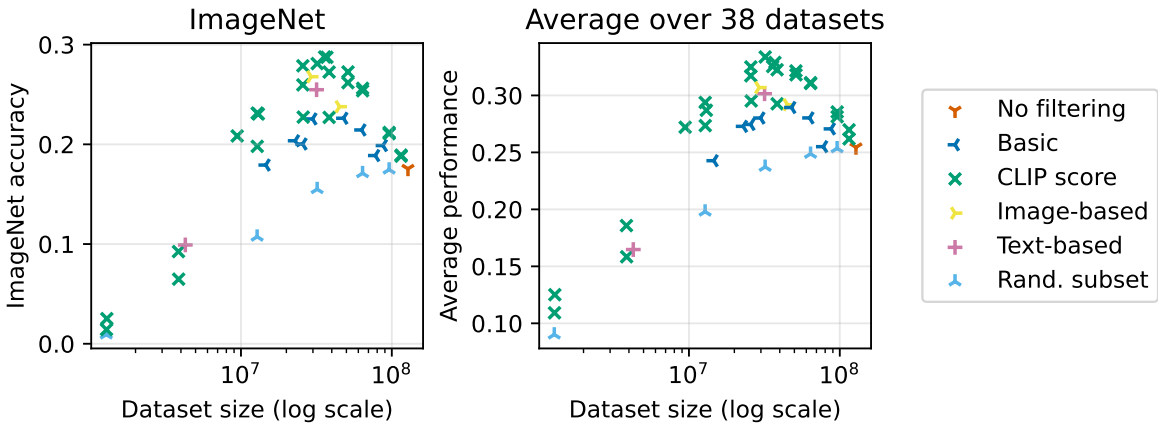


Figure 4: Performance as a function of the number of training samples from the `medium` scale. There is a significant variance in accuracy even when accounting for the size of the training set, suggesting that size is not the only determining factor of the quality of a dataset. Results for additional scales are shown in Appendix Figure 23.

5.2 DATACOMP design analyses

COMMONPOOL and LAION are comparable with the same filtering. To validate our pool construction, we show that we can build datasets comparable to LAION-2B by employing their filtering technique on our pool. LAION-2B selects all samples where the caption is in English and the cosine similarity score from a trained ViT-B/32 CLIP model is above 0.28. We compare this filtering approach on our pool using the same number samples, 130M samples at the `large` scale. Our experiments show that the different data sources perform comparably when using the same filtering strategy: 55.3% vs 55.7% accuracy on ImageNet, and 0.491 vs 0.479 average performance

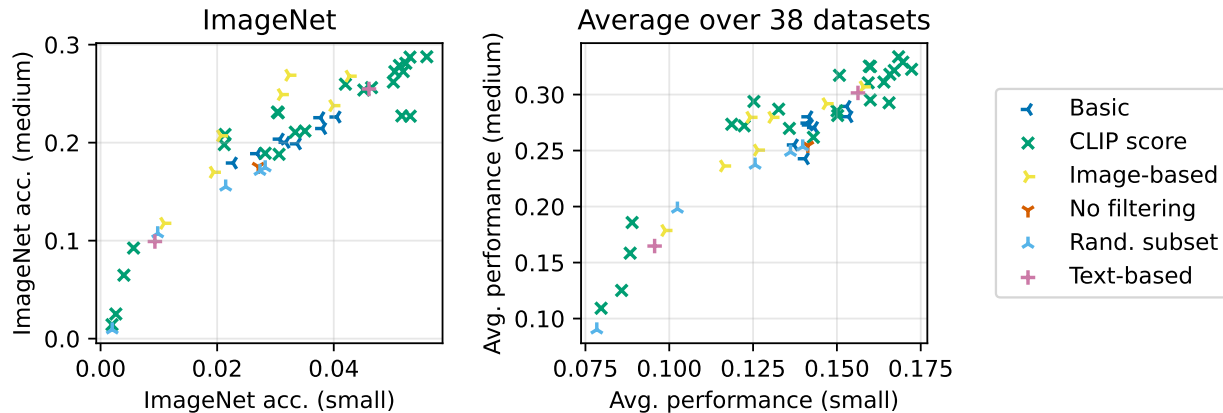


Figure 5: Correlation between performance at `small` and `medium` scales for various filtering strategies. The trends suggest that experiments at smaller scales can serve as useful guides for larger scales. Results for additional scales are shown in Appendix Figure 22.

over our evaluation sets using our pool and LAION-2B, respectively.

Training set size alone does not explain performance. We find a significant variation in accuracy even when accounting for the size of the filtered training set at a given scale. As shown in Figure 4, different choices of filtering can substantially impact performance, even when the size of the resulting dataset is comparable and the scale is fixed. For example, `cld3` English filtering and CLIP score top 20% are almost the same size, yet the CLIP score approach performs substantially better at all scales.

Consistency across scales. We find that the ranking between filtering strategies is typically consistent across different scales. This is illustrated in Figure 5, which shows that the baselines at `small` and `medium` scales are positively correlated. Moreover, as shown in Table 20 in the appendix, the rank correlations of performance is high, between 0.74 and 0.90 for different scale pairs.

Consistency across training hyperparameters. One potential concern is that modifying training hyperparameters changes the relative ordering of different data curation methods in terms of downstream performance. To test this, we examine the effect of increasing the number of training steps in `small` filtering track baselines by $10\times$. We find a rank correlation of 0.71 on zero-shot average performance. Though varying training hyperparameters can change the optimal filtering method, these initial experiments suggest that the ordering is relatively stable. For more information see Appendix L.

5.3 Evaluation trends

ImageNet accuracy is indicative, but not the complete picture. Similarly to Kornblith et al. [76], in Appendix Figure 25 we find that ImageNet performance is highly correlated with the average performance across all datasets we study, with an overall correlation of 0.99 using the full evaluation suite.⁵ However, ImageNet performance is not representative of all evaluation tasks,

⁵Note that unlike Kornblith et al. [76] we evaluate zero-shot performance rather than transfer learning.

as the correlation between ImageNet accuracy and accuracy on other individual datasets varies substantially, in some cases even exhibiting a negative correlation, as discussed in Appendix Q.

Robustness and fairness. While typical models trained on a target task suffer large performance drops under data distribution shift, zero-shot CLIP models exhibit consistently strong performance across a wide range of distributions [102]. In Appendix Figure 26, we show that models trained with data from our pool are more robust to distribution shift than ImageNet-trained models trained to the same ImageNet accuracy from Taori et al. [128]’s testbed. Examining geographic diversity, we find that our models are better than ImageNet-trained models, but fall short of models fine-tuned on diverse curated datasets (see Appendix Figure 21). We also perform a face classification analysis and identify demographic biases in our models: notably, introducing the BYOD datasets we consider can increase the risk of misclassification. Full details of our fairness and diversity analyses are presented in Appendix P.

6 Conclusion and future work

We introduce DATACOMP, a new benchmark for curating image-text datasets. DATACOMP allows for controlled experiments in dataset creation, enabling a similar paradigm as that seen in model development. Our benchmark supports experiments both augmenting our candidate pool with examples from new data sources, or coming up with new filtering approaches. In either case, our infrastructure makes experimenting with data curation ideas far simpler than creating an entire large dataset from scratch, and also provides a controlled environment that allows rigorous empirical experimentation. We believe that such an approach to dataset development will accelerate progress in machine learning because key datasets such as ImageNet or LAION-2B are currently rarely updated (if at all), while researchers develop many generations of new models on the same dataset.

In its current form, DATACOMP is a first step towards improving training datasets. We see several interesting directions for future work, including:

Curating more data sources. COMMONPOOL and LAION-2B only draw text annotations from `alt-text` in the `HTML img` tags. Parsing websites more intelligently will likely unlock higher quality text annotations. In addition, identifying further data repositories and conducting broader or more targeted web crawls will hopefully yield better training data. Beyond real data, synthetic data from generative models or physics-based rendering are also promising directions.

Improved data filtering. So far we only experimented with basic filtering techniques in our baselines. We expect that better text processing, using alternative multimodal models as features, or other clustering approaches will result in better filtering methods for multimodal dataset design.

Further supervision signals. COMMONPOOL relies entirely on the original captions from Common Crawl. Running image captioning models on the collected images may offer an alternative supervision signal and make it possible to train on images that do not come with a text annotation. In addition, bounding boxes for object detection or segmentation masks could be further useful information to incorporate into the training set.

More modalities. Beyond image-text pairs, contemporary machine learning relies on many additional forms of large pre-training datasets. Natural candidates for benchmarks similar to DATACOMP are text, video, structured documents, 3D objects, or graph-structured data. Moreover,

as researchers build foundation models for specific scientific domains such as remote sensing, understanding data curation in specialized domains is also an important direction for future work.

Broader evaluations. Beyond our evaluation suite, researchers could investigate additional domains and tasks such as image generation, visual question answering, captioning and embodied tasks such as vision-and-language navigation. Moreover, our evaluation suite could be expanded beyond English to include multilingual tasks.

Extended scaling trends. While medium-scale experiments in DATACOMP usually predict performance at larger scales well, there are also phenomena that still appear puzzling. For instance, the 12.8M scale does not always predict the larger scales accurately, and the gains from our current BYOD experiments shrink with increased scale. Reliably extrapolating these performance changes across compute and data scales would assist future dataset design. And ideally, experiments on ever smaller scales than 12.8M would yield useful signal. Finally, it would be important to better characterize how data curation methods compare under different choices for model size and compute budget.

Combining data sources. While combining different data sources often leads to better performance than any individual source, in many cases the combination is worse than simply using the best source. Even when combining multiple data sources is productive, there is still the question of whether and by how much to upsample each source, which has a direct impact on performance. While we present related initial experiments in the BYOD track, a more complete understanding of the optimal way to combine data sources is an exciting research direction for future work.

Acknowledgements

SYG and JH are supported by NSF Graduate Research Fellowships. GS is supported by the Onassis Foundation - Scholarship ID: F ZS 056-1/2022-2023. GD has been supported by the Onassis Fellowship (Scholarship ID: F ZS 012-1/2022-2023), the Bodossaki Fellowship and the Leventis Fellowship. This research has been supported by NSF Grants AF 1901292, CNS 2148141, DMS 2134012, TRIPODS II-DMS 2023166, Tripods CCF 1934932, IFML CCF 2019844 and research gifts by Western Digital, WNCG IAP, UT Austin Machine Learning Lab (MLL), Cisco, the Len Blavatnik and the Blavatnik Family Foundation, the Stanly P. Finch Centennial Professorship in Engineering, Open Philanthropy, Google, Microsoft, and the Allen Institute for AI.

We thank Stability AI and the Gauss Centre for Supercomputing e.V.⁶ for providing us with compute resources to train models. We are thankful for the compute time provided through the John von Neumann Institute for Computing (NIC) on the GCS Supercomputer JUWELS Booster [69] at Jülich Supercomputing Centre (JSC), and for storage resources on JUST [45] granted and operated by JSC, as well as computing and storage resources from the Helmholtz Data Federation (HDF).

We would like to thank Amro Abbas, Jessie Chapman, Brian Cheung, Joshua Gardner, Nancy Garland, Sachin Goyal, Huy Ha, Zaid Harchaoui, Andy Jones, Adam Klivans, Ronak Mehta, Ari Morcos, Raviteja Mullapudi, Jonathon Shlens, Brandon McKinzie, Alexander Toshev, David Grangier, Navdeep Jaitly, Kentrell Owens, Marco Tulio Ribeiro, Shiori Sagawa, Christoph Schuhmann, Matthew Wallingford, and Ross Wightman for helpful feedback at various stages of the project.

⁶<https://gauss-centre.eu>

We are particularly grateful to Daniel Levy and Alec Radford for early encouragement to pursue this project and feedback on the experimental design.

References

- [1] CLD3. <https://github.com/google/cld3>.
- [2] Amro Abbas, Kushal Tirumala, Dániel Simig, Surya Ganguli, and Ari S Morcos. Semdedup: Data-efficient learning at web-scale through semantic deduplication, 2023. <https://arxiv.org/abs/2303.09540>.
- [3] Pankaj K. Agarwal, Sariel Har-Peled, and Kasturi R. Varadarajan. Approximating extent measures of points. *Journal of the ACM (JACM)*, 2004. <https://doi.org/10.1145/1008731.1008736>.
- [4] Jean-Baptiste Alayrac, Jeff Donahue, Pauline Luc, Antoine Miech, Iain Barr, Yana Hasson, Karel Lenc, Arthur Mensch, Katie Millican, Malcolm Reynolds, et al. Flamingo: a visual language model for few-shot learning. In *Advances in Neural Information Processing Systems (NeurIPS)*, 2022. <https://openreview.net/forum?id=EbMuimAbPbs>.
- [5] Abhijeet Awasthi, Sabyasachi Ghosh, Rasna Goyal, and Sunita Sarawagi. Learning from rules generalizing labeled exemplars. In *International Conference on Learning Representations (ICLR)*, 2020. <https://openreview.net/forum?id=SkeuexBtDr>.
- [6] Stephen H Bach, Daniel Rodriguez, Yintao Liu, Chong Luo, Haidong Shao, Cassandra Xia, Souvik Sen, Alex Ratner, Braden Hancock, Houman Alborzi, Rahul Kuchhal, Christopher Ré, and Rob Malkin. Snorkel drybell: A case study in deploying weak supervision at industrial scale. In *Special Interest Group on Management of Data (SIGMOD)*, 2019. <https://arxiv.org/abs/1812.00417>.
- [7] Olivier Bachem, Mario Lucic, and Andreas Krause. Coresets for nonparametric estimation - the case of dp-means. In *International Conference on Machine Learning (ICML)*, 2015. <https://proceedings.mlr.press/v37/bachem15.html>.
- [8] Peter Bandi, Oscar Geessink, Quirine Manson, Marcory Van Dijk, Maschenka Balkenhol, Meyke Hermesen, Babak Ehteshami Bejnordi, Byungjae Lee, Kyunghyun Paeng, Aoxiao Zhong, et al. From detection of individual metastases to classification of lymph node status at the patient level: the camelyon17 challenge. *IEEE Transactions on Medical Imaging*, 2018. <https://pubmed.ncbi.nlm.nih.gov/30716025/>.
- [9] Andrei Barbu, David Mayo, Julian Alverio, William Luo, Christopher Wang, Dan Gutfreund, Josh Tenenbaum, and Boris Katz. Objectnet: A large-scale bias-controlled dataset for pushing the limits of object recognition models. In H. Wallach, H. Larochelle, A. Beygelzimer, F. d'Alché-Buc, E. Fox, and R. Garnett (eds.), *Advances in Neural Information Processing Systems (NeurIPS)*, volume 32. Curran Associates, Inc., 2019. <https://proceedings.neurips.cc/paper/2019/file/97af07a14cacba681feacf3012730892-Paper.pdf>.
- [10] Sara Beery, Elijah Cole, and Arvi Gjoka. The iwildcam 2020 competition dataset, 2020. <https://arxiv.org/abs/2004.10340>.
- [11] Vighnesh Birodkar, Hossein Mobahi, and Samy Bengio. Semantic redundancies in image-classification datasets: The 10% you don't need. *arXiv preprint arXiv:1901.11409*, 2019. <https://arxiv.org/abs/1901.11409>.

- [12] Yonatan Bitton, Nitzan Bitton Guetta, Ron Yosef, Yuval Elovici, Mohit Bansal, Gabriel Stanovsky, and Roy Schwartz. WinoGAViL: Gamified association benchmark to challenge vision-and-language models, 2022. <https://arxiv.org/abs/2207.12576>.
- [13] Lukas Bossard, Matthieu Guillaumin, and Luc Van Gool. Food-101—mining discriminative components with random forests. In *European Conference on Computer Vision (ECCV)*, 2014. https://link.springer.com/chapter/10.1007/978-3-319-10599-4_29.
- [14] Tom Brown, Benjamin Mann, Nick Ryder, Melanie Subbiah, Jared D Kaplan, Prafulla Dhariwal, Arvind Neelakantan, Pranav Shyam, Girish Sastry, Amanda Askell, Sandhini Agarwal, Ariel Herbert-Voss, Gretchen Krueger, Tom Henighan, Rewon Child, Aditya Ramesh, Daniel Ziegler, Jeffrey Wu, Clemens Winter, Chris Hesse, Mark Chen, Eric Sigler, Mateusz Litwin, Scott Gray, Benjamin Chess, Jack Clark, Christopher Berner, Sam McCandlish, Alec Radford, Ilya Sutskever, and Dario Amodei. Language models are few-shot learners. In H. Larochelle, M. Ranzato, R. Hadsell, M.F. Balcan, and H. Lin (eds.), *Advances in Neural Information Processing Systems (NeurIPS)*, 2020. https://proceedings.neurips.cc/paper_files/paper/2020/file/1457c0d6bfc4967418bfb8ac142f64a-Paper.pdf.
- [15] Minwoo Byeon, Beomhee Park, Haecheon Kim, Sungjun Lee, Woonhyuk Baek, and Saehoon Kim. Coyo-700m: Image-text pair dataset. <https://github.com/kakaobrain/coyo-dataset>, 2022.
- [16] Ethan Caballero, Kshitij Gupta, Irina Rish, and David Krueger. Broken neural scaling laws. *International Conference on Learning Representations (ICLR)*, 2023. <https://arxiv.org/abs/2210.14891>.
- [17] Nicholas Carlini, Matthew Jagielski, Christopher A Choquette-Choo, Daniel Paleka, Will Pearce, Hyrum Anderson, Andreas Terzis, Kurt Thomas, and Florian Tramèr. Poisoning web-scale training datasets is practical, 2023. <https://arxiv.org/abs/2302.10149>.
- [18] Stephanie C. Y. Chan, Adam Santoro, Andrew K. Lampinen, Jane X. Wang, Aaditya Singh, Pierre H. Richemond, Jay McClelland, and Felix Hill. Data distributional properties drive emergent in-context learning in transformers. In *Advances in Neural Information Processing Systems (NeurIPS)*, 2022. <https://arxiv.org/abs/2205.05055>.
- [19] Soravit Changpinyo, Piyush Sharma, Nan Ding, and Radu Soricut. Conceptual 12m: Pushing web-scale image-text pre-training to recognize long-tail visual concepts. In *Conference on Computer Vision and Pattern Recognition (CVPR)*, 2021. <https://arxiv.org/abs/2102.08981>.
- [20] Xi Chen, Xiao Wang, Soravit Changpinyo, AJ Piergiovanni, Piotr Padlewski, Daniel Salz, Sebastian Goodman, Adam Grycner, Basil Mustafa, Lucas Beyer, Alexander Kolesnikov, Joan Puigcerver, Nan Ding, Keran Rong, Hassan Akbari, Gaurav Mishra, Linting Xue, Ashish Thapliyal, James Bradbury, Weicheng Kuo, Mojtaba Seyedhosseini, Chao Jia, Burcu Karagol Ayan, Carlos Riquelme, Andreas Steiner, Anelia Angelova, Xiaohua Zhai, Neil Houlsby, and Radu Soricut. Pali: A jointly-scaled multilingual language-image model. In *International Conference on Learning Representations (ICLR)*, 2022. <https://arxiv.org/abs/2209.06794>.
- [21] Xinlei Chen, Hao Fang, Tsung-Yi Lin, Ramakrishna Vedantam, Saurabh Gupta, Piotr Dollár,

- and C Lawrence Zitnick. Microsoft COCO captions: Data collection and evaluation server, 2015. <https://arxiv.org/abs/1504.00325>.
- [22] Gong Cheng, Junwei Han, and Xiaoqiang Lu. Remote sensing image scene classification: Benchmark and state of the art. *Proceedings of the Institute of Electrical and Electronics Engineers (IEEE)*, 2017. <https://ieeexplore.ieee.org/abstract/document/7891544>.
- [23] Mehdi Cherti, Romain Beaumont, Ross Wightman, Mitchell Wortsman, Gabriel Ilharco, Cade Gordon, Christoph Schuhmann, Ludwig Schmidt, and Jenia Jitsev. Reproducible scaling laws for contrastive language-image learning, 2022. <https://arxiv.org/abs/2212.07143>.
- [24] Gordon Christie, Neil Fendley, James Wilson, and Ryan Mukherjee. Functional map of the world. In *Conference on Computer Vision and Pattern Recognition (CVPR)*, 2018. <https://arxiv.org/abs/1711.07846>.
- [25] Mircea Cimpoi, Subhransu Maji, Iasonas Kokkinos, Sammy Mohamed, and Andrea Vedaldi. Describing textures in the wild. In *Conference on Computer Vision and Pattern Recognition (CVPR)*, 2014. https://openaccess.thecvf.com/content_cvpr_2014/html/Cimpoi_Describing_Textures_in_2014_CVPR_paper.html.
- [26] Adam Coates, Andrew Ng, and Honglak Lee. An analysis of single-layer networks in unsupervised feature learning. In *International Conference on Artificial Intelligence and Statistics (AISTATS)*, 2011. <https://proceedings.mlr.press/v15/coates11a.html>.
- [27] Michael B. Cohen, Cameron Musco, and Christopher Musco. Input sparsity time low-rank approximation via ridge leverage score sampling. In *ACM-SIAM Symposium on Discrete Algorithms*, 2017. <https://dl.acm.org/doi/10.5555/3039686.3039801>.
- [28] C Coleman, C Yeh, S Mussmann, B Mirzasoleiman, P Bailis, P Liang, J Leskovec, and M Zaharia. Selection via proxy: Efficient data selection for deep learning. In *International Conference on Learning Representations (ICLR)*, 2020. <https://arxiv.org/abs/1906.11829>.
- [29] Alexis Conneau, Kartikay Khandelwal, Naman Goyal, Vishrav Chaudhary, Guillaume Wenzek, Francisco Guzmán, Edouard Grave, Myle Ott, Luke Zettlemoyer, and Veselin Stoyanov. Unsupervised cross-lingual representation learning at scale. In *Annual Meeting of the Association for Computational Linguistics (ACL)*, 2019. <https://arxiv.org/abs/1911.02116>.
- [30] R Dennis Cook. Detection of influential observation in linear. *Technometrics*, 19(1):15–18, 1977.
- [31] Achal Dave, Tarasha Khurana, Pavel Tokmakov, Cordelia Schmid, and Deva Ramanan. Tao: A large-scale benchmark for tracking any object. In *European Conference on Computer Vision (ECCV)*, 2020. <https://arxiv.org/abs/2005.10356>.
- [32] Jia Deng, Wei Dong, Richard Socher, Li-Jia Li, Kai Li, and Li Fei-Fei. Imagenet: A large-scale hierarchical image database. In *Conference on Computer Vision and Pattern Recognition (CVPR)*, 2009. <https://ieeexplore.ieee.org/abstract/document/5206848>.
- [33] Karan Desai, Gaurav Kaul, Zubin Aysola, and Justin Johnson. Redcaps: Web-curated image-text data created by the people, for the people, 2021. <https://arxiv.org/abs/2111.11431>.

- [34] Alexey Dosovitskiy, Lucas Beyer, Alexander Kolesnikov, Dirk Weissenborn, Xiaohua Zhai, Thomas Unterthiner, Mostafa Dehghani, Matthias Minderer, Georg Heigold, Sylvain Gelly, Jakob Uszkoreit, and Neil Houlsby. An image is worth 16x16 words: Transformers for image recognition at scale. In *International Conference on Learning Representations (ICLR)*, 2021. <https://openreview.net/forum?id=YicbFdNTTy>.
- [35] Matthijs Douze, Giorgos Tolias, Ed Pizzi, Zoë Papanikolaou, Lowik Chanussot, Filip Radenovic, Tomas Jenicek, Maxim Maximov, Laura Leal-Taixé, Ismail Elezi, Ondrej Chum, and Cristian Canton-Ferrer. The 2021 image similarity dataset and challenge, 2021. <https://arxiv.org/abs/2106.09672>.
- [36] Kawin Ethayarajh, Yejin Choi, and Swabha Swayamdipta. Understanding dataset difficulty with v-usable information. In *International Conference on Machine Learning (ICML)*, 2022. <https://arxiv.org/abs/2110.08420>.
- [37] M. Everingham, L. Van Gool, C. K. I. Williams, J. Winn, and A. Zisserman. The PASCAL Visual Object Classes Challenge 2007 (VOC2007) Results, 2007. <http://www.pascal-network.org/challenges/VOC/voc2007/workshop/index.html>.
- [38] Sabri Eyuboglu, Bojan Karlaš, Christopher Ré, Ce Zhang, and James Zou. dcbench: a benchmark for data-centric ai systems. In *Proceedings of the Sixth Workshop on Data Management for End-To-End Machine Learning*, 2022. <https://dl.acm.org/doi/abs/10.1145/3533028.3533310>.
- [39] Alex Fang, Gabriel Ilharco, Mitchell Wortsman, Yuhao Wan, Vaishaal Shankar, Achal Dave, and Ludwig Schmidt. Data determines distributional robustness in contrastive language image pre-training (clip). In *International Conference on Machine Learning (ICML)*, 2022. <https://arxiv.org/abs/2205.01397>.
- [40] Li Fei-Fei, Rob Fergus, and Pietro Perona. Learning generative visual models from few training examples: An incremental Bayesian approach tested on 101 object categories. *Conference on Computer Vision and Pattern Recognition (CVPR) Workshop*, 2004. <https://ieeexplore.ieee.org/document/1384978>.
- [41] Dan Feldman, Matthew Faulkner, and Andreas Krause. Scalable training of mixture models via coresets. In *Advances in Neural Information Processing Systems (NeurIPS)*, 2011. https://proceedings.neurips.cc/paper_files/paper/2011/file/2b6d65b9a9445c4271ab9076ead5605a-Paper.pdf.
- [42] Daniel Y. Fu, Mayee F. Chen, Frederic Sala, Sarah M. Hooper, Kayvon Fatahalian, and Christopher Ré. Fast and three-rious: Speeding up weak supervision with triplet methods. In *International Conference on Machine Learning (ICML)*, 2020. <https://arxiv.org/abs/2002.11955>.
- [43] Andreas Geiger, Philip Lenz, and Raquel Urtasun. Are we ready for autonomous driving? the kitti vision benchmark suite. In *Conference on Computer Vision and Pattern Recognition (CVPR)*, 2012. <https://ieeexplore.ieee.org/abstract/document/6248074>.
- [44] Amirata Ghorbani and James Zou. Data shapley: Equitable valuation of data for machine learning. In *International Conference on Machine Learning*, pp. 2242–2251. PMLR, 2019.

- [45] Stephan Graf and Olaf Mextorf. Just: Large-scale multi-tier storage infrastructure at the jülich supercomputing centre. *Journal of large-scale research facilities JLSRF*, 7:180, 2021.
- [46] Chengcheng Guo, Bo Zhao, and Yanbing Bai. Deepcore: A comprehensive library for coresets selection in deep learning, 2022. <https://arxiv.org/abs/2204.08499>.
- [47] Han Guo, Nazneen Fatema Rajani, Peter Hase, Mohit Bansal, and Caiming Xiong. Fastif: Scalable influence functions for efficient model interpretation and debugging. *arXiv preprint arXiv:2012.15781*, 2020.
- [48] Jia Guo, Jiankang Deng, Alexandros Lattas, and Stefanos Zafeiriou. Sample and computation redistribution for efficient face detection. In *International Conference on Learning Representations (ICLR)*, 2021. <https://arxiv.org/abs/2105.04714>.
- [49] Suchin Gururangan, Swabha Swayamdipta, Omer Levy, Roy Schwartz, Samuel Bowman, and Noah A. Smith. Annotation artifacts in natural language inference data. In *Conference of the North American Chapter of the Association for Computational Linguistics (NAACL)*, 2018. <https://aclanthology.org/N18-2017>.
- [50] Kelvin Guu, Albert Webson, Ellie Pavlick, Lucas Dixon, Ian Tenney, and Tolga Bolukbasi. Simfluence: Modeling the influence of individual training examples by simulating training runs. *arXiv preprint arXiv:2303.08114*, 2023.
- [51] Frank R Hampel. The influence curve and its role in robust estimation. *Journal of the american statistical association*, 69(346):383–393, 1974.
- [52] Xiaochuang Han, Byron C Wallace, and Yulia Tsvetkov. Explaining black box predictions and unveiling data artifacts through influence functions. *arXiv preprint arXiv:2005.06676*, 2020.
- [53] Laura Hanu and Unitary team. Detoxify, 2020. <https://github.com/unitaryai/detoxify>.
- [54] Sariel Har-Peled and Soham Mazumdar. On coresets for k-means and k-median clustering. In *Symposium on Theory of Computing (STOC)*, 2004. <https://doi.org/10.1145/1007352.1007400>.
- [55] Kaiming He, Xiangyu Zhang, Shaoqing Ren, and Jian Sun. Deep residual learning for image recognition. In *Conference on Computer Vision and Pattern Recognition (CVPR)*, 2016. <https://arxiv.org/abs/1512.03385>.
- [56] Patrick Helber, Benjamin Bischke, Andreas Dengel, and Damian Borth. Eurosat: A novel dataset and deep learning benchmark for land use and land cover classification. *Journal of Selected Topics in Applied Earth Observations and Remote Sensing*, 2019. <https://arxiv.org/abs/1709.00029>.
- [57] Dan Hendrycks, Steven Basart, Norman Mu, Saurav Kadavath, Frank Wang, Evan Dorundo, Rahul Desai, Tyler Zhu, Samyak Parajuli, Mike Guo, Dawn Song, Jacob Steinhardt, and Justin Gilmer. The many faces of robustness: A critical analysis of out-of-distribution generalization. *ICCV*, 2021. <https://arxiv.org/abs/2006.16241>.
- [58] Dan Hendrycks, Kevin Zhao, Steven Basart, Jacob Steinhardt, and Dawn Song. Natural adversarial examples. In *Conference on Computer Vision and Pattern Recognition (CVPR)*, 2021. <https://arxiv.org/abs/1907.07174>.

- [59] Jordan Hoffmann, Sebastian Borgeaud, Arthur Mensch, Elena Buchatskaya, Trevor Cai, Eliza Rutherford, Diego de Las Casas, Lisa Anne Hendricks, Johannes Welbl, Aidan Clark, et al. Training compute-optimal large language models, 2022. <https://arxiv.org/abs/2203.15556>.
- [60] Raphael Hoffmann, Congle Zhang, Xiao Ling, Luke Zettlemoyer, and Daniel S Weld. Knowledge-based weak supervision for information extraction of overlapping relations. In *Annual Meeting of the Association for Computational Linguistics (ACL)*, 2011. <https://aclanthology.org/P11-1055/>.
- [61] Gabriel Ilharco, Mitchell Wortsman, Ross Wightman, Cade Gordon, Nicholas Carlini, Rohan Taori, Achal Dave, Vaishaal Shankar, Hongseok Namkoong, John Miller, Hannaneh Hajishirzi, Ali Farhadi, and Ludwig Schmidt. OpenCLIP, July 2021. <https://doi.org/10.5281/zenodo.5143773>.
- [62] Andrew Ilyas, Sung Min Park, Logan Engstrom, Guillaume Leclerc, and Aleksander Madry. Datamodels: Predicting predictions from training data, 2022. <https://arxiv.org/abs/2202.00622>.
- [63] Tanuj Jain, Christopher Lennan, Zubin John, and Dat Tran. Imagededup, 2019. <https://github.com/ideal0/imagededup>.
- [64] Chao Jia, Yinfei Yang, Ye Xia, Yi-Ting Chen, Zarana Parekh, Hieu Pham, Quoc V Le, Yunhsuan Sung, Zhen Li, and Tom Duerig. Scaling up visual and vision-language representation learning with noisy text supervision. In *International Conference on Machine Learning (ICML)*, 2021. <https://arxiv.org/abs/2102.05918>.
- [65] Mon-Fong Jiang, Shian-Shyong Tseng, and Chih-Ming Su. Two-phase clustering process for outliers detection. *Pattern recognition letters*, 2001. <https://www.sciencedirect.com/science/article/abs/pii/S0167865500001318>.
- [66] Jeff Johnson, Matthijs Douze, and Hervé Jégou. Billion-scale similarity search with GPUs. *IEEE Transactions on Big Data*, 2019. <https://arxiv.org/abs/1702.08734>.
- [67] Justin Johnson, Bharath Hariharan, Laurens van der Maaten, Li Fei-Fei, C. Lawrence Zitnick, and Ross B. Girshick. CLEVR: A diagnostic dataset for compositional language and elementary visual reasoning. *Conference on Computer Vision and Pattern Recognition (CVPR)*, 2017. <https://arxiv.org/abs/1612.06890>.
- [68] Armand Joulin, Edouard Grave, Piotr Bojanowski, and Tomas Mikolov. Bag of tricks for efficient text classification. In *Conference of the European Chapter of the Association for Computational Linguistics (EACL)*, 2017. <https://arxiv.org/abs/1607.01759>.
- [69] Juelich Supercomputing Center. JUWELS Booster Supercomputer, 2020. <https://apps.fz-juelich.de/jsc/hps/juwels/configuration.html#hardware-configuration-of-the-system-name-booster-module>.
- [70] Jared Kaplan, Sam McCandlish, Tom Henighan, Tom B Brown, Benjamin Chess, Rewon Child, Scott Gray, Alec Radford, Jeffrey Wu, and Dario Amodei. Scaling laws for neural language models, 2020. <https://arxiv.org/abs/2001.08361>.
- [71] Kimmo Karkkainen and Jungseock Joo. Fairface: Face attribute dataset for balanced race,

- gender, and age for bias measurement and mitigation. In *IEEE/CVF Winter Conference on Applications of Computer Vision*, 2021. <https://arxiv.org/abs/1908.04913>.
- [72] Diederik P Kingma and Jimmy Ba. Adam: A method for stochastic optimization. In *International Conference on Learning Representations (ICLR)*, 2014. <https://arxiv.org/abs/1412.6980>.
- [73] Pang Wei Koh and Percy Liang. Understanding black-box predictions via influence functions. In *International Conference on Machine Learning (ICML)*, 2017.
- [74] Pang Wei Koh, Kai-Siang Ang, Hubert Teo, and Percy S Liang. On the accuracy of influence functions for measuring group effects. *Advances in Neural Information Processing Systems (NeurIPS)*, 2019.
- [75] Pang Wei Koh, Shiori Sagawa, Henrik Marklund, Sang Michael Xie, Marvin Zhang, Akshay Balsubramani, Weihua Hu, Michihiro Yasunaga, Richard Lanus Phillips, Irena Gao, Tony Lee, Etienne David, Ian Stavness, Wei Guo, Berton A. Earnshaw, Imran S. Haque, Sara Beery, Jure Leskovec, Anshul Kundaje, Emma Pierson, Sergey Levine, Chelsea Finn, and Percy Liang. WILDS: A benchmark of in-the-wild distribution shifts. In *International Conference on Machine Learning (ICML)*, 2021. <https://arxiv.org/abs/2012.07421>.
- [76] Simon Kornblith, Jonathon Shlens, and Quoc V Le. Do better imagenet models transfer better? In *Conference on Computer Vision and Pattern Recognition (CVPR)*, 2019. <https://arxiv.org/abs/1805.08974>.
- [77] Jonathan Krause, Michael Stark, Jia Deng, and Li Fei-Fei. 3d object representations for fine-grained categorization. In *International Conference on Computer Vision Workshops (ICML)*, 2013. https://www.cv-foundation.org/openaccess/content_iccv_workshops_2013/W19/html/Krause_3D_Object_Representations_2013_ICCV_paper.html.
- [78] Alex Krizhevsky, Geoffrey Hinton, et al. Learning multiple layers of features from tiny images, 2009. <https://www.cs.toronto.edu/~kriz/learning-features-2009-TR.pdf>.
- [79] Alex Krizhevsky, Ilya Sutskever, and Geoffrey E Hinton. Imagenet classification with deep convolutional neural networks. In *Advances in Neural Information Processing Systems (NeurIPS)*, 2012.
- [80] Ronan Le Bras, Swabha Swayamdipta, Chandra Bhagavatula, Rowan Zellers, Matthew Peters, Ashish Sabharwal, and Yejin Choi. Adversarial filters of dataset biases. In *International Conference on Machine Learning (ICML)*, 2020. <https://arxiv.org/abs/2002.04108>.
- [81] Yann LeCun. The MNIST database of handwritten digits, 1998. <http://yann.lecun.com/exdb/mnist/>.
- [82] Katherine Lee, Daphne Ippolito, Andrew Nystrom, Chiyuan Zhang, Douglas Eck, Chris Callison-Burch, and Nicholas Carlini. Deduplicating training data makes language models better. In *Annual Meeting of the Association for Computational Linguistics (ACL)*, 2021. <https://arxiv.org/abs/2107.06499>.
- [83] Yi Li and Nuno Vasconcelos. Repair: Removing representation bias by dataset resampling.

- In *Conference on Computer Vision and Pattern Recognition (CVPR)*, 2019. <https://arxiv.org/abs/1904.07911>.
- [84] Ilya Loshchilov and Frank Hutter. Sgdr: Stochastic gradient descent with warm restarts. In *International Conference on Learning Representations (ICLR)*, 2016. <https://arxiv.org/abs/1608.03983>.
- [85] Ilya Loshchilov and Frank Hutter. Decoupled weight decay regularization. In *International Conference on Learning Representations (ICLR)*, 2019. <https://openreview.net/forum?id=Bkg6RiCqY7>.
- [86] Mario Lucic, Matthew Faulkner, Andreas Krause, and Dan Feldman. Training gaussian mixture models at scale via coresets. *Journal of Machine Learning Research (JMLR)*, 2018. <http://jmlr.org/papers/v18/15-506.html>.
- [87] S. Maji, J. Kannala, E. Rahtu, M. Blaschko, and A. Vedaldi. Fine-grained visual classification of aircraft, 2013. <https://arxiv.org/abs/1306.5151>.
- [88] Gideon S Mann and Andrew McCallum. Generalized expectation criteria for semi-supervised learning with weakly labeled data. *Journal of Machine Learning Research (JMLR)*, 2010. <https://www.jmlr.org/papers/v11/mann10a.html>.
- [89] Mark Mazumder, Colby Banbury, Xiaozhe Yao, Bojan Karlaš, William Gaviria Rojas, Sudnya Diamos, Greg Diamos, Lynn He, Douwe Kiela, David Jurado, David Kanter, Rafael Mosquera, Juan Ciro, Lora Aroyo, Bilge Acun, Sabri Eyuboglu, Amirata Ghorbani, Emmett Goodman, Tariq Kane, Christine R. Kirkpatrick, Tzu-Sheng Kuo, Jonas Mueller, Tristan Thrush, Joaquin Vanschoren, Margaret Warren, Adina Williams, Serena Yeung, Newsha Ardalani, Praveen Paritosh, Ce Zhang, James Zou, Carole-Jean Wu, Cody Coleman, Andrew Ng, Peter Mattson, and Vijay Janapa Reddi. Dataperf: Benchmarks for data-centric ai development, 2022. <https://arxiv.org/abs/2207.10062>.
- [90] Baharan Mirzasoleiman, Jeff Bilmes, and Jure Leskovec. Coresets for data-efficient training of machine learning models. In *International Conference on Machine Learning (ICML)*, 2020. <https://arxiv.org/abs/1906.01827>.
- [91] Yuval Netzer, Tao Wang, Adam Coates, Alessandro Bissacco, Bo Wu, and Andrew Y Ng. Reading digits in natural images with unsupervised feature learning. In *Advances in Neural Information Processing Systems (NeurIPS) Workshops*, 2011. <https://storage.googleapis.com/pub-tools-public-publication-data/pdf/37648.pdf>.
- [92] Andrew Ng, Dillon Laird, and Lynn He. Data-centric ai competition, 2021. <https://https-deeplearning-ai.github.io/data-centric-comp/>.
- [93] Thao Nguyen, Gabriel Ilharco, Mitchell Wortsman, Sewoong Oh, and Ludwig Schmidt. Quality not quantity: On the interaction between dataset design and robustness of clip. In *Advances in Neural Information Processing Systems (NeurIPS)*, 2022. <https://openreview.net/forum?id=LTCBavFwP5C>.
- [94] Maria-Elena Nilsback and Andrew Zisserman. Automated flower classification over a large number of classes. In *Indian Conference on Computer Vision, Graphics and Image Processing*, 2008. <https://ieeexplore.ieee.org/document/4756141>.

- [95] OpenAI. Gpt-4 technical report, 2023. <https://arxiv.org/abs/2303.08774>.
- [96] Vicente Ordonez, Girish Kulkarni, and Tamara L. Berg. Im2text: Describing images using 1 million captioned photographs. In *Advances in Neural Information Processing Systems (NeurIPS)*, 2011. https://papers.nips.cc/paper_files/paper/2011/file/5dd9db5e033da9c6fb5ba83c7a7ebea9-Paper.pdf.
- [97] Omkar M. Parkhi, Andrea Vedaldi, Andrew Zisserman, and C. V. Jawahar. Cats and dogs. In *Conference on Computer Vision and Pattern Recognition (CVPR)*, 2012. <https://ieeexplore.ieee.org/document/6248092>.
- [98] Mansheej Paul, Surya Ganguli, and Gintare Karolina Dziugaite. Deep learning on a data diet: Finding important examples early in training. In *Advances in Neural Information Processing Systems (NeurIPS)*, 2021. <https://arxiv.org/abs/2107.07075>.
- [99] Hieu Pham, Zihang Dai, Golnaz Ghiasi, Hanxiao Liu, Adams Wei Yu, Minh-Thang Luong, Mingxing Tan, and Quoc V. Le. Combined scaling for zero-shot transfer learning, 2021. <https://arxiv.org/abs/2111.10050>.
- [100] Garima Pruthi, Frederick Liu, Satyen Kale, and Mukund Sundararajan. Estimating training data influence by tracing gradient descent. *Advances in Neural Information Processing Systems (NeurIPS)*, 2020. <https://arxiv.org/abs/2002.08484>.
- [101] Filip Radenovic, Abhimanyu Dubey, Abhishek Kadian, Todor Mihaylov, Simon Vandenhende, Yash Patel, Yi Wen, Vignesh Ramanathan, and Dhruv Mahajan. Filtering, distillation, and hard negatives for vision-language pre-training. In *Conference on Computer Vision and Pattern Recognition (CVPR)*, 2023. <https://arxiv.org/abs/2301.02280>.
- [102] Alec Radford, Jong Wook Kim, Chris Hallacy, Aditya Ramesh, Gabriel Goh, Sandhini Agarwal, Girish Sastry, Amanda Askell, Pamela Mishkin, Jack Clark, Gretchen Krueger, and Ilya Sutskever. Learning transferable visual models from natural language supervision. In *International Conference on Machine Learning (ICML)*, 2021. <https://arxiv.org/abs/2103.00020>.
- [103] Alec Radford, Jong Wook Kim, Tao Xu, Greg Brockman, Christine McLeavey, and Ilya Sutskever. Robust speech recognition via large-scale weak supervision. *arXiv preprint arXiv:2212.04356*, 2022.
- [104] Colin Raffel, Noam Shazeer, Adam Roberts, Katherine Lee, Sharan Narang, Michael Matena, Yanqi Zhou, Wei Li, and Peter J Liu. Exploring the limits of transfer learning with a unified text-to-text transformer. *The Journal of Machine Learning Research (JMLR)*, 2020. <https://arxiv.org/abs/1910.10683>.
- [105] Vikram V. Ramaswamy, Sing Yu Lin, Dora Zhao, Aaron B. Adcock, Laurens van der Maaten, Deepti Ghadiyaram, and Olga Russakovsky. Beyond web-scraping: Crowd-sourcing a geodiverse dataset, 2023. <https://arxiv.org/abs/2301.02560>.
- [106] Aditya Ramesh, Mikhail Pavlov, Gabriel Goh, Scott Gray, Chelsea Voss, Alec Radford, Mark Chen, and Ilya Sutskever. Zero-shot text-to-image generation. In *International Conference on Machine Learning (ICML)*, 2021. <https://arxiv.org/abs/2102.12092>.

- [107] Aditya Ramesh, Prafulla Dhariwal, Alex Nichol, Casey Chu, and Mark Chen. Hierarchical text-conditional image generation with clip latents, 2022. <https://arxiv.org/abs/2204.06125>.
- [108] A. J. Ratner, B. Hancock, J. Dunmon, F. Sala, S. Pandey, and C. Ré. Training complex models with multi-task weak supervision. In *Association for the Advancement of Artificial Intelligence (AAAI)*, 2019. <https://arxiv.org/abs/1810.02840>.
- [109] Alexander J Ratner, Christopher M De Sa, Sen Wu, Daniel Selsam, and Christopher Ré. Data programming: Creating large training sets, quickly. In *Advances in Neural Information Processing Systems (NeurIPS)*, 2016. <https://arxiv.org/abs/1605.07723>.
- [110] Alexander J Ratner, Stephen H Bach, Henry Ehrenberg, Jason Fries, Sen Wu, and Christopher Ré. Snorkel: Rapid training data creation with weak supervision. In *Very Large Data Bases Conference (VLDB)*, 2017. <https://arxiv.org/abs/1711.10160>.
- [111] Christopher Ré. Overton: A data system for monitoring and improving machine-learned products. In *10th Conference on Innovative Data Systems Research, CIDR 2020, Amsterdam, The Netherlands, January 12-15, 2020, Online Proceedings*. [www.cidrdb.org](http://cidrdb.org), 2020. URL <http://cidrdb.org/cidr2020/papers/p33-re-cidr20.pdf>.
- [112] Benjamin Recht, Rebecca Roelofs, Ludwig Schmidt, and Vaishaal Shankar. Do ImageNet classifiers generalize to ImageNet? In *International Conference on Machine Learning (ICML)*, 2019. <http://proceedings.mlr.press/v97/recht19a.html>.
- [113] William A Gaviria Rojas, Sudnya Damos, Keertan Ranjan Kini, David Kanter, Vijay Janapa Reddi, and Cody Coleman. The dollar street dataset: Images representing the geographic and socioeconomic diversity of the world. In *Advances in Neural Information Processing Systems (NeurIPS) Datasets and Benchmarks Track*, 2022. <https://openreview.net/forum?id=qnfYsave0U4>.
- [114] Robin Rombach, Andreas Blattmann, Dominik Lorenz, Patrick Esser, and Björn Ommer. High-resolution image synthesis with latent diffusion models. In *Conference on Computer Vision and Pattern Recognition (CVPR)*, 2022. <https://arxiv.org/abs/2112.10752>.
- [115] Peter J Rousseeuw and Mia Hubert. Robust statistics for outlier detection. *Wiley interdisciplinary reviews: Data mining and knowledge discovery*, 2011. <http://i2pc.es/coss/Docencia/SignalProcessingReviews/Rousseeuw2011.pdf>.
- [116] Peter J Rousseeuw and Mia Hubert. Anomaly detection by robust statistics. *Wiley interdisciplinary reviews: Data mining and knowledge discovery*, 2018. <https://wires.onlinelibrary.wiley.com/doi/pdf/10.1002/widm.1236>.
- [117] Olga Russakovsky, Jia Deng, Hao Su, Jonathan Krause, Sanjeev Satheesh, Sean Ma, Zhiheng Huang, Andrej Karpathy, Aditya Khosla, Michael Bernstein, Alexander C. Berg, and Li Fei-Fei. ImageNet Large Scale Visual Recognition Challenge. *International Journal of Computer Vision (IJCV)*, 2015. <https://arxiv.org/abs/1409.0575>.
- [118] Shiori Sagawa, Pang Wei Koh, Tony Lee, Irena Gao, Sang Michael Xie, Kendrick Shen, Ananya Kumar, Weihua Hu, Michihiro Yasunaga, Henrik Marklund, Sara Beery, Etienne David, Ian Stavness, Wei Guo, Jure Leskovec, Kate Saenko, Tatsunori Hashimoto, Sergey Levine, Chelsea Finn, and Percy Liang. Extending the wilds benchmark for unsupervised

- adaptation. In *International Conference on Learning Representations (ICLR)*, 2022. <https://arxiv.org/abs/2112.05090>.
- [119] Christoph Schuhmann, Richard Vencu, Romain Beaumont, Robert Kaczmarczyk, Clayton Mullis, Aarush Katta, Theo Coombes, Jenia Jitsev, and Aran Komatsuzaki. LAION-400M: Open dataset of clip-filtered 400 million image-text pairs, 2021. <https://arxiv.org/abs/2111.02114>.
- [120] Christoph Schuhmann, Romain Beaumont, Richard Vencu, Cade W Gordon, Ross Wightman, Mehdi Cherti, Theo Coombes, Aarush Katta, Clayton Mullis, Mitchell Wortsman, Patrick Schramowski, Srivatsa R Kundurthy, Katherine Crowson, Ludwig Schmidt, Robert Kaczmarczyk, and Jenia Jitsev. LAION-5B: An open large-scale dataset for training next generation image-text models. In *Thirty-sixth Conference on Neural Information Processing Systems (NeurIPS), Datasets and Benchmarks Track*, 2022. <https://openreview.net/forum?id=M3Y74vmsMcY>.
- [121] Ozan Sener and Silvio Savarese. Active learning for convolutional neural networks: A core-set approach. In *International Conference on Learning Representations (ICLR)*, 2018. <https://openreview.net/forum?id=H1aIuk-RW>.
- [122] Piyush Sharma, Nan Ding, Sebastian Goodman, and Radu Soricut. Conceptual captions: A cleaned, hypernymed, image alt-text dataset for automatic image captioning. In *Annual Meeting of the Association for Computational Linguistics (ACL)*, 2018. <https://aclanthology.org/P18-1238/>.
- [123] Changho Shin, Winfred Li, Harit Vishwakarma, Nicholas Roberts, and Frederic Sala. Universalizing weak supervision. In *International Conference on Learning Representations (ICLR)*, 2022. <https://openreview.net/forum?id=YpPiNigTzMT>.
- [124] Ben Sorscher, Robert Geirhos, Shashank Shekhar, Surya Ganguli, and Ari S. Morcos. Beyond neural scaling laws: beating power law scaling via data pruning. In *Advances in Neural Information Processing Systems (NeurIPS)*, 2022. <https://openreview.net/forum?id=UmvS1P-PyV>.
- [125] Krishna Srinivasan, Karthik Raman, Jiecao Chen, Michael Bendersky, and Marc Najork. Wit: Wikipedia-based image text dataset for multimodal multilingual machine learning. In *44th International ACM SIGIR Conference on Research and Development in Information Retrieval*, 2021. <https://arxiv.org/abs/2103.01913>.
- [126] Johannes Stallkamp, Marc Schlipsing, Jan Salmen, and Christian Igel. The german traffic sign recognition benchmark: a multi-class classification competition. In *International Joint Conference on Neural Networks (IJCNN)*, 2011. <https://ieeexplore.ieee.org/document/6033395>.
- [127] Swabha Swayamdipta, Roy Schwartz, Nicholas Lourie, Yizhong Wang, Hannaneh Hajishirzi, Noah A. Smith, and Yejin Choi. Dataset cartography: Mapping and diagnosing datasets with training dynamics. In *Conference on Empirical Methods in Natural Language Processing (EMNLP)*, 2020. <https://aclanthology.org/2020.emnlp-main.746>.
- [128] Rohan Taori, Achal Dave, Vaishaal Shankar, Nicholas Carlini, Benjamin Recht, and Ludwig

- Schmidt. Measuring robustness to natural distribution shifts in image classification. In *Advances in Neural Information Processing Systems (NeurIPS)*, 2020. <https://dl.acm.org/doi/abs/10.5555/3495724.3497285>.
- [129] Bart Thomee, David A Shamma, Gerald Friedland, Benjamin Elizalde, Karl Ni, Douglas Poland, Damian Borth, and Li-Jia Li. YFCC100M: The new data in multimedia research. *Communications of the ACM*, 2016. <https://arxiv.org/abs/1503.01817>.
- [130] Mariya Toneva, Alessandro Sordoni, Remi Tachet des Combes, Adam Trischler, Yoshua Bengio, and Geoffrey J Gordon. An empirical study of example forgetting during deep neural network learning. In *International Conference on Learning Representations (ICLR)*, 2018. <https://arxiv.org/abs/1812.05159>.
- [131] Bastiaan S Veeling, Jasper Linmans, Jim Winkens, Taco Cohen, and Max Welling. Rotation equivariant CNNs for digital pathology, 2018. <https://arxiv.org/abs/1806.03962>.
- [132] Haohan Wang, Songwei Ge, Zachary Lipton, and Eric P Xing. Learning robust global representations by penalizing local predictive power. In *Advances in Neural Information Processing Systems (NeurIPS)*, 2019. <https://arxiv.org/abs/1905.13549>.
- [133] Ryan Webster, Julien Rabin, Loic Simon, and Frederic Jurie. On the de-duplication of laion-2b, 2023. <https://arxiv.org/abs/2303.12733>.
- [134] Kai Wei, Rishabh Iyer, and Jeff Bilmes. Submodularity in data subset selection and active learning. In *International Conference on Machine Learning (ICML)*, 2015. <https://proceedings.mlr.press/v37/wei15.html>.
- [135] Jianxiong Xiao, Krista A Ehinger, James Hays, Antonio Torralba, and Aude Oliva. Sun database: Exploring a large collection of scene categories. *International Journal of Computer Vision (IJCV)*, 2016. <https://link.springer.com/article/10.1007/s11263-014-0748-y>.
- [136] Kaiyu Yang, Jacqueline H Yau, Li Fei-Fei, Jia Deng, and Olga Russakovsky. A study of face obfuscation in ImageNet. In *International Conference on Machine Learning (ICML)*, 2022. <https://arxiv.org/abs/2103.06191>.
- [137] Lewei Yao, Runhui Huang, Lu Hou, Guansong Lu, Minzhe Niu, Hang Xu, Xiaodan Liang, Zhenguo Li, Xin Jiang, and Chunjing Xu. Filip: Fine-grained interactive language-image pre-training. In *International Conference on Learning Representations (ICLR)*, 2022. <https://arxiv.org/abs/2111.07783>.
- [138] Shuhei Yokoo. Contrastive learning with large memory bank and negative embedding subtraction for accurate copy detection, 2021. <https://arxiv.org/abs/2112.04323>.
- [139] Peter Young, Alice Lai, Micah Hodosh, and Julia Hockenmaier. From image descriptions to visual denotations: New similarity metrics for semantic inference over event descriptions. *Transactions of the Association for Computational Linguistics*, 2014. <https://aclanthology.org/Q14-1006/>.
- [140] Dantong Yu, Gholamhosein Sheikholeslami, and Aidong Zhang. Findout: Finding outliers in very large datasets. *Knowledge and information Systems*, 2002. <https://link.springer.com/article/10.1007/s101150200013>.

- [141] Lu Yuan, Dongdong Chen, Yi-Ling Chen, Noel Codella, Xiyang Dai, Jianfeng Gao, Houdong Hu, Xuedong Huang, Boxin Li, Chunyuan Li, et al. Florence: A new foundation model for computer vision, 2021. <https://arxiv.org/abs/2111.11432>.
- [142] Man-Ching Yuen, Irwin King, and Kwong-Sak Leung. A survey of crowdsourcing systems. In *SocialCom*. IEEE, 2011. <https://ieeexplore.ieee.org/document/6113213>.
- [143] Matei Zaharia, Reynold S Xin, Patrick Wendell, Tathagata Das, Michael Armbrust, Ankur Dave, Xiangrui Meng, Josh Rosen, Shivaram Venkataraman, Michael J Franklin, et al. Apache spark: a unified engine for big data processing. *Communications of the ACM*, 2016. <https://dl.acm.org/doi/10.1145/2934664>.
- [144] Xiaohua Zhai, Joan Puigcerver, Alexander Kolesnikov, Pierre Ruysen, Carlos Riquelme, Mario Lucic, Josip Djolonga, André Susano Pinto, Maxim Neumann, Alexey Dosovitskiy, Lucas Beyer, Olivier Bachem, Michael Tschannen, Marcin Michalski, Olivier Bousquet, Sylvain Gelly, and Neil Houlsby. The visual task adaptation benchmark, 2019. <http://arxiv.org/abs/1910.04867>.
- [145] Jieyu Zhang, Yue Yu, Yinghao Li, Yujing Wang, Yaming Yang, Mao Yang, and Alexander Ratner. WRENCH: A comprehensive benchmark for weak supervision. In *NeurIPS*, 2021. URL <https://openreview.net/forum?id=Q9SKS5k8io>.
- [146] Jieyu Zhang, Cheng-Yu Hsieh, Yue Yu, Chao Zhang, and Alexander Ratner. A survey on programmatic weak supervision, 2022. <https://arxiv.org/abs/2202.05433>.
- [147] Zhifei Zhang, Yang Song, and Hairong Qi. Age progression/regression by conditional adversarial autoencoder. In *IEEE Conference on Computer Vision and Pattern Recognition (CVPR)*, 2017. <https://arxiv.org/abs/1702.08423>.

Appendix

Contents

1	Introduction	2
2	Related Work	4
3	DATACOMP	5
3.1	Competition design	6
3.2	COMMONPOOL generation	8
3.3	Bring your own data (BYOD)	9
3.4	Training	9
3.5	Evaluation	10
4	Baselines	10
4.1	Filtering baselines	10
4.2	BYOD baselines	11
5	Results and discussion	11
5.1	Building better datasets	11
5.2	DATACOMP design analyses	14
5.3	Evaluation trends	15
6	Conclusion and future work	16
A	Benchmark rules	33
A.1	Filtering track rules	33
A.2	Bring your own data track: amendments	34
B	Contributions	35
B.1	Candidate pool	35
B.2	Participant tooling	35
B.3	Baselines	35
B.4	Leadership and Advising	35
C	Additional related work	36
D	Parsing Common Crawl	36
E	Not safe for work (NSFW) filtering	37
F	Deduplication against evaluation sets	38
G	Face blurring	39
H	DATACOMP COMMONPOOL creation pipeline	40

I	COMMONPOOL statistics	42
J	Efficient training on data subsets	46
K	Effect of duplicates in the training data	46
L	Training with additional steps	47
M	Training details	49
N	Evaluation details	49
O	Baseline details	52
	O.1 Filtering track	56
	O.2 BYOD track	58
	O.2.1 Additional results	58
P	Fairness and biases	60
	P.1 Diversity	60
	P.2 Fairness	61
Q	Extra figures and tables	63
R	Datasheet	71
	R.1 Motivation	71
	R.2 Composition	71
	R.3 Collection Process	74
	R.4 Preprocessing, Cleaning, and/or Labeling	76
	R.5 Uses	77
	R.6 Distribution	78
	R.7 Maintenance	79

A Benchmark rules

We provide concrete rules below for the two competition tracks that comprise DATACOMP: filtering and BYOD. Additionally, we provide a checklist, which encourages participants to specify design decisions, hence allowing for more granular comparison between submissions.

A.1 Filtering track rules

- Participants can enter submissions for one or many different scales: `small`, `medium`, `large` or `xlarge`, which represent the raw number of image-text pairs in CommonPool that should be filtered.
- After choosing a scale, participants generate a list of uids, where each uid refers to a COMMONPOOL sample. The list of uids is used to recover image-text pairs from the pool, which is used for downstream CLIP training.

- Duplicate uids are allowed.
- Participants are *not* allowed to modify the training procedure. Hence, changing hyperparameters, model architecture, optimizer, compute budget, or number of training steps is not allowed. Changing any other training details is also not allowed.
- Participants are strongly encouraged to submit and open-source both the list of uids and the code used to generate this list; however, this is not required.
- To avoid overfitting, we do not permit running any code or algorithmic dependence on the test images of the evaluation tasks. However, use of other images associated with these tasks (e.g., supervised training sets) is permitted.
- Participants can use templates or class labels from the downstream tasks in their filtering algorithms.

For clarity, we include some examples of permitted and forbidden uses:

- ✓ We **permit** using the ImageNet class label “triceratops” in a filtering algorithm.
- × We **forbid** examining individual or aggregate predictions on the test sets of the evaluation tasks.

A.2 Bring your own data track: amendments

To facilitate more open-ended exploration, we provide amendments to the Track 1 competition to allow for more diverse submissions in Track 2.

- Participants are allowed to augment COMMONPOOL data with existing datasets, so long as these data sources do not contain test images from the evaluation tasks. Participants can use data from any COMMONPOOL; however, they are not required to do so.
- Assembling one’s own dataset is allowed; however, test images from the evaluation tasks can neither be contained nor otherwise used to construct said dataset. We encourage releasing the image urls or the images themselves in addition to the text for each image. We also encourage rigorous documentation of face-blurring and other data safety checks (see Section 3.2 for more details). We reserve the right to run our own safety code on participant provided data and disqualify entries that do not meet adequate safety standards.

Checklist. The following checklist provides the basis for more fine-grained comparison between submissions.

- Images from the evaluation tasks are included in my submission. If yes, please specify which datasets.
- I used an existing datasets (e.g., YFCC100M [129]) in my submission. If yes, please specify which datasets. (Note: applies to BYOD only)
- I curated my own data. If yes, please provide (1) image data or urls, (2) text for each image, (3) list of safety steps taken including but not limited to face blurring, explicit content image and text filtering. (Note: applies to BYOD only)

B Contributions

For this section, contributors are ordered alphabetically.

B.1 Candidate pool

Candidate pool lead. Vaishaal Shankar

Data collection. Romain Beaumont, Vaishaal Shankar

Pre-processing and metadata. Giannis Daras, Alex Fang (content filtering lead), Samir Yitzhak Gadre (metadata lead), Ryan Marten (deduplication lead), Vivek Ramanujan, Vaishaal Shankar, George Smyrnis (face blurring lead)

B.2 Participant tooling

Participant tooling lead. Gabriel Ilharco

Resharder. Romain Beaumont, Yair Carmon, Alex Fang, Jonathan Hayase (lead), Gabriel Ilharco, Vivek Ramanujan, Vaishaal Shankar, Georgios Smyrnis

Training. Mehdi Cherti, Gabriel Ilharco, Jenia Jitsev, Vivek Ramanujan, Georgios Smyrnis, Mitchell Wortsman (lead)

Evaluation. Romain Beaumont, Yonatan Bitton, Mehdi Cherti, Dhruva Ghosh (lead), Gabriel Ilharco

Additional infrastructure. Stephen Mussmann, Sarah Pratt

B.3 Baselines

Baselines lead. Yair Carmon

Filtering track. Yair Carmon, Rahim Enterazi, Alex Fang, Samir Yitzhak Gadre, Gabriel Ilharco, Kalyani Marathe, Thao Nguyen, Eyal Orgad (co-lead), Georgios Smyrnis, Mitchell Wortsman, Jieyu Zhang (co-lead)

BYOD track. Gabriel Ilharco, Thao Nguyen

Experiment babysitting. Alex Fang, Gabriel Ilharco, Samir Yitzhak Gadre

B.4 Leadership and Advising

Advising. Romain Beaumont, Yair Carmon, Alexandros G. Dimakis, Ali Farhadi, Hannaneh Hajishirzi, Jenia Jitsev, Pang Wei Koh, Ranjay Krishna, Stephen Mussmann, Sewoong Oh, Alexander Ratner, Olga Saukh, Ludwig Schmidt, Vaishaal Shankar, Shuran Song, Richard Vencu

Leadership. Yair Carmon, Alexandros G. Dimakis, Jenia Jitsev, Sewoong Oh, Ludwig Schmidt, Vaishaal Shankar

Overall project lead. Ludwig Schmidt

C Additional related work

Beyond data selection, Chan et al. [18] investigate the effects of dataset distribution on emergent properties of transformers, while Fang et al. [39] look at the relationship between data and model robustness to distribution shifts. We hope our extensive evaluation suite comprised of 38 diverse tasks To facilitate similar studies when training multimodal models at large scale.

Others study how to reduce the burdens of training data annotation in the curation process. Classic approaches include distant supervision [60], crowd-sourced labels [142], heuristic rules [5] and feature annotation [88], among others. A recent line of work known as data programming or programmatic weak supervision [109, 110, 145, 146] attempts to reduce annotation cost and is found in many industry applications [6, 111]. In data programming, developers write programmatic labeling functions to automatically label a large amount of unlabeled data. The labeling functions could produce noisy and conflicting labels, so researchers have developed methods to aggregate noisy votes to produce the final training labels [108, 42, 123].

Previous literature also studies methods for training data attribution, which seek to link a model’s behavior (e.g., its accuracy on a particular task or subset of data) to particular subsets of its training data. Such methods include influence functions, a classic technique from robust statistics [51, 30] that uses a second-order Taylor expansion to approximate the effect of removing a training point on the learned model parameters [73, 74, 52, 47], as well as methods that fit attribution functions directly to the dynamics of repeated training runs [44, 100, 62, 50]. Training data attribution methods assume that we have already trained a model, though they can be subsequently used to refine the training data (e.g., by identifying potentially mislabeled training points [73]). Our focus in this paper is instead on data curation methods—that is, methods for selecting a subset of the training data to train a model in the first place.

In the context of natural language processing, Swayamdipta et al. [127] proposes a tool for characterizing samples in a dataset based on training dynamics, labelling instances as ambiguous, easy to learn or hard to learn. Previous literature such as work by Le Bras et al. [80], Li & Vasconcelos [83], Gururangan et al. [49] advocate for removing easy instances from the training data. Ethayarajh et al. [36] propose a measure of how difficult a dataset is to learn, \mathcal{V} -usable information. Such techniques could be promising directions of further exploration in the context of our benchmark.

Finally, another related line of work is studying scaling trends. In addition to Sorscher et al. [124], researchers have investigated how model performance changes as a function of compute budget, model size, and number of training samples [70, 59, 16, 23]. However, this line of work does not consider how dataset design may affects scaling trends. Beyond dataset size, we measure the effects of different dataset sources and filtering strategies. While scaling trends are central to our investigations, the purpose of our benchmark is to search for the next generation of large multimodal datasets to facilitate more accurate and reliable models.

D Parsing Common Crawl

Common Crawl releases metadata files for the websites that they index (i.e., WAT files). They release these files approximately once a month. We consider all files available from 2014 through November of 2022. We first parse these files, utilizing Apache Spark [143] to extract image urls

Table 5: Detoxify positive rates by threshold on 1 million caption subset of Common Crawl.

Threshold	Toxicity	Severe Toxicity	Obscene	Identity Attack	Insult	Threat	Sexual Explicit
0.01	9.5%	1.0%	33.4%	1.8%	35.0%	1.3%	2.0%
0.1	3.6%	0.1%	0.8%	0.3%	1.4%	0.1%	1.0%

Table 6: Comparing LAION-2B CLIP based NSFW filtering model to Google Vision API Safe Search adult category on a 40,000 random subset of Common Crawl.

Threshold	False Positive Rate (Relative to Google)	True Positives (Manual Review)	Model Positive Rate	Google API Positive Rate
0.1	3.6%	2	14.4%	3.5%
0.2	0.6%	2	9.1%	3.5%
0.3	0.3%	3	7.2%	3.5%

and corresponding alt-text. We map each url, text pair to a uid hash and remove duplicates. This results in 88 billion url, text pairs, which are randomized via a distributed shuffle. Note, we do not consider image content when running uid deduplication at this step. Hence, two identical images with different urls and the same caption would both be retained.

E Not safe for work (NSFW) filtering

Our data is sourced from Common Crawl, which contains snapshots of the web. Therefore, we apply multiple layers of NSFW content filtering to remove problematic images and captions from COMMONPOOL.

First, we filter our captions with Detoxify [53], a language model for toxic comment classification. Specifically, we use the multilingual XLM-RoBERTa [29] variant. The model outputs scores between zero and one for the following categories: toxicity, severe toxicity, obscene, identity attack, insult, threat, and sexually explicit. As we had no ground truth for our data, we manually inspected a 1 million random subset of COMMONPOOL at varying thresholds. We found that a threshold of 0.1 provided good coverage of filtering out NSFW text. If any of the detoxify category scores exceeds the threshold, the sample is discarded. Qualitatively, we found that the model struggled with multilingual content, acronyms, and innuendo. Even at 0.1, we noticed there are some captions that are NSFW. However, lowering the threshold further heavily affected false positives. We therefore use a 0.1 threshold for all NSFW categories, which on a random subset of one million captions achieves positive rates shown in Table 5.

Second, on the vision side, we use a modified version of LAION-5B’s [120] CLIP-based binary classification NSFW model, which takes CLIP ViT-L/14 visual embeddings as input. We remove the initial multi-category encoder from the model, and retrain on the same data with an initial normalization layer followed by a 4-layer multilayer perceptron. Our retrained model matches the performance of the original model on their manually annotated testset. Specifically, we achieve 97.4% classification accuracy on a held out test set compared to 96.1% for the original LAION NSFW image filtering model. Additional details about the training data can be found in Appendix C.5 of the LAION-5B paper. In brief, the training data contains 682K images that is roughly balanced with images from safe for work and NSFW categories.



Figure 6: Candidate images (top) that are detected as duplicates against images in the evaluation sets (bottom) are removed from the pool. In addition to exact duplicate images, near-duplicates with variable aspect ratios, JPEG compression, overlays, color adjustment, and artistic rendering are also detected.

To evaluate our model and determine a threshold, we used Google Vision API’s SafeSearch explicit content detector to generate labels for an 40,000 random subset of our candidate pool. Specifically, an image is NSFW if SafeSearch classifies it as likely or very likely adult (i.e., sexually explicit). As shown in Table 6, we found that by thresholding at 0.1 we achieve high recall relative to SafeSearch and very few true positives after manual review. We also manually reviewed images classified by SafeSearch as likely or very likely racy and found that the images were either benign, subjectively suggestive but not explicit, or already found in the set of images labeled as adult.

F Deduplication against evaluation sets

To prevent data leakage, we filter COMMONPOOL by removing duplicate and near-duplicate matches of evaluation set images. See Figure 6 for example query images from Common Crawl and corresponding near-duplicates in our evaluations sets. We consider images as duplicates when the cosine similarity between a query (Common Crawl image) feature and a reference (evaluation image) feature is higher than a fixed threshold. We employ the deduplication model proposed by Yokoo [138], which earned 1st place in the Facebook AI Image Similarity Challenge (ISC) [35]. We choose a cosine similarity threshold of 0.604169 to maximize the true duplicates detected, without removing too many false duplicates from the pool. We compare against OpenAI’s CLIP ViT-B/32 as a baseline on ISC. We find that for our threshold, the ISC model achieves precision 0.9 and recall 0.8. At a threshold of 0.96, CLIP achieves the same precision 0.9, but a significantly worse recall of 0.02. Approximately 2.8% of downloaded samples are flagged as evaluation set near-duplicates.

To verify the performance of our de-duplication models with greater granularity, we modify the evaluation procedure in Douze et al. [35] to include transformations which are representative of naturally-occurring duplications on the Internet. Specifically, we study: 1) jpeg compression (encoding), 2) image flips, 3) image rotations, 4) aspect ratio modifications, and 5) grayscaling. To

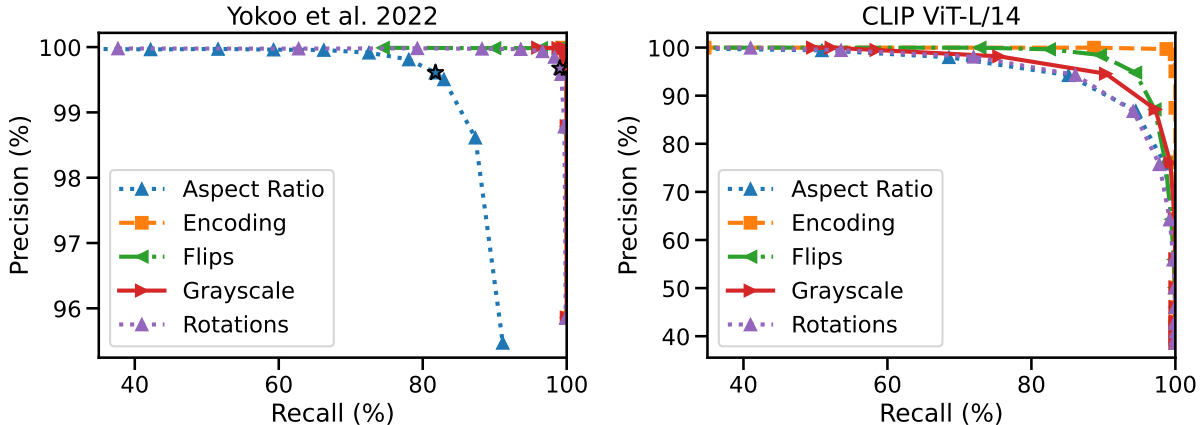


Figure 7: Analysis of different de-duplication strategies across a variety of image transformations. We see that the model introduced by Yokoo [138] is better in almost every transformation, with the exception of very aggressive aspect ratio modification.

do this, we sample 20% of the images from each of our evaluation datasets uniformly at random to serve as a reference set of about 140,000 images. Next we sample 560,000 images uniformly at random from LAION-2B to serve as distractors, for a 4-to-1 distractor to reference ratio. Finally, we apply each of the augmentations above and use threshold filtering to determine duplicates. Figure 7 shows the results from the deduplication model [138] compared with OpenAI’s CLIP ViT-L/14. At high recall values, we see that CLIP filtering results in removing over $2\times$ the data as that of the deduplication model from Yokoo [138].

G Face blurring

As an extra step to safeguard against issues of privacy that may arise from the use of data scraped from the web, we include face blurring as part of our pool creation. To create face metadata, we use the SCRFD face detector [48] to extract bounding boxes for the faces in our images. These bounding boxes are included as part of the image metadata in our pool. We make use of the pretrained SCRFD-10G model. We use the same preprocessing as the one described in the official repository of the paper, with the exception of providing 224×224 input images (by padding each image to square and then resizing) to limit computation costs. Invoking this model provides us with bounding boxes along with an associated score, which we then compare against a threshold of 0.3 to keep or discard this bounding box. This threshold is the default one used in the repository of SCRFD for the visualization of bounding boxes, and we found it to perform well on our data as discussed next.

In Table 7 we can see the result of face detection on a set of 3293 images from COMMONPOOL. We evaluate the detection on whether the image has visible faces or not (where images such as cartoon drawings of non-real human faces are not considered as positives), and whether the detector has detected these visible faces. We considered an image as a true positive if all the clearly visible faces in the image were detected, based on the above thresholding process. We did not do extensive box labeling. True positives are instead determined by human inspection. We compare the quality of these detections with the Amazon Rekognition system, which is the one upon which the face

Table 7: Face detection performance on a set of 3293 random images from COMMONPOOL.

	SCRFD-10G	Amazon Rekognition
Accuracy	93.87	96.57
Precision	75.87	86.09
Recall	90.53	93.75

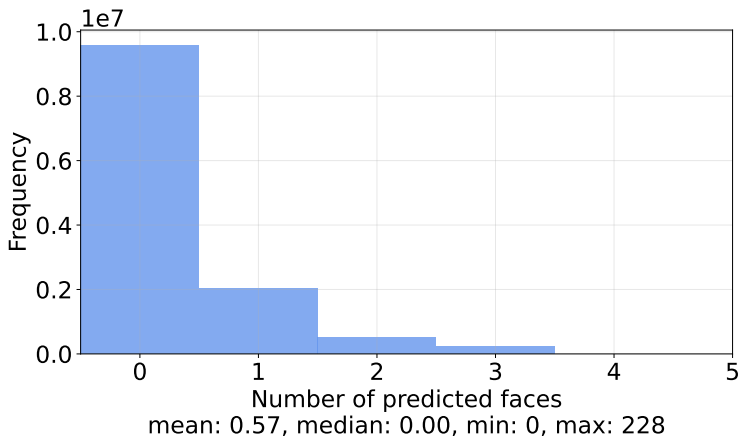


Figure 8: Frequency of predicted number of faces in the `small` COMMONPOOL.

detections on ImageNet were based [136]. Note that in this scenario, the recall of the detectors is more important than precision (as detecting a few more bounding boxes across our pool does not affect privacy).

To utilize these bounding boxes on our data, we apply a standard blurring pipeline, as proposed by Yang et al. [136]. The result of this process is an image where the faces is blurred and there is a smooth transition from blurred to clean parts of the image. In Figure 8 we see the distribution of faces for the `small` COMMONPOOL. Note that the majority of images do not contain faces.

As part of our competition pipeline, images are by default blurred during the download process. In Table 8 we can see the results of training on 100M images with and without the application of face blurring, as provided by our detector. We can see that the difference in performance is small, which suggests that the application of face blurring does not significantly affect the performance on our downstream tasks.

Finally, we evaluated the detector we used for potential biases. More specifically, we used the detector on the validation set of the FairFace dataset [71]. We found that the central face of the image was detected in all the images of the validation set, regardless of subgroup.

H DATACOMP COMMONPOOL creation pipeline

Table 8: Effect of face blurring on zero-shot performance. Face blurring improves the privacy preservation of our dataset, while affecting model performance negligibly. Results shown for the medium scale.

Filtering	Face blurring	ImageNet acc.	Avg. performance
CLIP score (B/32, thresh. 0.3) + English filtering	×	0.209	0.246
	✓	0.196	0.243
CLIP score (B/32, 30%)	×	0.287	0.301
	✓	0.282	0.298

Table 9: Provided metadata for COMMONPOOL.

Generation Time	Label	Additional notes
Step 2	uid	
	url	Link to the image.
	text	Image caption.
	original_width	
	original_height	
	sha256	Safeguard for data poisoning.
	Step 1	clip_b32_similarity_score
clip_b32_image_features		In separate file.
clip_b32_text_features		In separate file.
clip_114_similarity_score		
clip_114_image_features		In separate file.
clip_114_text_features		In separate file.
Step 2, dropped during Step 3	face_bboxes	
	nsfw_image_score	
	nsfw_text_score	
	dedup_score	

Creating COMMONPOOL was a multistep process, which involved (1) parsing image urls and alt-text from Common Crawl dumps and downloading these images, (2) tagging images with metadata and (3) conducting safety content filtering and evaluation set duplication. In this section we provide an overview of the data pipeline used to create COMMONPOOL. For an overview of our “data funnel” see Figure 2.

1. For the first step, we use parse Common Crawl metadata files to harvest image-text pairs (Section D). We use `img2dataset`⁷ to obtain ~16.8B downloaded samples. This is the first, unfiltered version of COMMONPOOL, and contains only basic information for our images (i.e., the original image height, width, and alt-text caption). During this step we also resize images such that their largest dimension does not exceed 512px. This eases storage requirements for large images, but is still larger than the 224px resolution used for later training stages.
2. For the second step, we process our unfiltered pool and create richer metadata for each image-text pair. We generate the following for each sample:
 - CLIP ViT-B/32 and CLIP ViT-L/14 image and text features, with their associated

⁷<https://github.com/rom1504/img2dataset>

similarities.

- NSFW scores for the image and the text, using the analysis described in Appendix E.
 - Deduplication score for the image, as described in Appendix F.
 - Bounding boxes for faces detected in the image, using the method described in Appendix G.
3. For the third and final step, we filter our image-text pairs based on the metadata generated during the second stage. We filter out image-text pairs where the NSFW and deduplication scores exceed the respective thresholds (Section E). From the images that pass through this filtering, we keep only the desired amount (e.g., 12.8B images from the `xlarge` COMMONPOOL). Smaller pools are telescoping subsets of larger pools. We package the metadata and image urls, which is made publicly available to the participants. Note, we do not release raw image data but rather image urls pointing to images.

A summary of the metadata for each sample is found in Table 9. To validate our pipeline for duplication and CLIP feature correctness, we additionally take ImageNet train though metadata generation as a unit test. Using the deduplication features, we detect that 100% of the images are in fact duplicates. Additionally using the CLIP ViT-B/32 and CLIP ViT-L/14 image features and corresponding text features from OpenAI’s 80-prompt ensemble, we achieve 63.36% and 75.54% top-1 accuracies, which match the performance reported in the CLIP paper [102].

When creating pools of different scale (i.e., number of samples), we ensure that smaller pools are subsets of larger pools. For instance, the `small` COMMONPOOL is a subset of the `xlarge` COMMONPOOL.

After COMMONPOOL is created, the participants can then download the final image-text pairs using the provided files via `img2dataset`. To further ease the computational burden on participants, we additionally provide metadata for each sample in COMMONPOOL. Note that when downloading, our `img2dataset` configuration automatically blurs faces. Hence this is an automatic step on not something participants must do ad hoc.

I COMMONPOOL statistics

To provide more information about the kinds of samples in our COMMONPOOL, we conduct additional analysis on the `small` pool, which is an i.i.d. sample of downloaded data and a subset of the larger pools.

In Figure 9 we show CLIP similarity scores between images and their corresponding text. We notice a flatter distribution of CLIP ViT-L/14 scores than corresponding B/32 scores.

Turning our attention to images in COMMONPOOL, in Figure 10, we visualize the aspect ratios and sizes of original images (i.e., before they are downloaded and resized). In Figure 11, we display a distribution of image height and width after *download* resizing. Notice that the majority of images are around 224×224 px, which is the final resized resolution used for training.

Analysing the textual component of each sample, we visualize frequency of the number of CLIP BPE tokens in the captions (Figure 12) and most common languages (Figure 13). Token counts

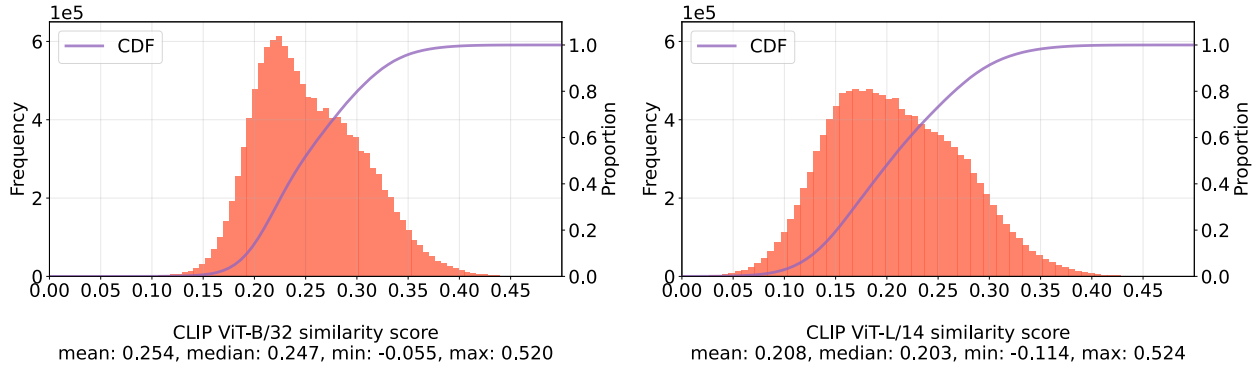


Figure 9: Image-text similarity score distributions using CLIP ViT-B/32 (*left*) and ViT-L/14 (*right*) models. We plot samples from the `small` COMMONPOOL, which are an i.i.d. sample of the `xlarge` COMMONPOOL.

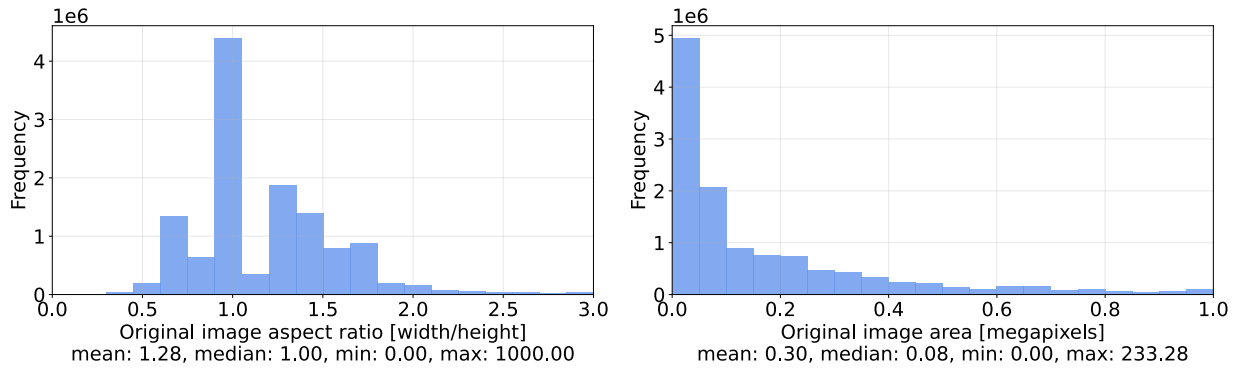


Figure 10: Statistics for images in the `small` COMMONPOOL, before applying resizing.

follow a long-tailed distribution with much more mass in the short sequence range, while English is the predominant language in COMMONPOOL according to `fasttext` and `cld3`.

We additionally look at url statistics. In Figure 14 we see common domain names in COMMONPOOL (e.g., wordpress domains) and common suffixes (e.g., `.com` or `.net`).

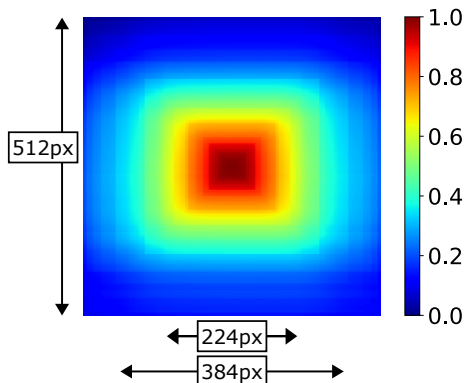


Figure 11: **Image pixel heatmap.** Each entry in the above heatmap represents the estimated probability that a pixel is occupied. The center entry has a value of 1.0 as every image has a center pixel. We compute the heatmap over the `small COMMONPOOL`. Note that image sizes are bounded as we resize all images such that their max dimension does not exceed 512px during dataset download.

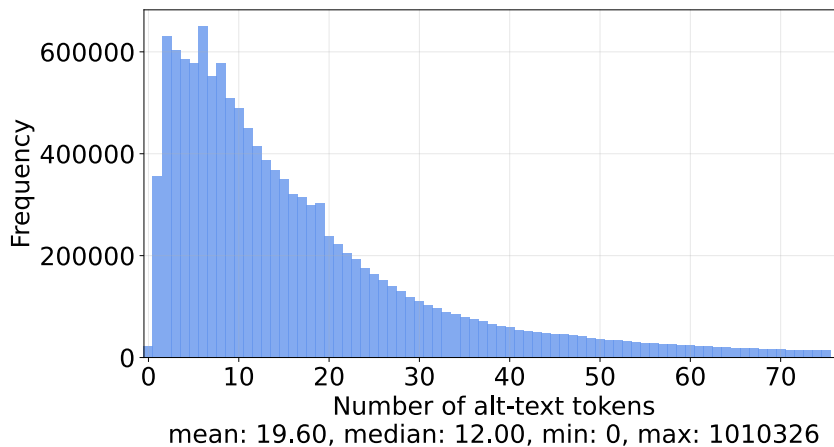


Figure 12: Distribution of token length for alt-text in the `small COMMONPOOL`. The CLIP BPE tokenizer is used for tokenization.

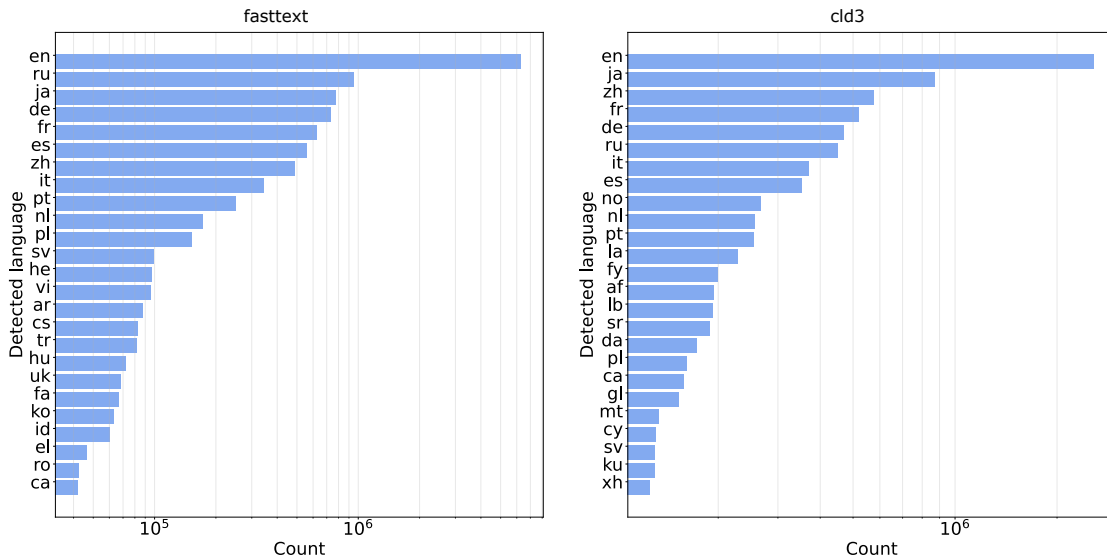


Figure 13: Counts for the top 25 most frequent languages in the `small COMMONPOOL`, as predicted by `fasttext` (left) and `cld3` (right).

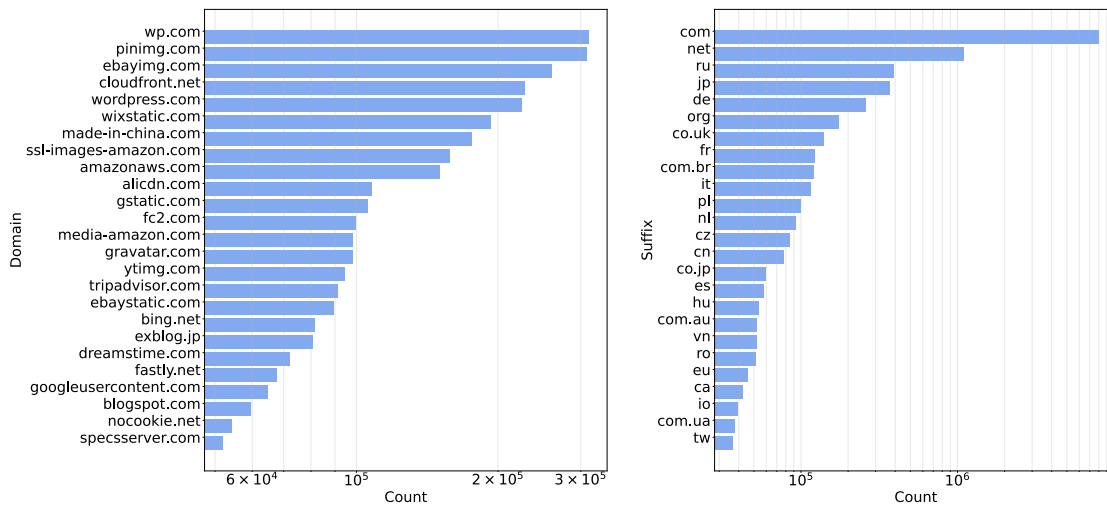


Figure 14: Counts for the top 25 most frequent domains (left) and suffixes (right) in the `small COMMONPOOL`.

J Efficient training on data subsets

When training at large scale, it is important to use efficient access patterns to load training data. This typically means that data must be loaded using large sequential reads instead of random reads in order to maximize throughput. In DATACOMP, this is facilitated by the WebDataset⁸ format which stores the training examples in tar files (called “shards”) and WebDataLoader which makes it easy to load data stored in this format.

Given an arbitrary subset of a pool, we would like to efficiently train on that subset. Because WebDataset format does not permit efficient random access (a feature inherited from tar), we must read through the entire pool to select the required images. There are two ways to implement this filtering:

1. **Filter during training:** we apply a predicate during training data loading that discards data not present in the subset.
2. **Filter before training:** we iterate over the pool, selecting the images in the subset, and write them to a new WebDataset.

After some profiling, we concluded that option 1 had too much overhead in the case where the subset is much smaller than the pool. To see why, note that if the subset is an p -fraction of the pool size, then we would end up reading a $1/p$ factor more data than needed for training. Instead, we give an implementation of option 2, which performs at most twice as many reads as needed for training.⁹

Our tool, called the *resharder*, reads a set of uids in NumPy array format, scans through the pool, selecting those examples, and writes them to a new WebDataset. The resharder uses multiprocessing to make good use of hardware and can be distributed over many computers to further increase throughput. The resharder also supports streaming data to and from cloud storage such as Amazon S3. The resharder is provided to participants as part of the competition tooling.

K Effect of duplicates in the training data

Given that COMMONPOOL was constructed by scraping the web for image and text pairs, there is a likelihood that some of our images are duplicates of each other, even if they originated from different web sources and have different captions. Here we examine the effect of removing such duplicates. We used the technique proposed by Webster et al. [133], where CLIP image features are first compressed and then used to do an approximate nearest neighbor search. After this process, two images x and y are considered duplicates if $\frac{|d_{ADC}(x,x)-d_{ADC}(x,y)|}{d_{ADC}(x,x)} < T_{ADC}$, where T_{ADC} is some threshold and $d_{ADC}(x,x)$ is the distance of a vector with its quantized version used for approximate nearest neighbor search. For each image, we search duplicates across its 1000 nearest neighbors, and keep it if it’s the one with the highest CLIP ViT-L/14 similarity score across its duplicates. Results can be seen in Table 10, both when this technique is used by itself and in conjunction with ViT-B/32 filtering. We can see that there are small improvements over using CLIP filtering by itself with respect to the average performance across evaluation datasets.

⁸<https://github.com/webdataset/webdataset>

⁹Since in DATACOMP, the number of examples seen is equal to the pool size.

Table 10: Effect of deduplication of training set for the medium size COMMONPOOL. The filtering performed here is CLIP B32 score top 30% (see Table 22). Higher threshold values lead to more samples being labeled as duplicates.

Subset	Training dataset size	ImageNet accuracy	Average performance
$T_{ADC} = 0.1$, without filtering	99.8M	0.195	0.272
$T_{ADC} = 0.2$, without filtering	85.9M	0.200	0.274
$T_{ADC} = 0.5$, without filtering	29.6M	0.227	0.292
$T_{ADC} = 0.1$, with filtering	33.5M	0.288	0.333
$T_{ADC} = 0.2$, with filtering	30.6M	0.289	0.333
$T_{ADC} = 0.5$, with filtering	15.5M	0.252	0.307

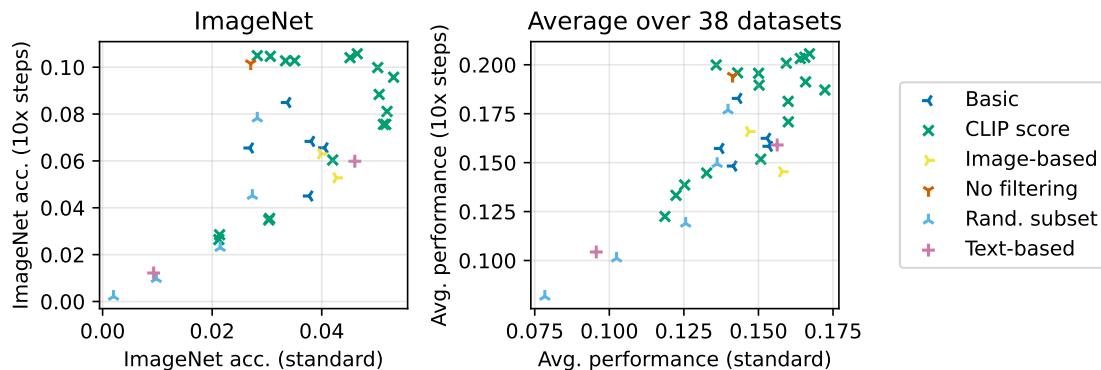


Figure 15: (left) The effect of training for $10\times$ steps for for `small` filtering track baselines on ImageNet. (right) Similar plot but for Avg. performance. While the ordering of some methods changes quite drastically, we, in general, see a positive correlation.

L Training with additional steps

Recall that one of our major design decisions for DATACOMP is to fix the hyperparameters associated with model training, following closely hyperparameters from prior work [102]. We choose to fix hyperparameters to place emphasis on data curation and remove confounders arising from hyperparameter differences between participants. Here we ablate our hyperparameter configuration by training `small` baselines for $10\times$ more steps. In Figure 15 we see positive correlation for ImageNet accuracy for the ablated and original hyperparameter configurations. We see similar correlation for average performance. See Table 11 for specific values.

Table 11: Experiment details when extending the number of steps by 10 times the standard amount for that scale.

Scale	Filtering	ImageNet	ImageNet dist. shifts	VTAB	Retrieval	Average over 38 datasets
small	No filtering	0.102	0.093	0.204	0.125	0.194
	Random subset(75%)	0.078	0.072	0.182	0.109	0.177
	Random subset(50%)	0.045	0.049	0.161	0.096	0.149
	Random subset(25%)	0.023	0.029	0.134	0.071	0.119
	Random subset(10%)	0.010	0.018	0.119	0.067	0.101
	Random subset(1%)	0.002	0.006	0.097	0.055	0.082
	Caption length	0.085	0.080	0.198	0.116	0.183
	Image size	0.066	0.064	0.153	0.101	0.157
	English (fasttext)	0.068	0.068	0.172	0.095	0.158
	English (fasttext) and caption length	0.066	0.065	0.182	0.095	0.162
	English (fasttext), caption length, and image size	0.045	0.048	0.164	0.084	0.148
	CLIP B32 score top 10%	0.035	0.046	0.162	0.072	0.139
	CLIP B32 score top 20%	0.076	0.076	0.182	0.088	0.171
	CLIP B32 score top 30%	0.096	0.090	0.221	0.104	0.204
	CLIP B32 score top 40%	0.081	0.077	0.200	0.107	0.191
	CLIP B32 score top 50%	0.106	0.097	0.211	0.113	0.203
	CLIP B32 score top 75%	0.103	0.096	0.210	0.126	0.196
	CLIP B32 score top 90%	0.105	0.096	0.212	0.127	0.200
	CLIP B32 threshold at 0.3 + English filter	0.029	0.036	0.152	0.071	0.133
	CLIP B32 threshold at 0.28 + English filter	0.035	0.041	0.168	0.080	0.145
	CLIP B32 threshold at 0.3	0.076	0.078	0.199	0.089	0.181
	CLIP L14 score top 10%	0.026	0.037	0.130	0.069	0.123
	CLIP L14 score top 20%	0.060	0.064	0.161	0.085	0.152
	CLIP L14 score top 30%	0.088	0.087	0.199	0.098	0.187
	CLIP L14 score top 40%	0.100	0.096	0.217	0.103	0.206
	CLIP L14 score top 50%	0.104	0.098	0.212	0.114	0.201
	CLIP L14 score top 75%	0.103	0.095	0.189	0.121	0.190
	CLIP L14 score top 90%	0.105	0.095	0.203	0.123	0.196
	Image-based clustering (ImageNet1k)	0.053	0.053	0.162	0.082	0.145
	Image-based clustering (ImageNet21k)	0.063	0.059	0.173	0.094	0.166
Text-based clustering (ImageNet1k)	0.012	0.018	0.120	0.060	0.104	
Text-based clustering (ImageNet21k)	0.060	0.064	0.170	0.090	0.159	
Intersect IN1k image clustering and CLIP B32 score top 30%	0.058	0.059	0.179	0.089	0.160	
Intersect IN1k image clustering and CLIP L14 score top 30%	0.049	0.051	0.171	0.083	0.149	
Intersect IN21k image clustering and CLIP B32 score top 30%	0.071	0.070	0.192	0.092	0.174	
Intersect IN21k image clustering and CLIP L14 score top 30%	0.064	0.065	0.200	0.085	0.172	
medium	No filtering	0.370	0.304	0.387	0.259	0.376
	English (fasttext), caption length, and image size	0.317	0.269	0.324	0.194	0.328
	CLIP B32 score top 30%	0.436	0.351	0.433	0.245	0.422
	CLIP B32 score top 40%	0.434	0.353	0.448	0.263	0.434
	CLIP B32 score top 50%	0.426	0.352	0.439	0.273	0.425
	CLIP B32 score top 75%	0.398	0.325	0.396	0.271	0.402
	Image-based clustering (ImageNet1k)	0.363	0.294	0.347	0.197	0.341
	Image-based clustering (ImageNet21k)	0.374	0.303	0.372	0.224	0.364
	Intersect IN1k image clustering and CLIP B32 score top 30%	0.415	0.330	0.413	0.218	0.396
	Intersect IN1k image clustering and CLIP L14 score top 30%	0.405	0.325	0.399	0.206	0.380

M Training details

The full set of hyperparameters used for each scale is shown in Table 12. For choosing hyperparameters, we follow the OpenCLIP library [61], an open source reproduction of OpenAI’s CLIP. For the **small**, **medium**, and **large** tracks, these hyperparameters are equal to those in the CLIP paper, except with reduced batch size so that training runs on reasonable hardware. For the **xlarge** track, batch size is increased from that in OpenAI’s CLIP to accelerate training by allowing the use of many GPUs simultaneously with high utilization. For this run we also double the learning rate following prior work [23].

N Evaluation details

Models are evaluated over a wide range of 38 tasks to measure proficiency in various domains. We include 22 of the 27 classification tasks in the test suite of Radford et al. [102], excluding the few datasets that have license restrictions, are in video format, or are no longer available in their original form. We include 6 datasets that were designed to test generalization of models trained on ImageNet. We also include a majority of the Visual Task Adaptation Benchmark, excluding 3 datasets that are ill-suited for zero-shot evaluation [144]. We include 3 datasets from the WILDS benchmark, which tests robustness to distribution shifts and spurious correlations [75, 118]. Finally, we include 2 additional datasets, Dollar Street and GeoDE, which test robustness of classification performance across income levels and geographical regions [113, 105]. Furthermore, we evaluate zero-shot image and text retrieval on the Flickr30k and MSCOCO datasets, and image association on the WinoGAViL dataset [139, 21, 12]. The complete list of evaluation tasks is given in Table 13. We show a sample from each dataset in Figure 16.

Prompt choice. Since we perform zero-shot evaluation, prompt and class name selection is important, and can have a significant impact on the results. To avoid heavy prompt engineering and overtuning to individual models, we opt to use the prompt templates used in Radford et al. [102] whenever possible. Most datasets come with pre-defined class names, but some are overwritten with more descriptive labels, again based on previous literature. For datasets with no precedent in zero-shot evaluation, we reuse prompt templates from other datasets with a similar domain and task (e.g., SVHN is evaluated with MNIST prompts and class names).

Evaluation metrics. For the majority of classification tasks, the primary evaluation metric is accuracy. For certain datasets with class imbalances, we instead compute mean per-class accuracy, as done in Radford et al. [102]. On the WILDS benchmark datasets, we use the primary metric specified for each dataset on their leaderboard. Dollar Street and GeoDE test model generalization across socioeconomic and geographic diversity. Thus, for Dollar Street, we compute worst-group

Table 12: Experimental configuration for each scale, including the size of the pool we provide, the model architecture and hyperparameters.

Scale	Model	Train compute (MACs)	Pool size	# samples seen	Learning rate	AdamW β_2	Warmup	Batch size
small	ViT-B/32	9.5×10^{16}	12.8M	12.8M	5e-4	0.98	500	4096
medium	ViT-B/32	9.5×10^{17}	128M	128M	5e-4	0.98	500	4096
large	ViT-B/16	2.6×10^{19}	1.28B	1.28B	5e-4	0.98	500	8192
xlarge	ViT-L/14	1.1×10^{21}	12.8B	12.8B	1e-3	0.95	10k	90112

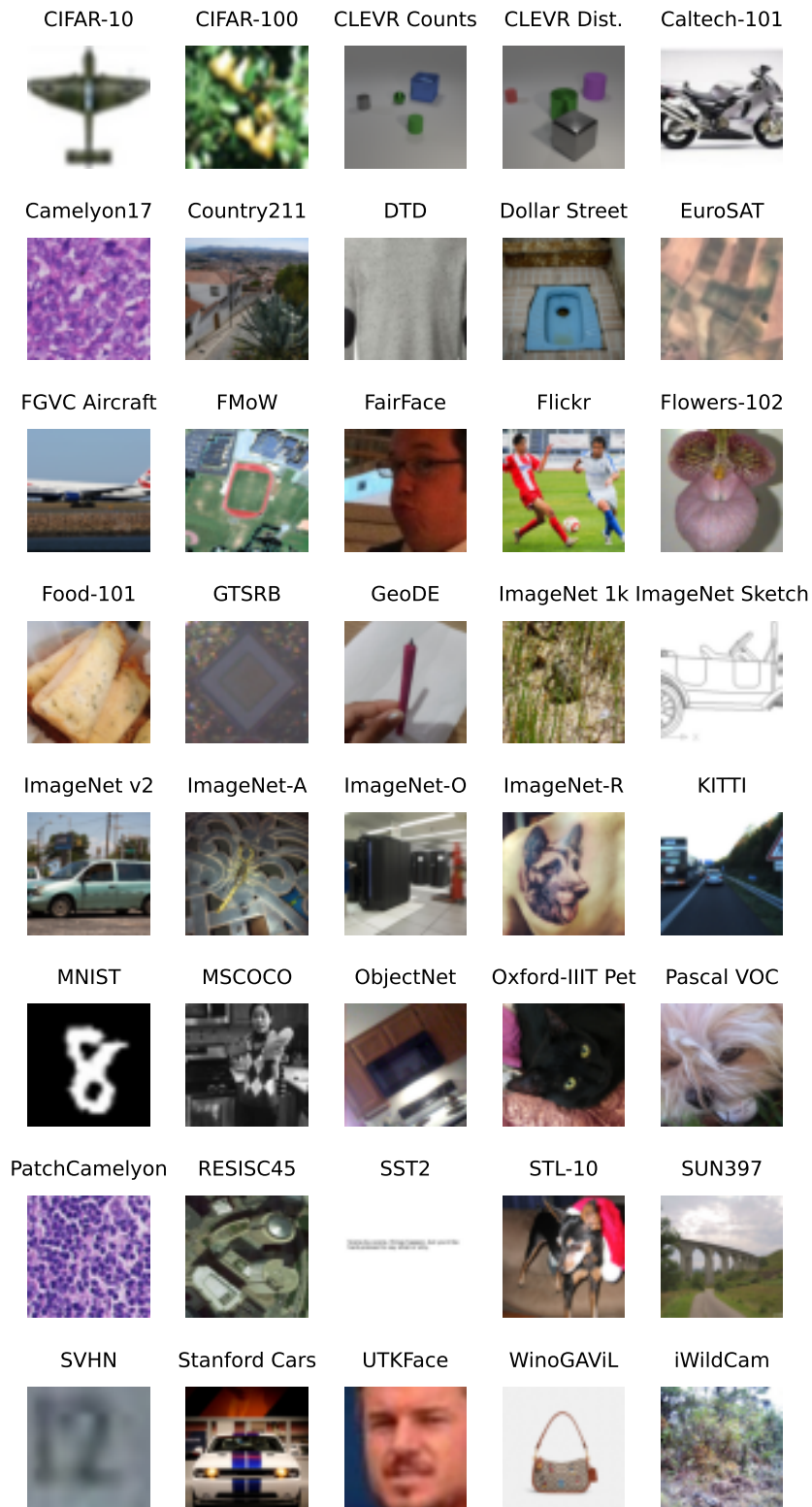


Figure 16: Randomly sampled images from the evaluation datasets we consider.

Table 13: Evaluation tasks.

Task type	Dataset	Task	Test set size	Number of classes	Main metric	Clean
	Caltech-101 [40]	Object recognition	6,085	102	mean per class	✓
	CIFAR-10 [78]	Visual recognition	10,000	10	accuracy	✓
	CIFAR-100 [78]	Visual recognition	10,000	100	accuracy	✓
	CLEVR Counts [67, 144]	Counting	15,000	8	accuracy	
	CLEVR Distance [67, 144]	Distance prediction	15,000	6	accuracy	
	Country211 [102, 129]	Geolocation	21,100	211	accuracy	✓
	DTD [25]	Texture classification	1,880	47	accuracy	✓
	EuroSAT [56, 144]	Satellite imagery recognition	5,400	10	accuracy	✓
	FGVC Aircraft [87]	Aircraft recognition	3,333	100	mean per class	✓
	Food-101 [13]	Food recognition	25,250	101	accuracy	✓
	GTSRB [126]	Traffic sign recognition	12,630	43	accuracy	✓
	ImageNet 1k [32]	Visual recognition	50,000	1,000	accuracy	✓
	ImageNet Sketch [132]	Visual recognition	50,889	1,000	accuracy	✓
	ImageNet V2 [112]	Visual recognition	10,000	1,000	accuracy	✓
	ImageNet-A [58]	Visual recognition	7,500	200	accuracy	✓
	ImageNet-O [58]	Visual recognition	2,000	200	accuracy	✓
	ImageNet-R [57]	Visual recognition	30,000	200	accuracy	✓
Classification	KITTI distance [43, 144]	Distance prediction	711	4	accuracy	
	MNIST [81]	Digit recognition	10,000	10	accuracy	✓
	ObjectNet [9]	Visual recognition	18,574	113	accuracy	✓
	Oxford Flowers-102 [94]	Flower recognition	6,149	102	mean per class	✓
	Oxford-IIIT Pet [97, 144]	Pet classification	3,669	37	mean per class	✓
	Pascal VOC 2007 [37]	Object recognition	14,976	20	accuracy	✓
	PatchCamelyon [131, 144]	Metastatic tissue cls.	32,768	2	accuracy	
	Rendered SST2 [144]	Sentiment classification	1,821	2	accuracy	✓
	RESISC45 [22, 144]	Satellite imagery recognition	6,300	45	accuracy	✓
	Stanford Cars [77]	Vehicle recognition	8,041	196	accuracy	✓
	STL-10 [26]	Visual recognition	8,000	10	accuracy	✓
	SUN-397 [135]	Scene recognition	108,754	397	accuracy	✓
	SVHN [91, 144]	Digit recognition	26032	10	accuracy	✓
	iWildCam [10, 75]	Animal recognition	42,791	182	macro F1 score	✓
	Camelyon17 [8, 75]	Metastatic tissue cls.	85,054	2	accuracy	
	FMoW [24, 75]	Satellite imagery recognition	22,108	62	worst-region acc.	✓
	Dollar Street [113]	Object recognition	3,503	58	worst-income top-5 acc.	✓
	GeoDE [105]	Object recognition	12,488	40	worst-region acc.	✓
Retrieval	Flickr30k [139]	Image and text retrieval	31,014	N/A	R@1	✓
	MSCOCO [21]	Image and text retrieval	5,000	N/A	R@1	✓
	WinoGAViL [12]	Commonsense association	3,563	N/A	Jaccard score	✓

top-5 accuracy, with groups defined by income level, emulating Rojas et al. [113]; for GeoDE, we compute worst-group accuracy, with groups defined by region (Africa, Americas, West Asia, East Asia, Southeast Asia, and Europe), as defined in Ramaswamy et al. [105]. For the image-text retrieval tasks, Flickr and MSCOCO, we compute both image and text recall (fraction of text captions for which the correct image was selected and vice versa), and plot their arithmetic mean. On WinoGAViL, we compute the Jaccard score (intersection-over-union) for each example, and show results for the harder samples (10 and 12 candidates). More information on WinoGAViL evaluation can be found in Bitton et al. [12].

Clean subset. For five of our evaluation tasks (the two CLEVR tasks, the two Camelyon tasks, and KITTI) the zero-shot performance of all evaluated models appears to be close to that of random guessing, and lack correlation to the type of filtering method used (see Figure 27). Consequently, we studied performance averaged only on the remaining 33 tasks, but found not substantial qualitative

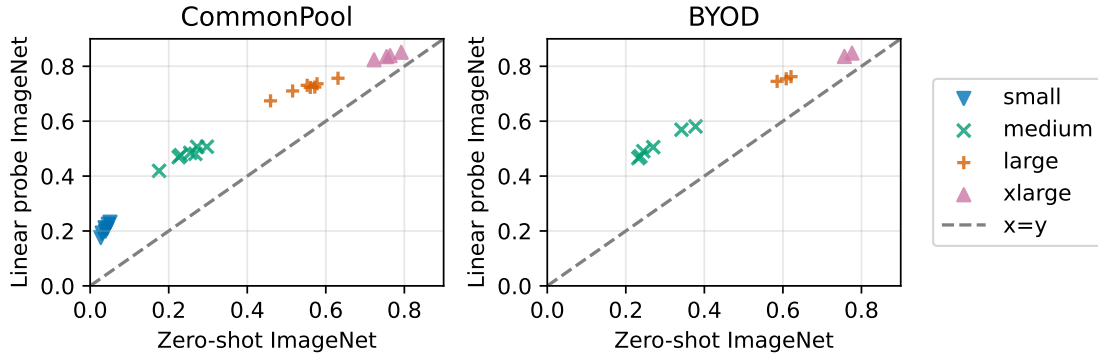


Figure 17: Zero-shot ImageNet and Linear probe ImageNet performance for models from Tables 3 and 4. Relative ordering of models demonstrates high rank correlations of 0.99 and 1.0 for COMMONPOOL and BYOD respectively.

differences in our results. As a result, we opted to report the average on the full evaluation suite throughout our study.

Zero-shot vs. fine-tuning protocols. One critical decision in DATACOMP is how exactly to evaluate models and whether or not to fine-tune models on evaluation tasks (i.e., supervised fine-tuning directly on task training sets). We opt for zero-shot evaluation, where a models are applied to downstream tasks directly to 1) ease computational burden on participants and 2) measure the out-of-the-box generalization capabilities of our models. To validate this design decision, we conduct linear probes on all models presented in Tables 3 and 4 on ImageNet. We follow a standard probing protocol and fine-tune the last linear layer from zero-shot initialization for 40 epochs with learning rate $1e-3$, batch size 256, AdamW optimizer with default settings with the exception of weight decay (that we set to zero), and a cosine annealing schedule. As seen in Figure 17, zero-shot and linear probe performance follow similar trends for both filtering and BYOD tracks. Moreover the Spearman rank correlation between the two protocols over the models considered is 0.99 for the filtering track and 1.0 for BYOD. This suggests that better zero-shot models on ImageNet are correlated with better representations of linear probe fine-tuning on ImageNet.

O Baseline details

Here we provide additional details on the creation of our baseline subsets. To highlight the qualitative differences between the filtering strategies we also provide visualization for *No filtering* (Figure 18), *Basic filtering* (Figure 19), and *CLIP score ($L/14$ 30%)* (Figure 20), which can all be found in Table 3. Notice that No filtering gives relatively noisy data (e.g., matching a bicycle with a caption: “IMG_2187.jpg”), while CLIP score samples give qualitatively more descriptive captions.



Organos muntoriales



20110531 4665RWw [F]
Grotte des Demoiselles
[Ganges]



【iPhone6s Plus/6 Plusケー
ス】WiFiブースター
LINKASE クリア with WiFi
スペースグレイ iPhone 6s
Plus/6 Plus_0



中村不折旧宅（書道博物館）



IMG_2187.jpg



Carregador portátil para
Smartphones 5000mAh 5V
2.1A - JS Soluções em
Segurança



NACIO EUROPA EN LA
EDAD MEDIA



JUMP LEADS HEAVY DUTY
COMMERCIAL 4.5 M 700
AMP



Energy Stocks Fuel Market
Rally



2019-02-08废金属价格相关
热搜新闻一览

Figure 18: An i.i.d. sample from `small COMMONPOOL` generated after applying the *No filter* strategy. Hence, these samples represent random images from `COMMONPOOL`.



status report templates -
12+ free word documents
download | free,
Powerpoint templates



Implication in the
classroom:
O Step 3: We Must Work it
Out
Say and mean "We have to
work it out". The behaviour
cannot
co...



City 39 mm Quartz



Astro ATA 3050 INSERTION
TOOL, 16/20 GA



1006: Rookwood pink mat
vase, 1929, 2382, 6"



WN | 2 Corinthians
10:1-18 | Meekness or
Boldness?



Chaussure De Running
Junior Asics Gt-1000 Gs
Bleu/vert - Asics - 37



Shopping Fairy Crochet
Pattern, crochet wings,
crochet shopping bags,
crochet doll

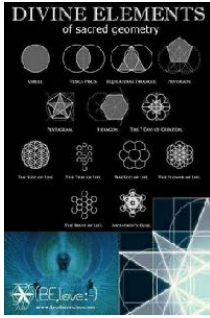


Luxardo, Maraschino
Cherries, 14 Fl Oz :
Grocery & Gourmet Food

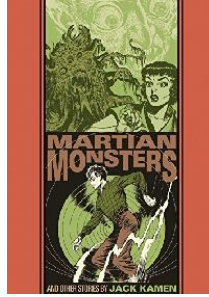


Essay Outlines Exles by
Writing Center Workshops
The Outline

Figure 19: An i.i.d. sample from small COMMONPOOL generated after applying the *Basic filter* strategy.



Sacred Geometry Egg Of Life, Sacred Geometry Symbols, Golden Ratio, Flower Of Life, Wicca, Magick, Tattoos, Geometric Nature, Geometric Mandala



The Martian Monster And Other Stories (The EC Comics Library) ()



Porsche Cayman S



Mesmerizing Black, Silver & Pink Handmade Modern Metal Wall Art Sculpture - Metallic One of a Kind Abstract Painting - OOK 546 by Jon Allen



ALPINESTARS Radar Short navy blue



Under Armour Heatgear Gotta Have It Shorty - Women's at Foot Locker



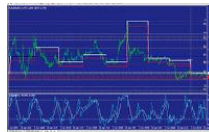
Tripod Delphin TPX3 Silver



Football Manager 2016



Mett.jpg auf www.funpot.net



Profitable forex trading systems

Figure 20: An i.i.d. sample from small COMMONPOOL generated after applying the CLIP score (L/14 30%) strategy.

O.1 Filtering track

Basic filtering. For language detection, we use Fasttext 0.92, version lid.176, and cld3 - library gld3 3.0.13. We count the number of words in each caption by splitting using whitespaces.

CLIP thresholds. We use OpenAI pretrained CLIP ViT-B/32 and ViT-L/14 models [102] to compute the cosine similarity text and image tower outputs as the CLIP scores. On the `small` and `medium` pools, we also experiment with baselines that filter out samples in the top few percentiles of CLIP scores. Specifically, we try baselines that use samples with top $\{1,2,5\}$ -30% CLIP scores (ViT-B/32 model), and the performance is slightly better on the `small` pool (at most 0.5 gain of averaged accuracy) while slightly worse on the `medium` pool (0.4-0.8 loss of averaged accuracy). In Table 14, we show how the CLIP score thresholds relate to the fraction of the pool retained by the filter.

Text-based filtering. Each synset is represented by a synset offset that can be used to retrieve the synset from WordNet. In order to verify if a caption has a word corresponding to a synset from our set we iterate over every word and retrieve the synsets that this word can describe (using `nlk.corpus` WordNet). Following that, we retrieve the most likely lemma representing that synset, find its synset offset, and check if the number is part of the IN21K or IN1K sets.¹⁰

Text-based sampling. This baseline uses text only to filter labels which mention concepts (synsets) appearing in IN21K, and applies a temperature parameter to control how equally-represented different concepts are in the dataset. For synset j , let N_j be the number of examples containing words matched to that synset, where as before for each word we only match the most likely synset. Furthermore, for image-text pair i let T_i be the set of synset matched to the caption.

The probability of sampling example i is proportional to either $\frac{1}{|T_i|} \sum_{j \in T_i} N_j^{\alpha-1}$ (average synset score in the data point) or $\max_{j \in T_i} N_j^{\alpha-1}$ (maximum synset score in the data point), where α is a “temperature” parameter controlling the flatness of the distribution. We sample examples with replacement but discard any example repeated more than 100 times.

Image-based filtering. We now provide a detailed description of the Image-based filtering procedure. First, since the core of the procedure concerns only image content, we begin with basic text-based filtering: we remove from the pool only all examples with non-English captions (as determined by `fasttext`), and all examples whose captions have less than two words or less than six characters.

Next, we use clustering of image embeddings to select a subset of examples whose image content is related to a clean training set of interest. Let e_1, \dots, e_M denote the CLIP image embeddings of the remaining examples in the pool. We cluster these embeddings into $K = 10^5$ clusters using Faiss with 20 iterations, and let c_1, \dots, c_K denote the resulting cluster centers. Due to memory constraints, for the `large` and `xlarge` pools, we perform the clustering on a random subset of about 160M examples (that pass the basic text-based filtering). For an embedding vector v , let

$$I(v) = \arg \max_{i \leq K} \langle v, c_i \rangle$$

denote the index of the cluster center nearest to v as measured by inner product. Let f_1, \dots, f_N denote the CLIP image embeddings of a clean supervised training set (we experiment with either

¹⁰For the ImageNet 21K synsets, we have used the list in https://storage.googleapis.com/bit_models/imagenet21k_wordnet_ids.txt

Table 14: CLIP threshold filtering configurations. “Fraction” denotes the size of the filtered subset relative to the pool.

CLIP model	En. filtering	Threshold	Fraction
ViT-B/32	✗	0.384	1%
ViT-B/32	✗	0.358	3%
ViT-B/32	✓	0.300	10.2%
ViT-B/32	✗	0.325	10%
ViT-B/32	✓	0.28	7.4%
ViT-B/32	✗	0.300	20%
ViT-B/32	✗	0.281	30%
ViT-B/32	✗	0.263	40%
ViT-B/32	✗	0.247	50%
ViT-B/32	✗	0.215	75%
ViT-B/32	✗	0.193	90%
ViT-L/14	✗	0.364	1%
ViT-L/14	✗	0.334	3%
ViT-L/14	✓	0.300	5.4%
ViT-L/14	✗	0.295	10%
ViT-L/14	✓	0.280	3.3%
ViT-L/14	✗	0.266	20%
ViT-L/14	✗	0.243	30%
ViT-L/14	✗	0.222	40%
ViT-L/14	✗	0.203	50%
ViT-L/14	✗	0.160	75%
ViT-L/14	✗	0.129	90%

ImageNet 1K or ImageNet 21K), and let

$$\mathcal{S} = \{I(f_i) \mid 1 \leq i \leq N\}$$

be the set of cluster indices who are nearest neighbors to some clean training set image. We then keep only images in the pool whose nearest cluster center is in \mathcal{S} . That is, out of the M examples passing the text-based filtering, the output subset keeps the examples with indices

$$\{1 \leq j \leq M \mid I(e_j) \in \mathcal{S}\}.$$

Image-based sampling. In addition to filtering methods, we experiment with cluster-based sampling methods. First, we compute the score of i -th cluster s_i as the number of ImageNet data assigned to this cluster. Then, for parameter $\alpha > 0$ we define a distribution over the pool by sampling cluster i with probability $\frac{s_i^\alpha}{\sum_j s_j^\alpha}$ and uniformly sampling an example for the cluster, rejecting any example repeated more than 100 times. We try 5 different α , i.e., $\{0, 0.2, 0.5, 1.0, 2.0\}$, and the best average accuracy is obtained when $\alpha = 0.2$, while the performance is still worse than the image-based filtering on the **small** and **medium** pool. We therefore do not include this line of baselines in the experiments of **large** pool.

ImageNet distance filtering. We rank the samples in the pool by the minimum embedding distance (1 minus cosine similarity) between its image and the ImageNet images; both embeddings are obtained from OpenAI pretrained CLIP ViT-L/14 model [102]. Then we select top images by different fractions as in image-based filtering methods.

Table 15: Measuring the quality of external data sources

Dataset	Dataset size	ImageNet acc.	Avg. accuracy		Avg. cos. sim. (B/32)	Avg. cos. sim. (L/14)
			ImageNet	and OOD sets		
CC12M	10M	27.8	34.0		0.306	0.268
YFCC15M	15M	22.6	24.6		0.262	0.198
RedCaps	11M	26.8	31.5		0.281	0.240
Shutterstock	15M	21.0	28.3		0.314	0.273

O.2 BYOD track

We experiment with the following data sources:

- CC12M [19]: images and HTML alt-text crawled and filtered from web pages.
- YFCC15M: this is the 15M subset of the YFCC100M dataset [129] that Radford et al. [102] used for dataset ablation in their CLIP paper.
- RedCaps [33]: 12M images and corresponding captions were crawled from 350 manually curated subreddits between 2008 and 2020.
- Shutterstock: 106M images and captions were obtained from the Shutterstock website in 2021 [93]. We use the “photos” subset of this dataset, with 58M samples, which we found performed best, unless specified otherwise.
- WIT [125]: Image-text pairs from Wikipedia pages. We use the attribution fields as captions, which we found performed best.
- COYO [15]: A collection of 700M image-text pairs from Common Crawl.
- LAION-2B [120]: A 2.32 billion english subset of LAION-5B.
- LAION-COCO: A dataset with 600M images from LAION-5B and synthetic captions.¹¹
- LAION-A: According to laion.ai, LAION-A is a 900M subset of LAION-2B [120] with the aesthetic filtering procedure used in LAION-aesthetic¹² and pHash deduplication [63].

In Table 15, we use some heuristics to measure the quality of the external data sources. First, following Nguyen et al. [93], we train a CLIP model on a 5M random subset from each source, and evaluate the performance of the resulting models on ImageNet and ImageNet-derived distributions — ImageNet-V2 [112], ImageNet-R [57], ImageNet-Sketch [132] and ObjectNet [9]. Moreover, for each data source, we use OpenAI’s pretrained CLIP ViT-B/32 and ViT-L/14 models to compute the cosine similarity between image and text embeddings of a data point, and obtain the average cosine similarity score for the whole dataset.

O.2.1 Additional results

We present a series of additional results for the BYOD track in Table 16.

¹¹<https://laion.ai/blog/laion-coco/>

¹²<https://github.com/LAION-AI/laion-datasets/blob/main/laion-aesthetic.md>

Table 16: Zero-shot performance for select baselines in the BYOD track. Unless specified otherwise, COMMONPOOL means our pool filtered with CLIP score (L/14, 30%).

Scale	Data source	Training dataset size	ImageNet	ImageNet dist. shifts	VTAB	Retrieval	Average over 38 datasets
small	#0	CC12M	0.099	0.080	0.223	0.160	0.202
	#1	LAION15M	0.083	0.076	0.210	0.119	0.187
	#2	RedCaps	0.076	0.066	0.177	0.127	0.167
	#3	Shutterstock 15M	0.083	0.070	0.214	0.128	0.183
	#4	YFCC15M	0.071	0.046	0.182	0.120	0.162
	#5	#0 + #1 + #2	0.097	0.084	0.208	0.131	0.192
	#6	#0 + #1 + #3	0.091	0.081	0.222	0.138	0.202
	#7	#0 + #2 + #3 + #4	0.095	0.075	0.205	0.135	0.184
	#8	#0-4	0.093	0.076	0.205	0.135	0.191
medium	#9	CC12M	0.245	0.189	0.283	0.206	0.266
	#10	LAION15M	0.270	0.215	0.317	0.181	0.300
	#11	RedCaps	0.237	0.166	0.271	0.150	0.261
	#12	Shutterstock 15M	0.229	0.191	0.316	0.190	0.284
	#13	YFCC15M	0.232	0.137	0.263	0.174	0.251
	#14	#9 + #10 + #11	0.376	0.287	0.387	0.227	0.358
	#15	#9 + #10 + #12	0.342	0.278	0.362	0.242	0.349
	#16	#9 + #11 + #12 + #13	0.360	0.268	0.365	0.190	0.338
	#17	#9-13	0.371	0.285	0.408	0.194	0.361
	#18	Shutterstock illustration	0.053	0.094	0.205	0.112	0.179
	#19	Shutterstock photo	0.342	0.209	0.364	0.248	0.323
	#20	Shutterstock vectors	0.072	0.151	0.216	0.129	0.206
	#21	Shutterstock full	0.313	0.254	0.353	0.240	0.335
	#22	WIT full	0.096	0.063	0.196	0.088	0.175
	#23	WIT English	0.051	0.038	0.145	0.073	0.142
	#24	COYO	0.272	0.235	0.333	0.249	0.314
	#25	LAION-COCO	0.209	0.205	0.293	0.243	0.288
large	#26	Shutterstock illustration	0.337	0.203	0.307	0.223	0.298
	#27	Shutterstock photo	0.485	0.304	0.432	0.311	0.389
	#28	Shutterstock vectors	0.126	0.223	0.244	0.152	0.243
	#29	Shutterstock full	0.500	0.412	0.472	0.335	0.447
	#30	COYO	0.615	0.504	0.529	0.332	0.522
	#31	LAION-COCO	0.355	0.351	0.395	0.366	0.388
	#32	COYO + LAION-COCO	0.528	0.458	0.479	0.466	0.488
	#33	LAION-A	0.611	0.474	0.501	0.414	0.495
	#34	COMMONPOOL + #9-13	0.602	0.498	0.541	0.284	0.527
	#35	COMMONPOOL + #9-13 (2x upsampled)	0.613	0.507	0.559	0.293	0.532
	#36	COMMONPOOL + #9-13 (4x upsampled)	0.615	0.514	0.553	0.295	0.533
	#37	COMMONPOOL + #9-13 (6x upsampled)	0.620	0.519	0.558	0.301	0.538
	#38	COMMONPOOL + #9-13 (8x upsampled)	0.624	0.520	0.533	0.302	0.526
	#39	COMMONPOOL + #9-13 (10x upsampled)	0.621	0.520	0.540	0.303	0.527
	#40	COMMONPOOL + COYO	0.561	0.472	0.504	0.375	0.503
	#41	COMMONPOOL + LAION-A	0.607	0.480	0.531	0.386	0.517
	#42	COMMONPOOL + LAION-COCO	0.522	0.457	0.513	0.374	0.504
	#43	COMMONPOOL + #11+#13+#19	0.609	0.508	0.546	0.303	0.525
	#44	COMMONPOOL + #11+#13+#19 (2x upsampled)	0.621	0.509	0.547	0.315	0.530
	#45	COMMONPOOL + #11+#13+#19 (4x upsampled)	0.632	0.515	0.533	0.316	0.522
	#46	COMMONPOOL + #11+#13+#19 (6x upsampled)	0.635	0.515	0.535	0.329	0.521
	#47	COMMONPOOL + #11+#13+#19 (8x upsampled)	0.633	0.515	0.523	0.328	0.520
	#48	COMMONPOOL + #11+#13+#19 (10x upsampled)	0.630	0.513	0.523	0.317	0.510
xlarge	#49	COMMONPOOL + #11+#13+#19	0.766	0.660	0.662	0.394	0.648
	#50	COMMONPOOL + #11+#13+#19 (6x upsampled)	0.776	0.671	0.633	0.410	0.638
	#51	COMMONPOOL + #11+#13+#19 (18x upsampled)	0.771	0.667	0.629	0.418	0.633

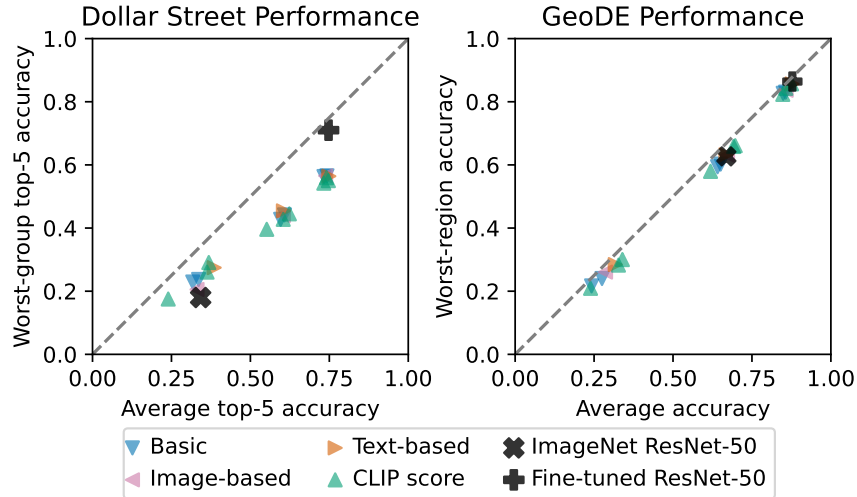


Figure 21: Comparison of average and worst-group scores for Dollar Street and GeoDE diversity datasets. On Dollar Street, our overall higher-performing models display a larger worst-group performance gap (corresponding to lower income households). GeoDE does not appear to show this trend.

P Fairness and biases

To study the biases displayed by our models, we include two diversity-related datasets, Dollar Street [113] and GeoDE [105], in our evaluation suite, and perform further analysis on the face datasets FairFace [71] and UTKFace [147] with demographic labels, following Radford et al. [102].

P.1 Diversity

We break down model performance on the Dollar Street and GeoDE datasets in Figure 21. Dollar Street consists of images of household items taken in homes around the world, and represents a wide socioeconomic range that includes homes with no Internet access [113]. The objects belong to ImageNet categories, and the task is image classification. Standard ImageNet-trained models achieve monotonically increasing performance levels with higher household income levels [113]. Here we use the income-based subgroups defined in Rojas et al. [113], and find a similar bias as discovered in their paper. While our trained models show a smaller worst-group performance gap than an ImageNet-trained ResNet-50, they underperform a model fine-tuned on Dollar Street. Models with higher average accuracy show a larger worst-group gap, which future work should try to address.

GeoDE consists of images of everyday items and objects, which again fall into ImageNet categories. The dataset represents six world regions equally, and primarily aims to promote geographic diversity of datasets [105]. Both ImageNet models and our models show less bias under this distribution compared to Dollar Street, with a smaller worst-group accuracy gap. The trends show that performance across all regions improves steadily with increased scale, and the performance approaches that of a model fine-tuned on GeoDE. While we know that classifiers trained specifically on ImageNet can display geographic biases [105], these biases are not apparent in our GeoDE model evaluations. Future work is needed to investigate the extent to which our models have geographic biases not evaluated in

GeoDE.

P.2 Fairness

Emulating Radford et al. [102], we evaluate our best models from the filtering and BYOD track baselines on the human face datasets FairFace and UTKFace, using zero-shot classification to predict race, gender, and age. Note that these are not intended end-goals of the model or benchmark, but rather probes into models behave differently across demographic subgroups. As described in Appendix G, our filtering track models are trained on images with faces blurred. Nevertheless, these models still perform significantly above random chance on face classification. We hypothesize that this is due to a combination of faces bypassing our face blurring filter in the training data, contextual clues outside of the face region, or signal associated with skin color. The BYOD track model performs even better than the Filtering track model. We hypothesize that this is because BYOD data is used off-the-shelf and hence contains non-blurred faces. In Table 17, we present overall accuracy for these three traits. Note that race is treated as a binary variable (white or non-white) to enable comparison to prior results; gender is a binary variable (male or female) according to annotations; and age is binned into 9 ranges according to the annotation precision of FairFace. The BYOD model, performs better at distinguishing gender, but is worse at distinguishing race and age.

We further break down these statistics over the intersection of race and gender, examining gender classification accuracies in Table 18. We find that there are drastic differences in accuracy across different subgroups, varying by both race and gender. The filtering models shows a tendency to misclassify Black, Southeast Asian, and East Asian males as females at 20.7%, 17%, and 19.3% respectively on FairFace. Furthermore, we find that while the BYOD model improves accuracy, in FairFace most of this improvement is on men (ranging from 1.7pp gain to 9.9pp gain), while on women, it offers little change (ranging from 0.6pp gain to 6.2pp drop).

Following Radford et al. [102], we also examined associations of particular demographics with potentially harmful language. We replicate their setup with two classification task: (1) including race-gender intersection classes (e.g. “black woman”, “indian man”, etc.), as well as several harmful crime-related terms (“thief”, “criminal”, “suspicious person”) and (2) out same race-gender intersection classes as well as non-human terms (“animal”, “gorilla”, “chimpanzee”, “orangutan”). We compute the frequency of misclassification of people into one of the harmful categories and run these experiments on FairFace and UTKFace separately. The results are shown in Table 19. Unlike in Radford et al. [102], we find that our models have a very small probability of classifying human faces as non-human, with a max score across all subgroups of 0.1%. However, a significant proportion of people are misclassified as criminal. The model is better at classifying race and gender, but also more susceptible to assigning unfounded associations with images. This again highlights the importance of dataset curation and the risks associated with zero-shot classification on models trained on such web-scraped datasets.

Table 17: Overall race, gender, and age classification accuracy of our two best `xlarge` baselines, Image-based \cap CLIP score (L/14 30%) for the filtering track and COMMONPOOL, CLIP score + 4 external sources (upsampled 6x) for the BYOD track. Race classification was binary (white or non-white) as in Karkkainen & Joo [71].

Dataset	Track	Race	Gender	Age
FairFace	Filtering	86.4	91.7	34.3
	BYOD	76.5	93.9	33.8
UTKFace	Filtering	86.2	93.8	39.5
	BYOD	86.1	95.5	38.6

Table 18: Gender classification accuracy of our two best `xlarge` baselines, Image-based \cap CLIP score (L/14 30%) for the filtering track and COMMONPOOL, CLIP score + 4 external sources (upsampled 6x) for the BYOD track.

FairFace								
Track	Gender	Race						
		Black	White	Indian	Latino/Hispanic	Middle Eastern	Southeast Asian	East Asian
Filtering	Male	79.3	91.3	90.8	90.4	95.7	83.0	80.7
	Female	95.4	96.6	94.2	96.6	96.5	97.2	98.2
BYOD	Male	89.2	94.8	93.2	93.4	97.4	90.2	90.6
	Female	89.2	96.0	94.2	96.0	96.2	97.1	97.0

UTKFace						
Track	Gender	Race				
		Black	White	Indian	Asian	Other
Filtering	Male	95.4	92.5	91.7	73.1	84.2
	Female	97.3	98.7	97.4	98.3	97.4
BYOD	Male	96.8	95.9	94.7	85.7	90.4
	Female	96.3	97.7	96.8	95.9	95.6

Table 19: Harmful misclassification rates of our two best `xlarge` baselines, Image-based \cap CLIP score (L/14 30%) for the filtering track and COMMONPOOL, CLIP score + 4 external sources (upsampled 6x) for the BYOD track. While very few samples are misclassified as non-human, the filter track model assigns a crime-related label to a significant portion of people, and this is exacerbated by the BYOD model in many cases.

FairFace								
Track		Race						
		Black	White	Indian	Latino/Hispanic	Middle Eastern	Southeast Asian	East Asian
Filtering	Crime-related	4.4	24.3	8.8	14.3	23.7	7.4	8.6
	Non-human	0.0	0.0	0.0	0.0	0.0	0.0	0.0
BYOD	Crime-related	18.4	16.8	21.5	22.9	20.9	35.3	30.9
	Non-human	0.0	0.1	0.0	0.1	0.0	0.1	0.1

UTKFace						
Track		Race				
		Black	White	Indian	Asian	Other
Filtering	Crime-related	6.8	16.1	9.1	6.9	13.9
	Non-human	0.0	0.2	0.0	0.1	0.0
BYOD	Crime-related	12.8	10.8	15.2	13.2	18.6
	Non-human	0.0	0.2	0.0	0.0	0.0

Table 20: Rank correlation between the performance obtained with various filtering strategies at two different scales. Our experimental suggest that the ranking is relatively consistent between scales, especially for the adjacent scale pairs.

Metric	small vs medium	small vs large	medium vs large
ImageNet acc.	0.901	0.830	0.863
Average pref. metric	0.862	0.738	0.889

Q Extra figures and tables

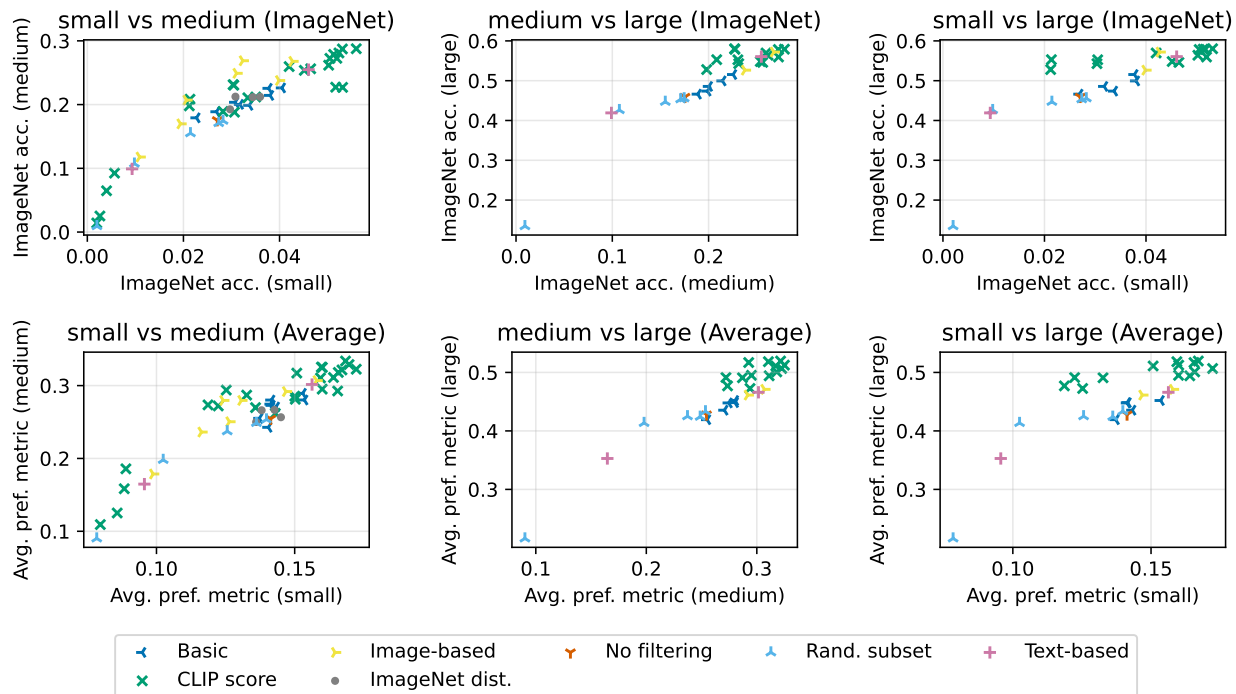


Figure 22: Improving downstream performance at smaller scales correlates positively with performance gains at larger scales. These trends suggests that dataset filtering can be studied effectively at smaller scales, even with less computational resources.

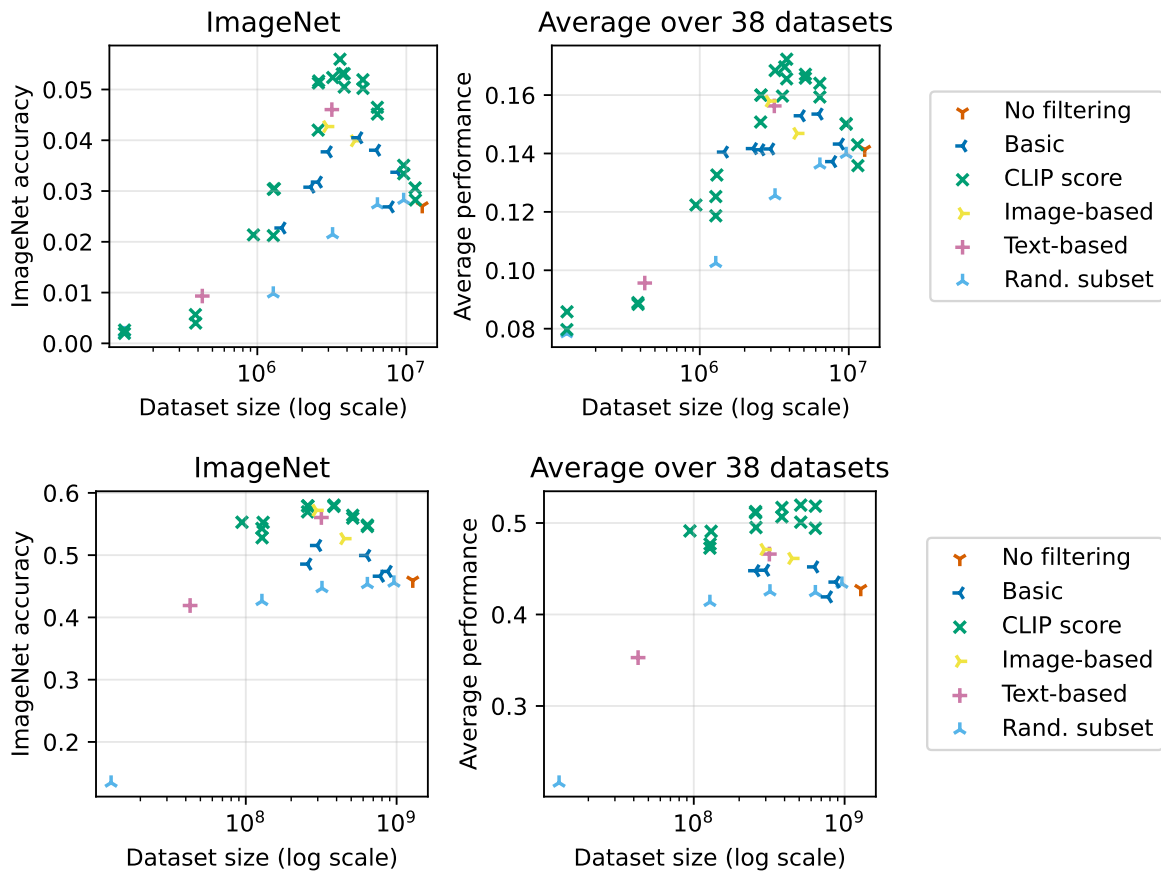


Figure 23: Performance as a function of the number of training samples from the `small` (top) and `large` (bottom) scales. There is a significant variance in accuracy even when accounting for the size of the training set.

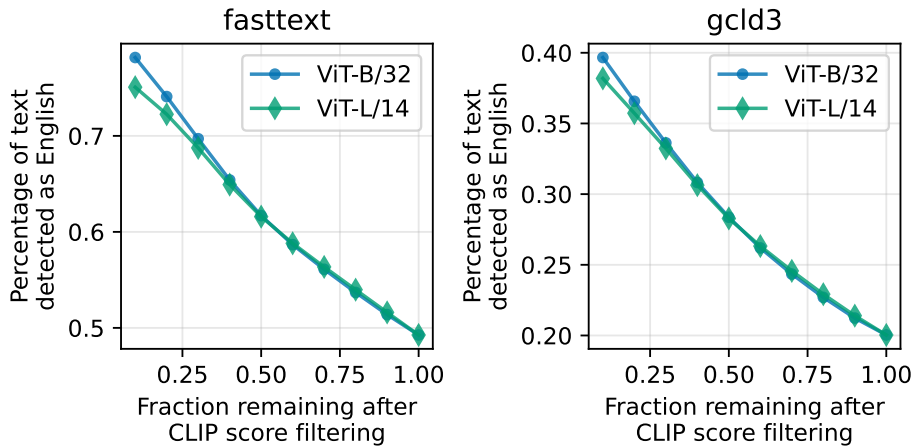


Figure 24: We examine the percentage of texts classified as English after taking the top fraction (on the x-axis) of the `large` billion pool as sorted by CLIP similarity score. We see that doing CLIP filtering implicitly does some English filtering, as image-text pairs with a higher CLIP score are more frequently classified as English.

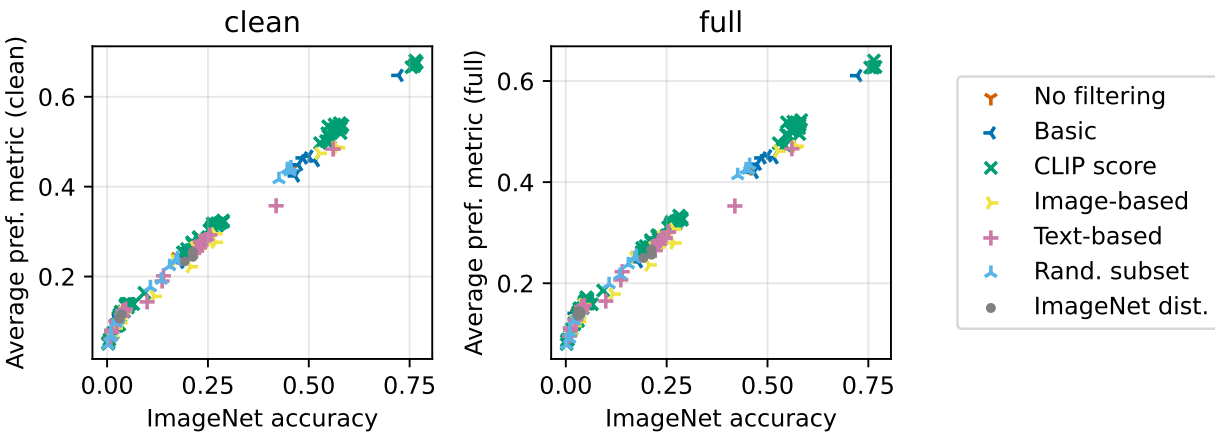


Figure 25: Correlation between ImageNet accuracy and average performance on our suite of evaluation tasks. While ImageNet accuracy strongly correlates with the average performance (both on the clean subset and the full suite), the same is not true for all individual datasets we study, as shown in Appendix Q.

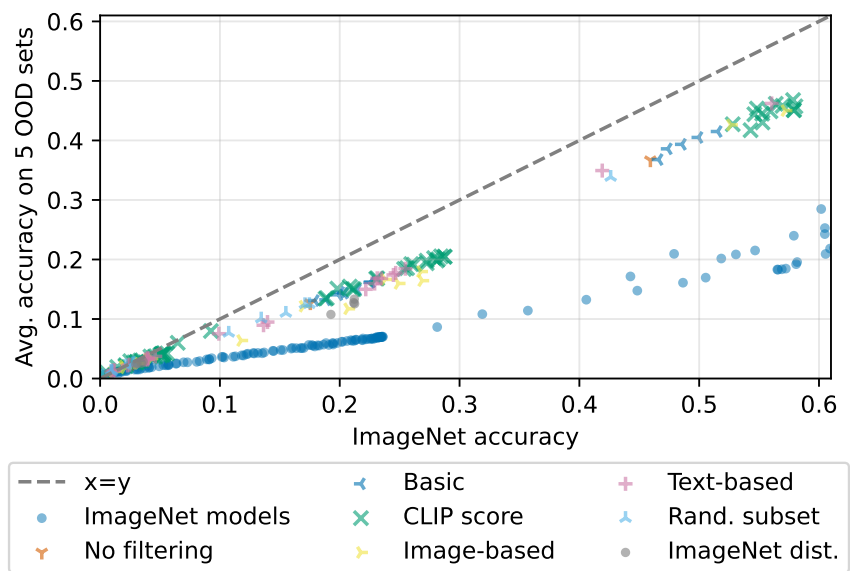


Figure 26: Zero-shot CLIP models trained with various filtering strategies form a reliable trend relating accuracy on ImageNet and related distribution shifts, exhibiting higher effective robustness when compared to ImageNet-trained models from Taori et al. [128].

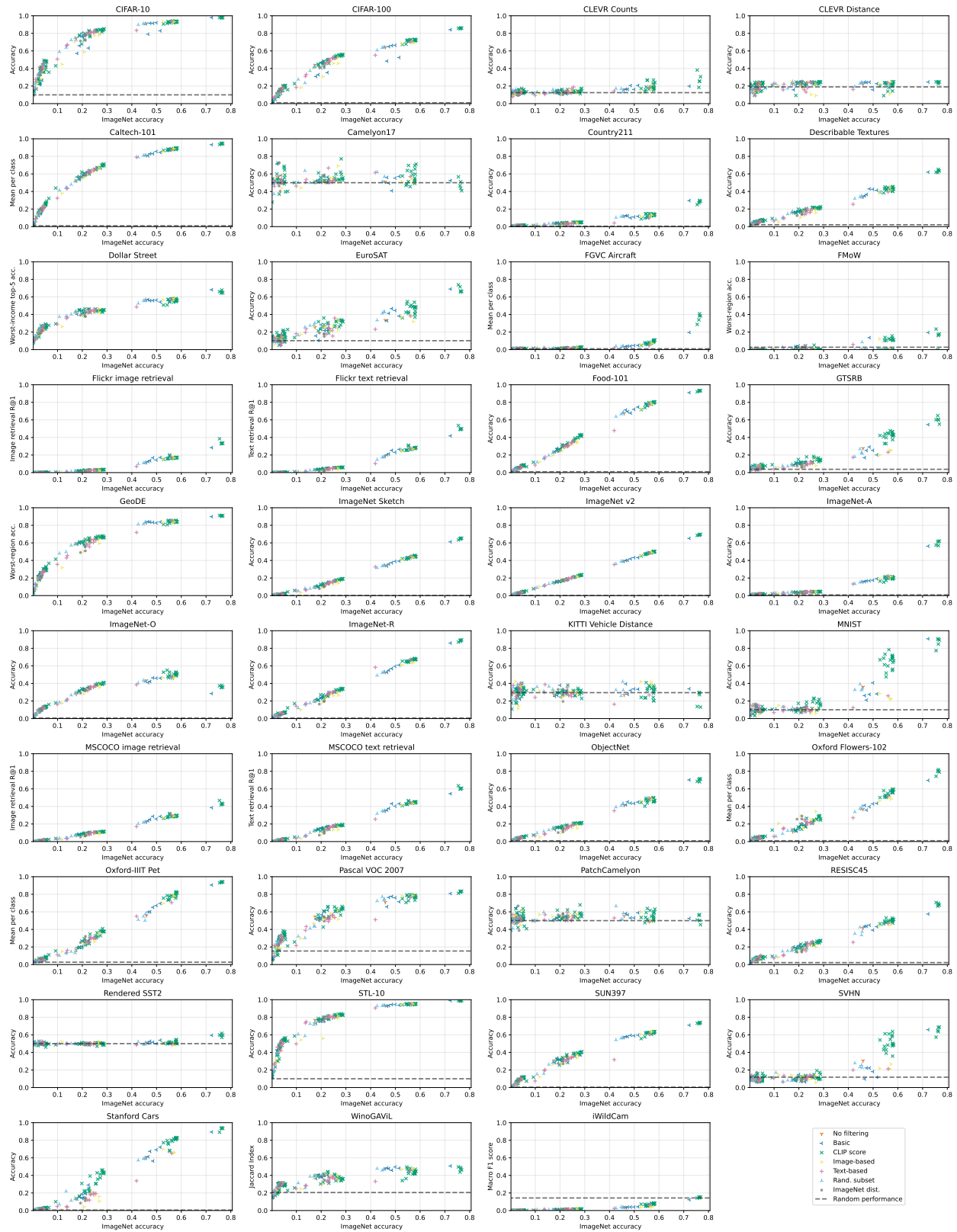


Figure 27: Zero-shot performance on other datasets is often positively correlated with that on ImageNet, but not always. In cases where ImageNet shows close to zero correlation with other datasets, performance on that dataset is often close to random chance.

Table 21: Baseline results for the filtering track, small scale.

Filtering	Training dataset size	ImageNet	ImageNet dist. shifts	VTAB	Retrieval	Average over 38 datasets
No filtering	12.8M	0.025	0.033	0.145	0.105	0.132
Random subset (75%)	9.6M	0.028	0.037	0.153	0.102	0.140
Random subset (50%)	6.4M	0.027	0.037	0.147	0.105	0.136
Random subset (25%)	3.2M	0.022	0.032	0.130	0.094	0.126
Random subset (10%)	1.3M	0.010	0.018	0.116	0.075	0.102
Random subset (1%)	128K	0.002	0.005	0.095	0.049	0.078
Caption length	8.7M	0.034	0.040	0.148	0.109	0.143
Image size	7.8M	0.027	0.036	0.154	0.111	0.137
English (fasttext)	6.3M	0.038	0.045	0.164	0.113	0.153
English (fasttext) and caption length	4.8M	0.041	0.048	0.159	0.111	0.153
English (fasttext), caption length, and image size	3.0M	0.030	0.040	0.149	0.111	0.137
English (cld3)	2.6M	0.032	0.039	0.143	0.100	0.141
English (cld3) and caption length	2.3M	0.031	0.038	0.153	0.103	0.142
English (cld3), caption length, and image size	1.5M	0.023	0.030	0.154	0.087	0.140
CLIP B32 score top 1%	129K	0.003	0.007	0.114	0.049	0.086
CLIP B32 score top 3%	384K	0.006	0.014	0.104	0.054	0.089
CLIP B32 score top 10%	1.3M	0.026	0.035	0.147	0.072	0.127
CLIP B32 score top 20%	2.6M	0.051	0.056	0.173	0.103	0.160
CLIP B32 score top 30%	3.8M	0.045	0.052	0.180	0.103	0.159
CLIP B32 score top 40%	5.1M	0.052	0.057	0.173	0.109	0.166
CLIP B32 score top 50%	6.4M	0.047	0.053	0.174	0.114	0.164
CLIP B32 score top 75%	9.6M	0.033	0.043	0.161	0.110	0.150
CLIP B32 score top 90%	11.5M	0.028	0.039	0.140	0.108	0.136
CLIP B32 threshold at 0.3 + English filter	942K	0.022	0.032	0.138	0.073	0.121
CLIP B32 threshold at 0.28 + English filter	1.3M	0.031	0.040	0.136	0.085	0.133
CLIP B32 threshold at 0.3	2.6M	0.052	0.056	0.166	0.102	0.160
CLIP B32 score 1% to 30%	3.7M	0.053	0.058	0.185	0.102	0.170
CLIP B32 score 2% to 30%	3.6M	0.056	0.059	0.173	0.108	0.160
CLIP B32 score 5% to 30%	3.2M	0.052	0.055	0.177	0.104	0.168
CLIP L14 score top 1%	128K	0.002	0.007	0.111	0.049	0.080
CLIP L14 score top 3%	386K	0.004	0.009	0.110	0.052	0.088
CLIP L14 score top 10%	1.3M	0.021	0.033	0.131	0.071	0.119
CLIP L14 score top 20%	2.6M	0.042	0.051	0.165	0.100	0.151
CLIP L14 score top 30%	3.8M	0.051	0.055	0.190	0.108	0.172
CLIP L14 score top 40%	5.1M	0.050	0.054	0.173	0.107	0.167
CLIP L14 score top 50%	6.4M	0.045	0.052	0.164	0.110	0.159
CLIP L14 score top 75%	9.6M	0.035	0.043	0.164	0.111	0.150
CLIP L14 score top 90%	11.5M	0.031	0.038	0.154	0.109	0.143
Image-based clustering (ImageNet1k)	2.9M	0.043	0.047	0.178	0.112	0.158
Image-based clustering (ImageNet21k)	4.5M	0.035	0.045	0.154	0.112	0.146
Image-based sampling, $\alpha=0$	12.8M	0.019	0.030	0.144	0.091	0.126
Image-based sampling, $\alpha=0.2$	12.8M	0.031	0.036	0.133	0.094	0.131
Image-based sampling, $\alpha=0.5$	12.8M	0.032	0.038	0.129	0.091	0.124
Image-based sampling, $\alpha=1$	12.8M	0.021	0.028	0.128	0.076	0.116
Image-based sampling, $\alpha=2$	12.8M	0.011	0.017	0.116	0.063	0.099
ImageNet distance (L14, top 30%) and English	2.0M	0.031	0.039	0.163	0.097	0.145
ImageNet distance (L14, top 20%)	2.6M	0.030	0.035	0.155	0.096	0.136
ImageNet distance (L14, top 30%)	3.9M	0.034	0.041	0.151	0.099	0.138
ImageNet distance (L14, top 40%)	5.1M	0.036	0.040	0.151	0.110	0.143
Text-based clustering (ImageNet1k)	427K	0.009	0.016	0.120	0.055	0.096
Text-based clustering (ImageNet21k)	3.2M	0.046	0.052	0.169	0.112	0.156
Text-based sampling with average score, $\alpha=0$	12.8M	0.011	0.020	0.128	0.078	0.112
Text-based sampling with average score, $\alpha=0.5$	12.8M	0.023	0.035	0.127	0.088	0.127
Text-based sampling with average score, $\alpha=1$	12.8M	0.040	0.044	0.163	0.105	0.154
Text-based sampling with average score, $\alpha=1.2$	12.8M	0.038	0.045	0.150	0.101	0.142
Text-based sampling with max score, $\alpha=0$	12.8M	0.012	0.020	0.126	0.073	0.107
Text-based sampling with max score, $\alpha=0.5$	12.8M	0.025	0.033	0.134	0.089	0.128
Text-based sampling with max score, $\alpha=1$	12.8M	0.040	0.046	0.159	0.106	0.149
Text-based sampling with max score, $\alpha=1.2$	12.8M	0.040	0.050	0.161	0.106	0.151
Intersect IN1k image clustering and CLIP B32 score top 30%	1.4M	0.049	0.053	0.150	0.095	0.147
Intersect IN1k image clustering and CLIP L14 score top 30%	1.4M	0.039	0.045	0.162	0.089	0.144
Intersect IN21k image clustering and CLIP B32 score top 30%	2.1M	0.052	0.057	0.179	0.103	0.166
Intersect IN21k image clustering and CLIP L14 score top 30%	2.1M	0.047	0.053	0.176	0.101	0.162

Table 22: Baseline results for the filtering track, medium scale.

Filtering	Training dataset size	ImageNet	ImageNet dist. shifts	VTAB	Retrieval	Average over 38 datasets
No filtering	128M	0.176	0.152	0.259	0.174	0.254
Random subset (75%)	96.0M	0.175	0.154	0.265	0.174	0.254
Random subset (50%)	64.0M	0.171	0.151	0.258	0.170	0.249
Random subset (25%)	32.0M	0.155	0.136	0.246	0.162	0.237
Random subset (10%)	12.8M	0.107	0.095	0.210	0.121	0.198
Random subset (1%)	1.3M	0.009	0.017	0.102	0.064	0.090
Caption length	87.5M	0.199	0.172	0.275	0.182	0.271
Image size	77.8M	0.189	0.163	0.248	0.182	0.255
English (fasttext)	63.0M	0.214	0.182	0.290	0.188	0.280
English (fasttext) and caption length	47.8M	0.226	0.193	0.297	0.192	0.289
English (fasttext), caption length, and image size	29.8M	0.226	0.193	0.284	0.192	0.280
English (cld3)	25.6M	0.200	0.175	0.296	0.181	0.275
English (cld3) and caption length	22.9M	0.204	0.175	0.287	0.181	0.273
English (cld3), caption length, and image size	14.6M	0.179	0.159	0.243	0.167	0.243
CLIP B32 score top 1%	1.3M	0.025	0.037	0.140	0.072	0.125
CLIP B32 score top 3%	3.9M	0.093	0.096	0.205	0.103	0.186
CLIP B32 score top 10%	12.8M	0.231	0.199	0.305	0.152	0.294
CLIP B32 score top 20%	25.7M	0.279	0.234	0.337	0.178	0.325
CLIP B32 score top 30%	38.4M	0.285	0.240	0.355	0.187	0.333
CLIP B32 score top 40%	51.3M	0.273	0.227	0.333	0.193	0.318
CLIP B32 score top 50%	64.0M	0.256	0.219	0.322	0.196	0.311
CLIP B32 score top 75%	96.1M	0.211	0.180	0.301	0.185	0.285
CLIP B32 score top 90%	115M	0.189	0.165	0.279	0.178	0.270
CLIP B32 threshold at 0.3 + English filter	9.4M	0.208	0.184	0.292	0.156	0.272
CLIP B32 threshold at 0.28 + English filter	13.0M	0.230	0.198	0.307	0.170	0.287
CLIP B32 threshold at 0.3	25.9M	0.282	0.233	0.340	0.178	0.327
CLIP B32 score 1% to 30%	37.1M	0.287	0.238	0.347	0.187	0.329
CLIP B32 score 2% to 30%	35.9M	0.288	0.238	0.338	0.184	0.325
CLIP B32 score 5% to 30%	32.0M	0.281	0.230	0.352	0.187	0.334
CLIP L14 score top 1%	1.3M	0.014	0.025	0.136	0.059	0.109
CLIP L14 score top 3%	3.9M	0.065	0.077	0.176	0.088	0.158
CLIP L14 score top 10%	12.8M	0.198	0.183	0.283	0.142	0.274
CLIP L14 score top 20%	25.7M	0.260	0.225	0.326	0.173	0.317
CLIP L14 score top 30%	38.4M	0.273	0.230	0.338	0.183	0.323
CLIP L14 score top 40%	51.2M	0.262	0.226	0.330	0.192	0.322
CLIP L14 score top 50%	64.1M	0.254	0.218	0.322	0.199	0.310
CLIP L14 score top 75%	96.1M	0.212	0.180	0.287	0.190	0.281
CLIP L14 score top 90%	115M	0.188	0.164	0.258	0.178	0.262
Image-based clustering (ImageNet1k)	29.2M	0.268	0.213	0.319	0.193	0.307
Image-based clustering (ImageNet21k)	45.1M	0.238	0.198	0.304	0.193	0.292
Image-based sampling, $\alpha=0$	128M	0.170	0.150	0.266	0.162	0.250
Image-based sampling, $\alpha=0.2$	128M	0.249	0.193	0.292	0.168	0.280
Image-based sampling, $\alpha=0.5$	128M	0.269	0.196	0.301	0.163	0.280
Image-based sampling, $\alpha=1$	128M	0.207	0.145	0.264	0.130	0.236
Image-based sampling, $\alpha=2$	128M	0.118	0.082	0.207	0.094	0.179
ImageNet distance (L14, top 30%) and English	19.8M	0.212	0.158	0.272	0.148	0.257
ImageNet distance (L/14, top 20%)	25.8M	0.193	0.138	0.276	0.149	0.250
ImageNet distance (L/14, top 30%)	38.5M	0.212	0.159	0.283	0.165	0.266
ImageNet distance (L/14, top 40%)	51.3M	0.212	0.165	0.273	0.171	0.267
Text-based clustering (ImageNet1k)	4.3M	0.099	0.090	0.173	0.095	0.165
Text-based clustering (ImageNet21k)	31.7M	0.255	0.215	0.328	0.183	0.301
Text-based sampling with average score, $\alpha=0$	128M	0.136	0.110	0.213	0.114	0.207
Text-based sampling with average score, $\alpha=0.5$	128M	0.222	0.178	0.273	0.157	0.265
Text-based sampling with average score, $\alpha=1$	128M	0.245	0.204	0.302	0.189	0.289
Text-based sampling with average score, $\alpha=1.2$	128M	0.231	0.200	0.298	0.182	0.284
Text-based sampling with max score, $\alpha=0$	128M	0.140	0.116	0.242	0.114	0.223
Text-based sampling with max score, $\alpha=0.5$	128M	0.229	0.190	0.290	0.155	0.279
Text-based sampling with max score, $\alpha=1$	128M	0.247	0.209	0.300	0.183	0.290
Text-based sampling with max score, $\alpha=1.2$	128M	0.235	0.200	0.298	0.178	0.285
Intersect IN1k image clustering and CLIP B32 score top 30%	14.2M	0.305	0.243	0.342	0.182	0.322
Intersect IN1k image clustering and CLIP L14 score top 30%	14.0M	0.297	0.239	0.346	0.170	0.323
Intersect IN21k image clustering and CLIP B32 score top 30%	21.1M	0.298	0.244	0.347	0.184	0.330
Intersect IN21k image clustering and CLIP L14 score top 30%	20.8M	0.290	0.241	0.339	0.182	0.323

Table 23: Baseline results for the filtering track, **large** scale.

Filtering	Training dataset size	ImageNet	ImageNet dist. shifts	VTAB	Retrieval	Average over 38 datasets
No filtering	1.28B	0.459	0.378	0.426	0.305	0.428
Random subset (75%)	960M	0.456	0.379	0.435	0.302	0.434
Random subset (50%)	640M	0.453	0.377	0.427	0.298	0.424
Random subset (25%)	320M	0.447	0.373	0.424	0.294	0.425
Random subset (10%)	128M	0.426	0.350	0.417	0.286	0.414
Random subset (1%)	12.8M	0.135	0.118	0.219	0.105	0.216
Caption length	874M	0.474	0.392	0.438	0.322	0.435
Image size	777M	0.466	0.375	0.421	0.316	0.419
English (fasttext)	630M	0.500	0.414	0.449	0.337	0.452
English (fasttext), caption length, and image size	298M	0.516	0.423	0.446	0.353	0.448
English (cld3)	256M	0.486	0.405	0.462	0.343	0.448
CLIP B32 score top 10%	128M	0.543	0.440	0.471	0.307	0.473
CLIP B32 score top 20%	257M	0.578	0.465	0.516	0.338	0.505
CLIP B32 score top 30%	384M	0.578	0.466	0.525	0.349	0.517
CLIP B32 score top 40%	512M	0.560	0.454	0.512	0.352	0.501
CLIP B32 score top 50%	640M	0.546	0.450	0.504	0.353	0.494
CLIP B32 threshold at 0.3 + English filter	94.3M	0.553	0.447	0.511	0.351	0.491
CLIP B32 threshold at 0.28 + English filter	130M	0.553	0.453	0.510	0.365	0.491
CLIP B32 threshold at 0.3	258M	0.579	0.464	0.501	0.338	0.495
CLIP L14 score top 10%	128M	0.528	0.444	0.482	0.293	0.477
CLIP L14 score top 20%	257M	0.570	0.466	0.524	0.331	0.511
CLIP L14 score top 30%	384M	0.578	0.474	0.538	0.342	0.520
CLIP L14 score top 40%	512M	0.564	0.462	0.533	0.346	0.520
CLIP L14 score top 50%	641M	0.548	0.455	0.539	0.345	0.518
Image-based clustering (ImageNet1k)	294M	0.572	0.454	0.483	0.353	0.471
Image-based clustering (ImageNet21k)	450M	0.527	0.433	0.468	0.337	0.461
Text-based clustering (ImageNet1k)	42.7M	0.419	0.355	0.340	0.210	0.353
Text-based clustering (ImageNet21k)	317M	0.561	0.465	0.465	0.352	0.466
Intersect IN1k image clustering and CLIP B32 score top 30%	143M	0.632	0.498	0.525	0.371	0.517
Intersect IN1k image clustering and CLIP L14 score top 30%	140M	0.631	0.508	0.546	0.369	0.527
Intersect IN21k image clustering and CLIP B32 score top 30%	211M	0.605	0.481	0.531	0.363	0.509
Intersect IN21k image clustering and CLIP L14 score top 30%	208M	0.506	0.416	0.466	0.300	0.461

Table 24: Baseline results for the filtering track, **xlarge** scale.

Filtering	Training dataset size	ImageNet	ImageNet dist. shifts	VTAB	Retrieval	Average over 38 datasets
No filtering	12.8B	0.723	0.612	0.611	0.441	0.611
CLIP B32 score top 30%	3.84B	0.764	0.640	0.628	0.474	0.628
CLIP B32 threshold at 0.28 + English filter	1.3B	0.755	0.637	0.624	0.503	0.627
CLIP L14 score top 20%	2.56B	0.761	0.649	0.630	0.452	0.626
CLIP L14 score top 25%	3.2B	0.768	0.656	0.621	0.465	0.628
CLIP L14 score top 30%	3.84B	0.764	0.655	0.643	0.468	0.641
Intersect IN1k image clustering and CLIP L14 score top 30%	1.38B	0.792	0.679	0.652	0.489	0.653

R Datasheet

R.1 Motivation

Q1 **For what purpose was the dataset created?** Was there a specific task in mind? Was there a specific gap that needed to be filled? Please provide a description.

- The purpose of DATACOMP and the associated COMMONPOOL dataset is to enable study of what makes a strong image-text dataset, which supports a broad range of applications. Prior work mainly focuses on data curation in the context of supervised datasets and smaller scales. For a fuller treatment see Section 2. In our initial release of DATACOMP we focus on 38 downstream image classification and image retrieval tasks. We additionally explore two fairness datasets. For details see Section 3.5 and Appendix N.

Q2 **Who created the dataset (e.g., which team, research group) and on behalf of which entity (e.g., company, institution, organization)?**

- DATACOMP and COMMONPOOL were created by a group of researchers with the following affiliations, listed in alphabetical order: Allen Institute for Artificial Intelligence (AI2), Apple, Columbia University, Graz University of Technology, Hebrew University, Juelich Supercomputing Center, LAION, Research Center Juelich, StabilityAI, Tel Aviv University, University of Illinois Urbana-Champaign, University of Texas at Austin, University of Washington.

Q3 **Who funded the creation of the dataset?** If there is an associated grant, please provide the name of the grantor and the grant name and number.

- Compute for this research was generously provided by StabilityAI. For more specific acknowledgments, see the acknowledgment section at the end of the main paper.

Q4 **Any other comments?**

- No.

R.2 Composition

Q5 **What do the instances that comprise the dataset represent (e.g., documents, photos, people, countries)?** *Are there multiple types of instances (e.g., movies, users, and ratings; people and interactions between them; nodes and edges)? Please provide a description.*

- Each instance is a pair of url and corresponding image alt-text. The url points to an image that a user can then try to download. Each sample is also tagged with metadata, discussed in Q25.

Q6 **How many instances are there in total (of each type, if appropriate)?**

- There are 12.8B instances in COMMONPOOL. For breakdowns and statistics see Appendix I.

Q7 **Does the dataset contain all possible instances or is it a sample (not necessarily random) of instances from a larger set?** *If the dataset is a sample, then what is the larger set? Is the sample representative of the larger set (e.g., geographic coverage)? If so, please*

describe how this representativeness was validated/verified. If it is not representative of the larger set, please describe why not (e.g., to cover a more diverse range of instances, because instances were withheld or unavailable).

- We find ~ 88 B possible samples in common crawl. These samples are globally shuffled to ensure i.i.d. sampling for all sampling based parts of the downstream pipeline. Of these samples we attempt to download ~ 40 B samples. Due to various download issues, such as dead links and throttling, we are able to successfully download ~ 16.8 B samples. After NSFW filtering and evaluation set deduplication we end up with ~ 13.1 B viable samples, from which we randomly sample 12.8B for COMMONPOOL. For a complete treatment and visualization of our data processing funnel, see Appendix H. For each sample we also release metadata shown in Table 9.

Q8 What data does each instance consist of? “Raw” data (e.g., unprocessed text or images) or features? In either case, please provide a description.

- Each sample contains an image url for download and an associated alt-text caption. Additionally, each sample contains metadata fields shown in Table 9 (e.g., image aspect ratio and CLIP features).

Q9 Is there a label or target associated with each instance? If so, please provide a description.

- We do not provide any category labels; however, the text associated with each image can be considered a soft, noisy label for each sample. Such labels are common in modern image-text training paradigms (e.g., image-text representation alignment, image captioning objectives, text-conditional image generation objectives, etc.).

Q10 Is any information missing from individual instances? If so, please provide a description, explaining why this information is missing (e.g., because it was unavailable). This does not include intentionally removed information, but might include, e.g., redacted text.

- No.

Q11 Are relationships between individual instances made explicit (e.g., users’ movie ratings, social network links)? If so, please describe how these relationships are made explicit.

- No.

Q12 Are there recommended data splits (e.g., training, development/validation, testing)? If so, please provide a description of these splits, explaining the rationale behind them.

- No. The test tasks are existing image classification tasks. We run a deduplication model to try to prevent test set contamination in COMMONPOOL.

Q13 Are there any errors, sources of noise, or redundancies in the dataset? If so, please provide a description.

- COMMONPOOL is sourced from Common Crawl, which can be thought of as a snapshot of the internet. Hence, there can be considerable noise (e.g., alt-text being unrelated to its associated image), duplicate data, etc.

Q14 Is the dataset self-contained, or does it link to or otherwise rely on external resources (e.g., websites, tweets, other datasets)? *If it links to or relies on external resources, a) are there guarantees that they will exist, and remain constant, over time; b) are there official archival versions of the complete dataset (i.e., including the external resources as they existed at the time the dataset was created); c) are there any restrictions (e.g., licenses, fees) associated with any of the external resources that might apply to a future user? Please provide descriptions of all external resources and any restrictions associated with them, as well as links or other access points, as appropriate.*

- The data is not self-contained and rather links other external resources on the internet. Links point to resources distributed across the internet. There is no guarantee that the resources will exist in perpetuity or that that the resources will not change. To mitigate against data poisoning in future COMMONPOOL downloads, we release SHA256 hashes of images. Due to the size of the dataset, it is not possible to provide it in an archival form.

Q15 Does the dataset contain data that might be considered confidential (e.g., data that is protected by legal privilege or by doctor–patient confidentiality, data that includes the content of individuals’ non-public communications)? *If so, please provide a description.*

- The dataset is comprised of data that was readily available on the internet at the time of our download. However, it is possible that the dataset contains confidential information (e.g., private data that is hosted publicly for nefarious reasons or out of ignorance of said data being confidential).

Q16 Does the dataset contain data that, if viewed directly, might be offensive, insulting, threatening, or might otherwise cause anxiety? *If so, please describe why.*

- Considering the plurality of people and their backgrounds across the world, it is highly likely that there is content in COMMONPOOL that may upset people. Common Crawl scrapes the internet, which has pornographic, hateful, racist, sexist, and otherwise abhorrent and toxic material. While we attempt to do thorough NSFW filtering, these methods are not 100% accurate. At the 12.8B scale at which we operate it is highly likely that there is still toxic content in the dataset. We consider the dataset as a research artifact and hope future work will look critically at COMMONPOOL in the hopes of developing even better safety filters.

Q17 Does the dataset relate to people? *If not, you may skip the remaining questions in this section.*

- People may appear in the dataset; however, in an effort to preserve privacy, our downloading tooling automatically blurs all detected faces in COMMONPOOL images.

Q18 Does the dataset identify any subpopulations (e.g., by age, gender)?

- While COMMONPOOL does not explicitly identify subpopulations in its metadata, it is plausible to extract such information for some images using the corresponding textual caption.

Q19 Is it possible to identify individuals (i.e., one or more natural persons), either

directly or indirectly (i.e., in combination with other data) from the dataset? If so, please describe how.

- We conjecture that even with our face blurring procedure, it may still be possible to identify individuals. Face blurring relies on a face detection model, which could fail (See Appendix G for experimental validation of the employed detector). It is also possible to identify certain celebrities or athletes, who may wear distinctive clothing that is associated with them. It is also likely that names are contained in textual captions, though it is not guaranteed that these names correspond to people in images due to the inherent noisiness of internet captions.

Q20 Does the dataset contain data that might be considered sensitive in any way (e.g., data that reveals racial or ethnic origins, sexual orientations, religious beliefs, political opinions or union memberships, or locations; financial or health data; biometric or genetic data; forms of government identification, such as social security numbers; criminal history)? If so, please provide a description.

- Yes. COMMONPOOL is created using images and corresponding alt-text that are available on the public internet. Given the 12.8B scale of COMMONPOOL, it is highly likely that there is sensitive data in the dataset. To mitigate against making sensitive content more accessible, we 1) run NSFW image filtering and 2) NSFW text filtering when generating COMMONPOOL, discarding all samples that are flagged. Additionally we 3) provide automatic face blurring in our COMMONPOOL download scripts to blur all detected faces.

Q21 Any other comments?

- No.

R.3 Collection Process

Q22 How was the data associated with each instance acquired? Was the data directly observable (e.g., raw text, movie ratings), reported by subjects (e.g., survey responses), or indirectly inferred/derived from other data (e.g., part-of-speech tags, model-based guesses for age or language)? If data was reported by subjects or indirectly inferred/derived from other data, was the data validated/verified? If so, please describe how.

- Data is directly downloaded from the public internet.

Q23 What mechanisms or procedures were used to collect the data (e.g., hardware apparatus or sensor, manual human curation, software program, software API)? How were these mechanisms or procedures validated?

- We iterate on the LAION-5B data collection process, making an effort to emphasize safety. We ran python based processing scripts to parse Common Crawl dumps, download images, filter out NSFW content, deduplicate samples against downstream test sets, blur faces, and compute CLIP features. We ran processes on 100s of AWS CPU nodes for Common Crawl parsing and data download. Other steps were run on one of StabilityAI's GPU cluster. For software links see Q37. For software validation related to NSFW content filtering and face blurring see Appendices E and G respectively. In brief, for NSFW image filtering, we validate against commercial APIs and on the NSFW test set introduced in

LAION-5B. For face detection (used for face blurring), we evaluate against commercial APIs and on the FairFace dataset. We find strong performance for both modules.

Q24 If the dataset is a sample from a larger set, what was the sampling strategy (e.g., deterministic, probabilistic with specific sampling probabilities)?

- See Q7.

Q25 Who was involved in the data collection process (e.g., students, crowdworkers, contractors) and how were they compensated (e.g., how much were crowdworkers paid)?

- The researching authors were involved in the data collection as an open source effort. No researchers were compensated specifically for their involvement in this project.

Q26 Over what timeframe was the data collected? Does this timeframe match the creation timeframe of the data associated with the instances (e.g., recent crawl of old news articles)? If not, please describe the timeframe in which the data associated with the instances was created.

- Data was downloaded between December 2022 and March 2023. The urls are collected from Common Crawl dumps between 2014 and 2022. Common Crawl dumps may include urls from the early days of the internet. Hence, the download/collection timeframe does not match the creation timeframe. Additionally, future users of COMMONPOOL and its subsets will have to download data themselves using our tooling.

Q27 Were any ethical review processes conducted (e.g., by an institutional review board)? If so, please provide a description of these review processes, including the outcomes, as well as a link or other access point to any supporting documentation.

- Our dataset collection process iterates on the LAION-5B process, which found IRB review was not necessary as they “do not intervene with the people depicted in the data as well as the data being public.” Additionally, the NeurIPS ethics review found no serious ethical issues with LAION-5B. We take even more stringent safety measures than the original LAION-5B dataset, in that we filter out data that is flagged as NSFW by our detection pipeline and blur detected faces in COMMONPOOL in our download scripts. All this being said, a formal ethics review has not been conducted to date.

Q28 Does the dataset relate to people? If not, you may skip the remaining questions in this section.

- Yes. People may appear in the dataset. Detected faces are blurred when downloading COMMONPOOL with our tooling.

Q29 Did you collect the data from the individuals in question directly, or obtain it via third parties or other sources (e.g., websites)?

- We collect data from websites across the internet.

Q30 Were the individuals in question notified about the data collection? If so, please describe (or show with screenshots or other information) how notice was provided, and provide

a link or other access point to, or otherwise reproduce, the exact language of the notification itself.

- Individuals were not notified about the data collection.

Q31 Did the individuals in question consent to the collection and use of their data? *If so, please describe (or show with screenshots or other information) how consent was requested and provided, and provide a link or other access point to, or otherwise reproduce, the exact language to which the individuals consented.*

- Following our usage of Common Crawl and <https://github.com/rom1504/img2dataset> for download images, we respect `robots.txt` files, which specify parts of websites that a crawler may access. It is, however, possible that images of people, medical images, etc. were uploaded to the internet without a person’s consent. To mitigate against such safety concerns we make an effort to do rigorous NSFW filtering and blur all detected faces automatically in our download tooling.

Q32 If consent was obtained, were the consenting individuals provided with a mechanism to revoke their consent in the future or for certain uses? *If so, please provide a description, as well as a link or other access point to the mechanism (if appropriate).*

- In conjunction with LAION, we use <https://laion.ai/dataset-requests/> to monitor user takedown requests. We will also make an effort to provide a user with the url at which their sensitive content is hosted—if they do not have this information already—, so they can take further action as they see fit (e.g., contacting the host to request that the content is taken down from the internet).

Q33 Has an analysis of the potential impact of the dataset and its use on data subjects (e.g., a data protection impact analysis) been conducted? *If so, please provide a description of this analysis, including the outcomes, as well as a link or other access point to any supporting documentation.*

- We conduct a fairness evaluation on models trained on COMMONPOOL and its derivative. See Appendix P for details. [Birhane, et al. 2021](#) conduct an extensive study in the context of LAION-400M, which is an image-text dataset also sourced from Common Crawl, finding a plethora of dangerous and unsafe data. Our dataset differs from LAION-400M in that we conduct NSFW filtering and face blurring for detected faces in our download tooling. However, since COMMONPOOL is created from the internet, it is still likely that COMMONPOOL contains some harmful data.

Q34 Any other comments?

- No.

R.4 Preprocessing, Cleaning, and/or Labeling

Q35 Was any preprocessing/cleaning/labeling of the data done (e.g., discretization or bucketing, tokenization, part-of-speech tagging, SIFT feature extraction, removal of instances, processing of missing values)? *If so, please provide a description. If not, you may skip the remainder of the questions in this section.*

- Yes. See Q7. For more details see Appendix H.

Q36 Was the “raw” data saved in addition to the preprocessed/cleaned/labeled data (e.g., to support unanticipated future uses)? *If so, please provide a link or other access point to the “raw” data.*

- Raw data is not available or distributed due to safety considerations. We distribute only urls that are in the dataset on HuggingFace—and not urls of images our preprocessing flagged as NSFW.

Q37 Is the software used to preprocess/clean/label the instances available? *If so, please provide a link or other access point.*

- We use the following, open-source software to aid in data processing:
 - Apache Spark: <https://spark.apache.org>
 - Ray: <https://www.ray.io>
 - img2dataset: <https://github.com/rom1504/img2dataset>
 - OpenAI CLIP: <https://github.com/openai/CLIP>
 - Near deduplicate detector: <https://github.com/lyakaap/ISC21-Descriptor-Track-1st>
 - Face detector: <https://github.com/deepinsight/insightface>
 - Detoxify, for detecting toxic language: <https://github.com/unitaryai/detoxify>
 - A modified version of the following NSFW image detector: <https://github.com/LAION-AI/CLIP-based-NSFW-Detector>. Specifically, we use the dataset used to train this model to train our own 4-layer MLP classifier.

Q38 Any other comments?

- No.

R.5 Uses

Q39 Has the dataset been used for any tasks already? *If so, please provide a description.*

- The full dataset (and subsets) have been used to train several CLIP models at various scales and compute budgets as presented in our main paper. We evaluate these models zero-shot on 38 downstream image classification and retrieval tasks. We additionally evaluate on 2 fairness datasets. See Section 3.5 and Appendix N for more details.

Q40 Is there a repository that links to any or all papers or systems that use the dataset? *If so, please provide a link or other access point.*

- No. However, there is a leaderboard associated with DATACOMP. Interested parties can investigate the submissions and further study publications that make use of our data. See: <https://www.datacomp.ai/leaderboard.html>.

Q41 What (other) tasks could the dataset be used for?

- The dataset could also be used for training image captioning models and language-conditional image generation models. Note: generative image models trained on COMMONPOOL are not expected to generate recognizable human faces as our download tooling automatically blurs detected faces. COMMONPOOL could be used for sociological studies, for example, examining societal biases or to better understand what is on the public internet.

Q42 Is there anything about the composition of the dataset or the way it was collected and preprocessed/cleaned/labeled that might impact future uses? *For example, is there anything that a future user might need to know to avoid uses that could result in unfair treatment of individuals or groups (e.g., stereotyping, quality of service issues) or other undesirable harms (e.g., financial harms, legal risks) If so, please provide a description. Is there anything a future user could do to mitigate these undesirable harms?*

- In our initial analysis of models trained on COMMONPOOL and its subsets, we notice disproportionate misclassification rates for identifying Black women (see Section P for more details on our fairness and bias evaluation). COMMONPOOL and its derivatives are not intended for production ready products, including but not limited to those related to race, gender identity or expression, ethnicity, sexual orientation, age, socioeconomic status, disability, religion, national origin or creed. COMMONPOOL is not suitable for any software that makes decisions involving people. COMMONPOOL is collected from the internet and hence reflects many of the biases, unfairness, and stereotypes currently existing in our societies.

Q43 Are there tasks for which the dataset should not be used? *If so, please provide a description.*

- COMMONPOOL in its current form or the subsets presented in this paper should not be used in software that makes decisions related to people. The known biases make deploying software, especially widely decimated production-level products, built on COMMONPOOL incredibly irresponsible. COMMONPOOL is designed as a research artifact for academic exploration. We also do not condone the use of COMMONPOOL in surveillance or military applications.

Q44 Any other comments?

- No.

R.6 Distribution

Q45 Will the dataset be distributed to third parties outside of the entity (e.g., company, institution, organization) on behalf of which the dataset was created? *If so, please provide a description.*

- Yes. We use HuggingFace datasets for public release.

Q46 How will the dataset be distributed (e.g., tarball on website, API, GitHub)? *Does the dataset have a digital object identifier (DOI)?*

- The dataset will be distributed via HuggingFace datasets at https://huggingface.co/datasets/mlfoundations/datacomp_pools/tree/main

Q47 **When will the dataset be distributed?**

- DATACOMP will be available starting May 2023.

Q48 **Will the dataset be distributed under a copyright or other intellectual property (IP) license, and/or under applicable terms of use (ToU)?** *If so, please describe this license and/or ToU, and provide a link or other access point to, or otherwise reproduce, any relevant licensing terms or ToU, as well as any fees associated with these restrictions.*

- We distribute the url-text sample and metadata under a standard CC-BY-4.0 licence.

Q49 **Have any third parties imposed IP-based or other restrictions on the data associated with the instances?** *If so, please describe these restrictions, and provide a link or other access point to, or otherwise reproduce, any relevant licensing terms, as well as any fees associated with these restrictions.*

- We do not copyright samples in the dataset.

Q50 **Do any export controls or other regulatory restrictions apply to the dataset or to individual instances?** *If so, please describe these restrictions, and provide a link or other access point to, or otherwise reproduce, any supporting documentation.*

- No.

Q51 **Any other comments?**

- No.

R.7 Maintenance

Q52 **Who will be supporting/hosting/maintaining the dataset?**

- HuggingFace currently hosts the url-text pairs and metadata. The DATACOMP team will be responsible for maintaining the dataset.

Q53 **How can the owner/curator/manager of the dataset be contacted (e.g., email address)?**

- We can be contacted at contact@datacomp.ai.

Q54 **Is there an erratum?** *If so, please provide a link or other access point.*

- Currently there are no errata. If issues are discovered, we will communicate with the public via our website <https://datacomp.ai>.

Q55 **Will the dataset be updated (e.g., to correct labeling errors, add new instances, delete instances)?** *If so, please describe how often, by whom, and how updates will be communicated to users (e.g., mailing list, GitHub)?*

- At the present time there is no intention to update COMMONPOOL for scientific reasons. However, we will respond to user takedown requests (see Q56). COMMONPOOL is inherently noisy and the purpose of releasing it is to encourage researchers in the community to study dataset cleaning in the context of image-text samples.

Q56 **If the dataset relates to people, are there applicable limits on the retention of the data associated with the instances (e.g., were individuals in question told that their data would be retained for a fixed period of time and then deleted)?** *If so, please describe these limits and explain how they will be enforced.*

- We will use the following website, <https://laion.ai/dataset-requests>, for user takedown requests, where “Sample ID” is the sample uid.

Q57 **Will older versions of the dataset continue to be supported/hosted/maintained?** *If so, please describe how. If not, please describe how its obsolescence will be communicated to users.*

- This is the first version of DATACOMP and the associated COMMONPOOL dataset. We do not intend to maintain deprecated version of COMMONPOOL. We will communicate deprecation notices through our website: <https://datacomp.ai>.

Q58 **If others want to extend/augment/build on/contribute to the dataset, is there a mechanism for them to do so?** *If so, please provide a description. Will these contributions be validated/verified? If so, please describe how. If not, why not? Is there a process for communicating/distributing these contributions to other users? If so, please provide a description.*

- All alterations to the dataset will be handled on a case-by-case basis.

Q59 **Any other comments?**

- No.